TU BERGAKADEMIE FREIBERG
FACULTY OF CHEMISTRY AND PHYSICS
Institute of Biosciences

UNIVERSIDAD DE SANTIAGO DE CHILE
FACULTY OF CHEMISTRY AND BIOLOGY
Department of Biology

CHARACTERIZATION OF ARSENIC-BINDING SIDEROPHORES FROM ENVIRONMENTAL BACTERIA AND EVALUATION OF THEIR ROLE IN ARSENIC TOLERANCE

GERARDO RETAMAL MORALES

Tutor: Gloria Levicán Jaque
Michael Schlömann

Graduate work presented in accordance with the requirements to obtain the Academic Degree of PhD in Biotechnology.

Santiago – Chile
2018

CHARACTERIZATION OF ARSENIC-BINDING SIDEROPHORES FROM ENVIRONMENTAL BACTERIA AND EVALUATION OF THEIR ROLE IN ARSENIC TOLERANCE.

GERARDO ENRIQUE RETAMAL MORALES

This work was prepared under the supervision of Dr. Gloria Levicán Jaque of the Faculty of Chemistry and Biology, of the University of Santiago de Chile, and Dr. Michael Schlömann, of the Institute of Bioscience of the Technical University of Freiberg, Germany and approved by the commission of follow-up

Prof. Dr. Gloria Levicán Tutor	Prof. Dr. Michael Schlömann Co-tutor
Prof. Dr. Diego Venegas	Prof. Dr. Juan P.García-Huidrobro
Prof. Dr. Claudia Saavedra	Prof. Dr. Rodrigo de la Iglesia

Prof. Dr. Alexis Aspée
Vicedecano de Investigación y Posgrado

CHARACTERIZATION OF ARSENIC-BINDING SIDEROPHORES FROM ENVIRONMENTAL BACTERIA AND EVALUATION OF THEIR ROLE IN ARSENIC TOLERANCE.

GERARDO ENRIQUE RETAMAL MORALES

_____	_____
Prof. Dr. Gero Frisch.	Prof. Dr. Jörg Matschullat
_____	_____
Prof. Dr. Dirk Tischler	Prof. Dr. Britta Planer-Friedrich

Chemical characterization of arsenic-binding siderophores from environmental bacteria and their role in arsenic tolerance

GERARDO ENRIQUE RETAMAL MORALES

ABSTRACT

Arsenic (As) is a toxic metalloid and the remediation of soils and waters from this contaminant as well as the prevention of future contamination are still pending tasks in Chile. There are bacteria able to live in environments polluted with arsenic, as they have tolerance mechanisms for this metalloid, or even can use it for energy metabolism. The potential tolerance mechanisms include the production of siderophores, metabolites with chelating activity that can decrease the toxicity of metals and metalloids. Although a correlation between siderophore production and metalloid tolerance has been described, the structure of arsenic-binding siderophores and their implications in tolerance have not been elucidated yet. In this work, it is proposed that bacteria isolated from contaminated environments produce arsenic-binding siderophores. The main aims of this work are to study the production of the siderophores by arsenic-tolerant bacteria, to characterize these compounds and to determine their relation with tolerance to arsenic.

Fourteen arsenic-tolerant bacteria were isolated from contaminated water, From these, four strains belonging to the species *Rhodococcus erythropolis*, *Arthrobacter oxydans* and *Kocuria rosea* were selected, in addition to the previously isolated *Rhodococcus erythropolis* S43, for a more detailed study. The isolates were used to produce siderophore extracts, which were then evaluated for their iron- and arsenic-binding activity. To detect the latter, a new method (As-$_m$CAS) was set up, based on the Chrome Azurol S (CAS) test, an assay to detect iron-chelating activity of siderophores. After testing the extracts, *R. erythropolis* S43 was selected as the strain with the best arsenic-binding activity. For the subsequent chemical characterization, siderophores were produced under control conditions (iron-free M9 medium) and under stress conditions with arsenic (iron-free M9 medium with sodium arsenite). HPLC analysis of the extracts for both culture conditions showed the presence of a single compound with both an iron-chelating and an arsenic-binding activity. Analyses by nuclear magnetic resonance (NMR) spectroscopy and mass spectrometry (MS) for both culture conditions suggested the main presence of the siderophore heterobactin B.

In addition, the genome of strain S43 was sequenced. A cluster of *ars*-genes was predicted, probably responsible for the arsenic-tolerance of the strain. In addition, a complete gene cluster for heterobactin production was found. However, no significant difference was obtained in the expression of these determinants in the presence or absence of arsenic, suggesting that the production of this siderophore in strain S43 is not responsible for the tolerance to the metalloid.
Keywords: Siderophores, Actinobacteria, *Rhodococcus erythropolis* S43, bioremediation, arsenic.

RESUMEN

El arsénico (As) es un metaloide altamente tóxico y su remediación de suelos y aguas de este contaminante, tal como la prevención de futura contaminación es una tarea pendiente en Chile. Existen bacterias capaces de vivir en ambientes contaminados con arsénico, pues poseen mecanismos de tolerancia para este metaloide, o pueden utilizarlo para su metabolismo energético. Entre los potenciales mecanismos de tolerancia destaca la producción sideróforos, metabolitos con actividad quelante que pueden disminuir la toxicidad de metales y metaloides. Si bien se ha descrito una correlación entre la producción de sideróforos y la tolerancia al metaloide, la estructura de los sideróforos quelantes de arsénico y sus implicancias en la tolerancia no han sido descritas. En esta tesis se plantea que las bacterias aisladas de ambientes contaminados producen sideróforos quelantes de arsénico. El principal objetivo es estudiar la producción y caracterizar los sideróforos quelantes de arsénico producidos por las bacterias tolerantes y determinar su relación con la tolerancia al metaloide.

De catorce cepas tolerantes a arsénico aisladas a partir de aguas contaminadas, se seleccionaron cuatro cepas pertenecientes a las especies *Rhodococcus erythropolis*, *Arthrobacter oxydans* y *Kocuria rosea*. Adicionalmente, se incluyó *Rhodococcus erythropolis* S43, una cepa que fue previamente caracterizada como tolerante. Los aislados fueron utilizados para realizar extractos de sideróforos a los que se les evaluó su actividad quelante de hierro y arsénico. Para detectas esta última, se estandarizó un método (As-$_m$CAS), basado en el ensayo Cromo Azurol S (CAS), método para detectar la presencia de sideróforos quelantes de hierro. Luego de evaluar los extractos, se seleccionó la cepa *R. erythropolis* S43 como la cepa con mejor actividad quelante de arsénico. Para la caracterización química, se produjeron sideróforos en condición control (medio M9 libre de hierro) y condición de estrés con arsénico (medio M9 sin hierro, con arsenito de sodio). El análisis por HPLC de los extractos mostró la presencia un único compuesto con actividad quelante de hierro y arsénico para ambas condiciones. Los análisis realizados utilizando espectroscopía de resonancia magnética nuclear (RMN) y espectrometría de masas (EM) sugirieron la presencia mayoritaria del sideróforo heterobactina B para ambas condiciones de cultivo.

Además, se secuenció el genoma de la cepa S43 donde se predijo un cluster de genes para un *cluster ars*, probablemente responsable del fenotipo tolerante a arsénico de la cepa. Además, se encontró un *cluster* génico para la producción de heterobactina. Sin embargo, no se obtuvo diferencia significativa en la expresión de estos determinantes en presencia o ausencia de arsénico, sugiriendo que la producción de este sideróforo en la cepa S43 no es responsable de la tolerancia al metaloide.

Palabras Clave: Sideróforos, Actinobacteria, *Rhodococcus erythropolis* S43, biorremediación, arsénico.

ZUSAMMENFASSUNG

Arsen (As) ist ein giftiges Halbmetall, für das die Sanierung belasteter Flächen und Gewässer sowie die Vermeidung künftiger Verschmutzung in Chile noch weitgehend ausstehen. Es gibt Bakterien, die in arsenbelasteter Umgebung leben können, da sie über Toleranzmechanismen für dieses Halbmetall verfügen oder es sogar für den Energiestoffwechsel nutzen können. Zu den Toleranzmechanismen gehört die Produktion von Siderophoren, Metaboliten mit Chelataktivität, welche die Toxizität von Metallen und Halbmetallen verringern können. Obwohl eine Korrelation zwischen der Produktion von Siderophoren und der Halbmetalltoleranz beschrieben wurde, konnten die Struktur von arsenbindenden Siderophoren und ihre Auswirkungen auf die Toleranz noch nicht geklärt werden. In dieser Arbeit wird postuliert, dass aus kontaminierten Umweltproben isolierte Bakterien arsenbindende Siderophore produzieren. Hauptziele dieser Arbeit sind die Untersuchung der Produktionsbedingungen der Siderophore aus Arsen tolerierenden Bakterien, die Charakterisierung dieser Verbindungen sowie die Ermittlung ihres Einflusses auf die Toleranz gegen Arsen.

Aus kontaminiertem Wasser wurden 14 arsentolerante Bakterien isoliert, von denen vier Stämme der Spezies *Rhodococcus erythropolis*, *Arthrobacter oxydans* und *Kocuria rosea* zusätzlich zum bereits früher isolierten *Rhodococcus erythropolis* S43 für eine genauere Untersuchung ausgewählt wurden. Von den Isolaten wurden Siderophorextrakte hergestellt, die anschließend auf ihre Eisen- und Arsenbindungsaktivität untersucht wurden. Um Letztere zu erkennen, wurde eine neue Methode (As-$_m$CAS) auf Basis des Chrome Azurol S (CAS)-Tests, einem Test zum Nachweis der Eisenkomplexbildungsaktivität von Siderophoren, entwickelt. Nach dem Testen der Extrakte wurde *R. erythropolis* S43 als Stamm mit der besten Arsenbindungsaktivität ausgewählt. Für die chemische Charakterisierung wurden die Siderophore unter Kontrollbedingungen (eisenfreies M9-Medium) und unter Stressbedingungen mit Arsen (eisenfreies M9-Medium mit Natriumarsenit) hergestellt. Die HPLC-Analyse der Extrakte zeigte für beide Kultivierungsbedingungen die Anwesenheit einer einzelnen Verbindung mit einer sowohl Eisen komplexierenden als auch Arsen bindenden Aktivität. Analysen mittels Kernspinresonanz-(NMR-)Spektroskopie und Massenspektrometrie (MS) deuteten für beide Kultivierungsbedingungen auf die hauptsächliche Anwesenheit des Siderophors Heterobactin B hin.

Zusätzlich wurde das Genom von Stamm S43 sequenziert. Ein Cluster von *ars*-Genen wurde vorhergesagt, wahrscheinlich verantwortlich für die Arsentoleranz des Stammes. Zusätzlich wurde ein komplettes Gencluster für die Heterobactinproduktion gefunden. Die Expression dieser Genen in Gegenwart oder Abwesenheit von Arsen zeigte jedoch keinen signifikanten Unterschied, was nahelegt, dass die Produktion dieses Siderophors in Stamm S43 nicht für die Toleranz gegenüber dem Halbmetall verantwortlich ist.

Schlüsselwörter: Siderophore, Actinobakterien, *Rhodococcus erythropolis* S43, Bioremediation, Arsen.

DEDICATORY

This thesis work is dedicated to all the people that have supported me over the years of this PhD process, which with their guidance and support made this path more comfortable for me in the personal and professional level.

I would like to thank the unconditional support of my mother, my father and my brother, whom have shared this process with me, supported me in the difficult moments and reminded me to enjoy the small successes that I have been able to achieve during these years.

Also, I would like to thank Prof. Dr. Enrique González Villanueva from University of Talca, for showing me that research in science is a noble and a fulfilling road, which must be walked with hard work and integrity. Also to his wife and aunt of mine, Rebeca Espinoza for her constant motherly support during several years, and specially to my best friends Pamela González and Daniela González, for being my family in a place far from home and for keeping me sane during the difficult moments, I hope we can keep sharing our growth together for many years to come.

Finally, to my PhD classmates and lab-mates, Camila Calfio, Carlos Gil, Rodolfo Parada, Javier Rivera, Claudia Muñoz, Angel Olguín and Pamela Alamos, among many others, for their friendship, support and criticism during my work, I would not have grown the same without your help.

I am sure that the student that entered the PhD in 2014 is not the same that leaves in 2018.

ACKNOWLEDGMENTS

I would like to thank to all the people that helped and guided me during this thesis work. First, to the Chilean evaluation committee, Prof. Dr. Claudia Saavedra from Universidad Andrés Bello, Prof. Dr. Rodrigo de la Iglesia from Universidad Católica, Prof. Dr. Diego Venegas and Prof. Dr. Alejandro Urzúa from Universidad de Santiago, for their guidance, attention and criticism during these last years, and helping me to have a more complete vision of the scientific investigation.

I also must give a very heartfelt thank you the German evaluation committee, Prof. Dr. Britta Planer-Friedrich from University of Bayreuth, Prof. Dr. Jörg Matschullat and Prof. Dr. Gero Frisch from TU Bergakademie Freiberg, for their patience, understand and feedback on this work, which was a very important input to the developing and improving of this manuscript.

To my lab-mates and friends in TU Freiberg, Marika Mehnert, Fabian Giebner, Thomas Heine, Ringo Schwabe, Judith Tischler, among many others, and all the people from the Institute of Biosciences, which helped me with my scientific work, integration into the German culture, and made me feel at home in a place far away, where I feel I found great friends. Also, very importantly to Prof. Dr. Dirk Tischler, for his guidance, patience and support during not only my staying in Freiberg, but also during all the time we have met, for being a great role model of what is to come in the following years as a scientist.

To Prof. Dr. Michael Schlömann, for opening the doors of the Institute of Biosciences for me, for being an understanding, dedicated and incredibly supportive tutor, it has been a pleasure to learn from you, and I hope I have reached the expectations you had for Chilean students and I have represented fairly my country at your home University.

To the Professors from the Laboratory of Basic and Applied Microbiology in Universidad de Santiago, Prof. Dr. Renato Chávez and Prof. Dr. Marcela Wilkens, for their advice and patience during my process of development as a student.

And finally, to Prof. Dr. Gloria Levicán, for being an outstanding tutor, which without her support and advice not only in the professional but also in the personal sense, this process would not have been the same. Thank you for trusting in my capacities without knowing me when I arrived, guiding me and keep supporting me in the moments when I did not achieve the desired standards, I have learned and grown immensely under your tutelage.

DECLARATION

I hereby declare that I completed this work without any improper help from a third party and without using any aids other than those cited. All ideas derived directly or indirectly from other sources are identified as such.

In the selection and in the use of materials and in the writing of the manuscript I received support from the following persons:

Dr. Michael Schlömann
Dr. Gloria Levicán

Persons other than those above did not contribute to the writing of this thesis. I did not seek the help of a professional doctorate-consultant. Only persons identified as having done so received any financial payment from me for any work done for me. This thesis has been submitted to TU Bergakademie Freiberg and Universidad de Santiago, according to the “General Agreement on a joint Doctorate procedure” signed by both Universities.

TABLE OF CONTENTS

INDEX OF TABLES

INDEX OF FIGURES

I. INTRODUCTION

1.1. Arsenic diffusion to the environment

Arsenic (As) is naturally ubiquitous in several environments such as soil, water sources and rock (Mandal and Suzuki 2002), occupying the 20th place in abundance on Earth's crust (Gomez-Caminero et al. 2001). This metalloid is forming non-soluble minerals (the most common being arsenopyrite, enargite and scorodite) which are stable and low in toxicity. However, due to activities such as mining, dye or electronic industrial processes (Welch et al. 2000) it can be released into the environment where it can form highly toxic compounds, which spread through different processes such as rain and filtration of waste water or related to arsenic-bearing flotation tailings and mine waters (Cullen and Reimer 1989; Drewniak et al. 2014) (Fig. 1).

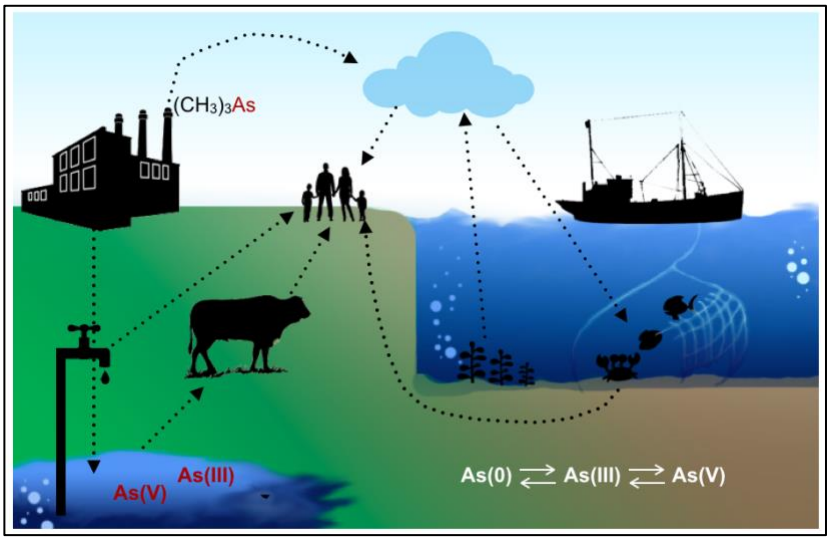

Figure 1.- The global arsenic geocycle and environmental contamination and anthropogenic sources polluting several environments.

In nature, arsenic is mostly found in sulfide minerals where it can occur as an arsenide or sulfarsenide anion bound to transition metals (for example, löllingite, $FeAs_2$ or arsenopyrite, FeAsS) or as part of iron containing minerals like scorodite ($FeAsO_4$) (Rousell et al. 2000; Al-Abed

et al. 2007), from where can be released into the environment through natural occurring processes like weathering reactions, biological activity and volcanic emissions, as well as through a range of anthropogenic activities, which involve mechanisms of dissolution, redox-reactions and adsorption-desorption processes. This mobility is dependent of the mineral form and the anthropogenic or natural form causing the mobilization, where the most prevalent arsenic species released are arsenite [As(III)] and arsenate [As(V)], although these are not the only arsenic species (where arsine As(-III) and arsenic (As0) must be also included). Arsenite is usually found as a neutral specie at neutral pH (with a pK_1 = 9.2) with high solubility in water, while arsenate is found in more oxidized conditions and is less soluble (Bowell et al. 2014).

When coming from anthropogenic sources arsenic can cycle among several reservoirs such as anthrosphere, lithosphere, atmosphere, hydrosphere and biosphere (Matschullat, 2000). The process usually starts with industrial activities such as mining of arsenic-containing minerals, where the metalloid is mobilized from the lithosphere to the other reservoirs, for example, through emissions of arsenic to the athmosphere product of ore smelting, where it can then contaminate water and soil product of precipitations into the land, or become part of the biomass of water-life. Regarding this phenomenon, several industrial processes can be involved in the release of the metalloid to the environment, such as mining of arsenic-containing ores, processing of arsenic and other metal concentrates and production of arsenic-containing products, among others (Chen et al. 2016)

1.2 Arsenic in water and its toxicity

Nowadays, arsenic derived from human activities can exceed natural metalloid sources up to 3-fold (Welch et al. 2000), being water sources one of the most problematic. In most natural groundwaters, it occurs either as As(III) or As(V), where organic arsenic forms may be produced by biological activity, mostly in surface waters, but are mostly present in biological tissues where the most dominant compound is arsenobetaine, which shows low toxicity in humans (Cullen and Reimer 1989).

Arsenic is generally present as an oxyanion in oxic environments, while in anaerobic soils, it is typically found combined with sulfur. Thus, in uncontaminated aerobic sediments and soils arsenate is the predominant species, whereas in anaerobic sediments and soils arsenite is the dominant species (Nordstrom and Archer 2003; Campbell and Nordstrom 2014). Methylated forms of arsenic can also form in surficial environments and are also pH sensitive. Over the natural range of Eh and pH, both As(III) and As(V) can occur in a range of stable aqueous forms, being arsenous acid (H_3AsO_3) the most common in groundwater (Bowell et al. 2014) (Supplementary material

Figure S1). The equilibrium constants for common arsenic species in aqueous solution, can be seen in Table 1.

Table 1.- Aqueous speciation of arsenic (obtained from Bowell et al. 2014).

Arsenic compound	**p*K*a**
Arsenic acid	
$H_3AsO_4 \leftrightharpoons H_2AsO_4^- + H^+$	p*K*a1 = 2.25
$H_2AsO_4^- \leftrightharpoons HAsO_4^{2-} + H^+$	p*K*a2 = 6.98
$HAsO_4^{2-} \leftrightharpoons AsO_4^{3-} + H^+$	p*K*a3 = 11.58
Arsenous acid	
$H_3AsO_3 \leftrightharpoons H_2AsO_3^- + H^+$	p*K*a1 = 9.24
Monomethylarsonic acid	
$CH_3AsO(OH)_2 \leftrightharpoons CH_3As(OH)O_2^- + H^+$	p*K*a1 = 4.19
$CH_3As(OH)O_2^- \leftrightharpoons CH_3AsO_3^{2-} + H^+$	p*K*a2 = 8.77
Dimethylarsinic acid	
$CH_3AsO(OH) \leftrightharpoons (CH_3)_2AsO_2^- + H_+$	p*K*a1 = 6.14

Independently of the majoritarian species present in water, around the world the total arsenic concentration is reported in order to determine if these sources achieve the limit of arsenic in water required by the World Health Organization (or the internal regulatory norms of each country), which states that the limit of arsenic in drinking water should be 10 µg/L (Gorchev et al. 2011). As expected, many natural aquifers affected by arsenic contamination exceed this standard containing concentrations above 50 µg/L. These areas have been reported to be in Bangladesh,West Bengal, Chile, Argentina, China, Mexico, Vietnam, and parts of Canada and the U.S.A. (Smedley and Kinniburgh 2002; McGuigen et al. 2010; Chappells et al. 2014). In Chile, some aquifers can present up to 500 mg/L (Supplementaty material, Table S1) of total arsenic content, these correspond to groundwater related to mining activity, and are connected to water-treatment plants to achieve the concentrations determined by the norm after the treatment (Marshall et al. 2007; Ferreccio and Sancha 2006).

The environmental problem lies not only in the presence of arsenic in water, since many of the water sources are related to water-purification plants, but does it in occupational exposure, which can lead to acute or chronic diseases product of excessive arsenic intake, where its toxicity is directly related to the species involved, where generally, organic compounds, for example the ones occurring in seafood, or the metabolites of inorganic arsenic forms, are much less toxic than the inorganic forms. These latter, when entering the human body through ingestion, inhalation, or skin absorption, can be a problem specially in miners which are in constant contact to arsenic-

containing ores or arsine-containing fumes. After entering the body, some of these arsenic-containing copounds can be absorbed in the gastrointestinal system and then distributed in a large number of organs including the lungs, liver, kidney and the skin (Mello de Capitani, 2011), where the clinical manifestations can be difficult to diagnose, since its early symptoms are non-specific and may be present in other diseases. So, classical early arsenic-produced diseases such as arsenicosis or keratosis which have respiratory, cardiovascular and topical effects are diagnosed many times at a late state (Ferrechio and Sancha 2006).

The many effects of arsenic in the human body include respiratory and cardiovascular effects such as irritation of the respiratory mucous membrane which can lead to laryngitis, bronchitis, chronic cough and over the years loug cancer. Also can cause thicken blood vessels and hypercontract the heart-muscle fibers. Aditionally, arsenic is filtered through the urinary sistem causing renal failure and is a risk factor to bladder cancer (Smith et al. 1992; Smith et al. 2009; Jomova et al. 2011).

Besides the afored mentioned complications arsenic can affect the gastrointestinal, neurological and hepatic systems, therefore, it can cause chronic damage in several bodily functions. While the carcinogenicity of arsenic (specially inorganic arsenic) has been confirmed, the mechanisms behind the diseases occurring after the exposure to the metalloid are not complelety understood. The most described toxic mechanism of arsenic is the impairment of cellular respiration through interference with oxidative phosphorylation caused by the inhibition of various mitochondrial enzymes, associated with inorganic arsenic species. As(III) is 2 to 10 times more toxic than As(V), the first suppresses the activity of more than 200 cellular enzymes by bonding with thiol or sulfhydryl groups, affecting the function numerous organs (Goyer, 2001). Meanwhile, As(V) can replace phosphorus, affecting numerous biochemical pathways including ATP synthesis (Hughes, 2002; Kaur et al. 2011). Although these tocixity mechanisms have been reported to be related to diseases after a exposure to high concentrations of arsenic, numerous studies have stated that also various health effects are caused by chronic exposure to low concentrations of the metalloid, which cause accumulative damage. Therefore, independently of the biologycal processes involved in arsenic toxicity it is possible to state, as other authors have (Hong et al. 2016), that arsenic contamination and chronic expossure to the metalloid are a public health issue which remains to be solved.

1.3. Current arsenic-removal technologies

As it has been commented, arsenic can be a risk factor for high mortality diseases which have complicated treatments, therefore, the main way to avoid arsenic toxicity is removing it from

water, and thus, their intake. However, arsenic cannot be destroyed, it can only be transformed into different forms or combined with other elements containing it into non-soluble compounds (Anjum et al. 2014). Here, a summarized review of some arsenic-removal methods is presented in order to give general context to this work.

Nowadays, there is a plethora of industrial technologies oriented to remove arsenic from water. One of the most commonly used are oriented to chemically oxidize arsenite to arsenate, a less toxic species, usually through addition of a chemical agent such as hypochlorite (ClO^-) or potassium permanganate. This is a very versatile method, which makes possible the coupling with other purification processes occurring in a water purification plant (Sen et al. 2010). However, a high level of technology and control is required, making this process necessary to be monitored by specialized staff.

Another common arsenic-removal process is the precipitation into non-soluble compounds, some of them, based in the low-solubility of certain inorganic As(V)-compounds, when several strategies can be used. For example, solid calcium arsenate reacts with carbon dioxide to form $CaCO_3$ while arsenic is remobilized, also the addition of magnesium salts can lead to the formation of $Mg_3(AsO_4)_2$. To a limited extent, this method is applied to achieve arsenate fixation in soils, sediments and wastes, where As(V) can be removed through precipitation of ferric arsenate (Magalhães 2002; Basha et al. 2008). Other type of arsenic precipitation is the production of the mineral scorodite, this arsenic-removal method that seems to be very useful via precipitation of As(V) in the $Fe\text{-}AsO_4\text{-}SO_4$ system, which can be carried out at pH < 1 in the temperature ranges 150 to 225˚C. Here, the production of scorodite as an arsenic-containing mineral solves the problem of high solubility of inorganic arsenic species. The nature of this process have some requirements, for example, the conversion to crystalline scorodite requires temperatures >90°C (Robins et al. 2001) and the precipitation is possible at pH values < 2 leading to an amorphous material with particle sizes of about 100 nm. Other options to obtain these crystals include the use of ferrous salts (as ferrous sulphate) and subsequent oxidation by means of ferrate ions (Vogels and Johnson 1998). This processing of arsenical compounds by the hydrothermal route has been named the "Scorodite Process" and this is considered to represent a realistic process option for arsenic disposal, where crystalline scorodite should have a low solubility for prolonged periods of time, and can be considered most stable arsenate compound formed in nature, being suitable for arsenic disposal purposes (Swash and Monhemius, 1998).

Among the most common industrial methods for arsenic detoxification, the membrane technologies are successful and versatile, since they can be coupled with the afore mentioned methods. Sorption has been described as an increasing technology in water treatment plants. it occurs in a fixed bed process through which ions in solution are removed by sorption at sorbent

active sites. When all active sites are occupied, the sorbent should be regenerated or replaced and properly disposed (Deschamps, 2011). Though the years, activated alumina was the first sorbent successfully applied in arsenic-removal technologies, while others, mostly Fe-based, were developed and made available on the market. Differences in the general composition of sorbents, such as: Fe valence state, crystalline structure, specific surface area, and other physico-chemical characteristics, result in different kinetics and sorption capacities. Studies and applications performed in commercial experiments have shown that the removal capacity of Fe-based sorbents exceeds that of alumina-based ones (EPA 2003). The performance of the treatment systems depends on various factors including concentration and speciation, pH, presence of competitor ions, adsorbent specific characteristics, average life and the extent to which they can be regenerated, making it a technology highly specific. The main disadvantage of these lies in the high sensitivity to the ion concentration and pH of the water, losing up to 90% of their effectivity when the pH of treated water is far from neutrality, a common occurrence in some mining derived waters (Kumar Kaushal 2007).

Nowadays, there are several types of biological systems in use for the removal of arsenic from water, which when coupled with the afored mentioned methods can improve the removal. One of these is the utilization of cultured bacteria to oxidize and precipitate iron and manganese in water. Other methods use anaerobic sulphate-reducing bacteria, and other reducing bacteria to precipitate arsenic from solution as insoluble arsenic-sulphide complexes, for example arsenic sulphide (As_2S_3) can be generated by adding ferrous sulphate solutions and by means of sulphate-reducing bacteria (Ayangbenro et al. 2018). The efficiency of these technologies is dependent of pH, available nutrients and temperature, and the removal rate is also sensitive to arsenic concentrations. To improve these methods, the use fungi can be applied to the removal technologies. Fungi can be used as biosorbents for arsenic removal, for example, dead fungal biomass of *Penicillium chrysogenum* , *Aspergillus niger* coated with iron oxide and *Penicillium purpurogenum* can be used for arsenic removal when coupled with a pre-treatment with the detergent hexadecyl-trimethyl ammonium bromide (HDTMA-Br) dodecylamine and a cationic polyelectrolyte to improve arsenate biosorption (Murugesan et al. 2006; Pokhrel and Viraraghavan, 2006). Other approaches use the combination of fungi and chitosan particles, chitosan beads are reported to remove As(III) and As(V) in both batch and continuous process from water (Dambies et al. 2000), so a chitosan/chitin mixture coupled with the biomass from the filamentous fungi (for example, *Rhizopus oryzae*) can be used for removal of arsenic from contaminated water (Elson et al. 1980; Mcafee et al. 2001).

Other researches have focused in phytoremediation, the utilization of plan biomass to remove metals/metalloids from water and soil. For example, the rhizofiltration (filtration trough the roots of plants) has been studied for the potential of different aquatic plant species to remove elements

which can be toxic when occurring in high concentrations in water, such as boron (B), chromium, copper, mercury, cadmium, nickel, selenium and arsenic (Mkandawire and Dudel 2005). This metal/metalloid sorption by plants is facilitated by transporter proteins present in plant cells. Here, due to the structural similarity between phosphate and As(V), this is sorbed by plants at the same sites as phosphate, which can be absorbed at high concentrations (Mkandawire et al. 2004).

To summarize, the current technologies seem to be effective and are safe for arsenic-removal from water, however, the implementation of these is not necessarily spread worldwide, thus, a wider promotion and implementation is still needed to avoid the health problems associated with excessive arsenic intake. Since, as it has been mentioned before, arsenic poisoning is mainly caused to excessive and uncontrolled industrialization which leads to the contamination of the natural resources. As it has been mention previously, the combination of biological solutions with current industrial technologies seems to be a good and versatile approach to face the environmental problem that is arsenic, in this work, an exploration of the capacity of microorganisms to deal with arsenic can light some clarity to keep developing or improving methods to face the current environmental problem.

Table 2.- Overview of the main arsenic-removal technologies described in this work.

Methods	Advantages	Disadvantages
Major oxidation/precipitation technologies		
Chemical oxidation	Oxidizes other impurities and inhibit microbial growth, simple and fast with minimum residual mass	Efficient control of the pH and oxidation step is required Mainly remove As(V) and accelerate the oxidation process
Coagulation / co-precipitation		
Sulfate coagulation	Simple in operation and low capital cost, effective over a wide range of pH	Produces toxic sludge, low removal of arsenic, pre-oxidation may be required
Precipitation as scorodite	Highly non-soluble product with low toxicity	Highly dependent of pH and temperature
Iron coagulation	Common chemicals available, more efficient that alum coagulation	intermediate removal rate of As(III), sedimentation and filtration is needed
Lime softening	Chemicals are available commercially	Readjustment of pH is required
Sorption and ion-exchange technologies		
Adsorption	Simple and cost effective, regenerated if required, effective arsenic removal	pH sensitve
Activated albumina/carbon	relatively well-known and commercially available	Need replacement after 4 to 5 regeneration
Ion-exchange resin	Well-studied, pH independent, exclusive ion specific resin to remove arsenic.	High cost, high-tech operation and mantainence, regeneration creates a sludge disposal problem, As(III) is difficult to remove, short life od resins
Biological technologies		
Anaerobic sulphate-reducing bacteria	High removal, possible to couple with existing technologies	pH and nutrient dependent
Fungi as bio-absorbents	No toxic solid waste is produced	High production of biomass required
Rhizofiltration	High versatility, many metal/metalloids can be filtrated	Death of plant biomass requires periodical exchange

1.4. How bacteria deal with arsenic

Bacteria are able to live in presence of several pollutants occurring in the environment (Strnad et al. 2014; Sekine et al. 2006; Slyemi and Bonnefoy, 2012). This is due to different mechanisms to deal with the toxicity of these elements that allow bacteria to survive in these unfavorable conditions. Thus, in order to understand these pathways and explore their biotechnological potential, several research groups have characterized different bacterial strains isolated from contaminated sites (Albarracín et al. 2005; Ueno et al. 2007; François et al. 2012), including arsenic-contaminated environments (Drewniak et al. 2008; Sultana et al. 2012; Srivastava et al. 2012; Retamal-Morales et al. 2018).

Until now, there have been no verifiable reports that indicate that intracellular arsenic is needed for the survival of any microorganism, and specific arsenic transporters have not been characterized or found. Therefore, in order to enter the bacterial cell, arsenic is carried by transport systems of analog molecules.

As it has been mentioned befote, due to their atomic similarity with phosphorus, As(V) can enter the cell through phosphate transport systems, usually through Pit (Phosphate Inorganic Transport), but it is also able to enter by the Pst system (Phosphate high-affinity transport) (Rosen and Liu 2009). Meanwhile, As(III) usually occurs as the neutral species arsenous acid [$As(OH)_3$] at physiological pH (lower than 9.3) and is structurally similar to glycerol. Therefore, its main uptake mechanism is through aquaglyceroporins, dedicated to the transport of water, glycerol and small uncharged molecules (Bhattacharjee et al. 2008). Once inside the cell, arsenic must face several bacterial tolerance mechanisms. Among them one of the most conserved tolerance strategies is the cytoplasmic reduction of As(V) to As(III), through several proteins encoded in the *ars* operon (Prithivirajsingh et al. 2001) which include an arsenate reductase (ArsC), an efflux pump for As(III) (ArsB) and a transcriptional regulator (ArsR). In some bacteria, this operon can also contain an ATPase protein coupled to the efflux pump (ArsA) (Fig. 2) and a chaperone (ArsD), which increases the extrusion capacity of ArsB (Yang et al. 2010). The strategy of reducing As(V) to As(III) is used by bacteria to minimize the competition of arsenic against phosphate, with the final aim of maintaining a normal ATP production. This detoxifying mechanism involving the reduction of As(V) and later extrusion of As(III) seems to be conserved from bacteria to plants (Ellis et al. 2006).

In relation to the mechanisms to detoxify As(III), methylation, dissimilatory oxidation and immobilization of arsenic are the most described by literature (Oremland and Stolz 2003, Slyemi and Bonnefoy, 2012). However, the dissimilatory oxidation of As(III) is usually performed by

bacteria to synthezise ATP, so it cannot be necessarily considered a detoxification mechanism, and although the oxidation of arsenite to arsenate lowers its toxicity, improving the capacity of bacteria to survive, it cannot be described a tolerance mechanism. This oxidation is performed by arsenite oxidases, which have been found widely in the Bacteria domain (Oremland and Stolz 2003; Stolz et al. 2006). These proteins can be AoxAB or ArxB. The AoxAB proteins have been extensively studied, they belong the DMSO-reductase protein family, use molybdenum as cofactor and have iron-sulfur clusters (Duval et al. 2010). Similarly, as the dissimilatory oxidation the dissimilatory reduction of arsenate should be not considered tolerance mechanisms since is also aimed to generate energy, although the current literature groups it in the traditional arsenic-tolerance mechanisms by bacteria (Slyemi and Bonnefoy, 2012). These pathways such as dissimilatory oxidation and reduction of the metalloid seem occur less frequently in bacteria (Oremland et al. 2009), and will not be the focus in this work.

Besides the enzymatic mechanisms, bacteria face arsenic toxicity through production of either organic or inorganic compounds, in the latter case usually sulfur- or iron-derived. An example of this is the extracellular precipitation of the metalloid, decreasing its uptake, and thus, lowering the toxicity (Battaglia-Brunet et al. 2009). Some microorganisms also use extracellular polymeric substances (EPS) to prevent the entry of arsenic to the inner cell (Harrison et al. 2007). Another proposed extracellular mechanism is the immobilization through synthesis of organic compounds such as siderophores. These have been described originally as organic chelators with high affinity for ferric iron [Fe(III)] in iron-depleting conditions (Schalk et al. 2011). However, some recent studies have suggested their participation in the tolerance against several metals/metalloids (Schalk et al. 2011; Braud et al. 2010), a novel perspective on the role of these compounds against toxic elements.

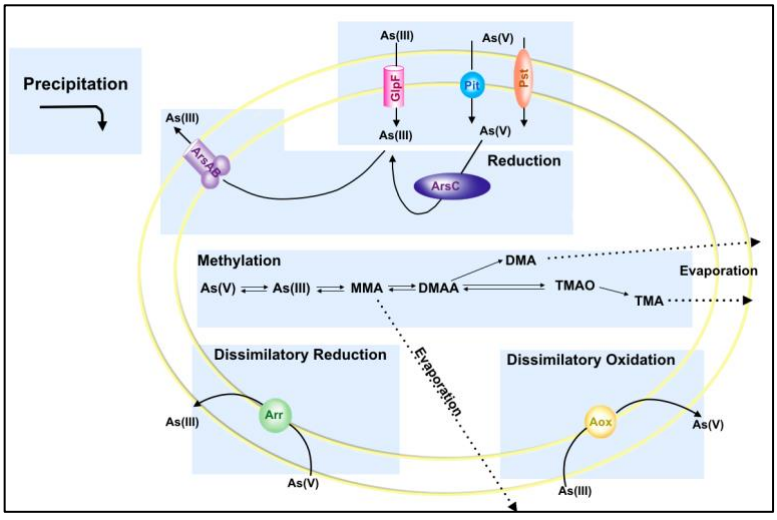

Figure 2.- Arsenic tolerance mechanisms present in bacteria (modified from: Slyemi and Bonnefoy, 2012).

1.5. Characteristics and function of bacterial siderophores

Siderophores are low molecular-weight organic molecules with high affinity for Fe(III). They are produced by plants, fungi and bacteria under nutrient-depleting conditions, specifically under iron depletion, since Fe(III) is a vital nutrient for development and growth of plants and microorganisms. Therefore, the traditional function of siderophores is the uptake of ferric iron from the extracellular medium to be used in metabolism (Kraemer 2004).

In bacteria, the synthesis of siderophores is usually performed by the combined action of non-ribosomal peptide synthetases (NRPS) and other enzymes, which can be encoded in a genetic cluster (Renshaw et al. 2002). NRPS are big multifunctional proteins with a modular structure able to synthesize peptides, independently of ribosomes (Mootz et al. 2002). The non-ribosomally synthesized peptides can be modified by action of other bacterial proteins (usually coded in the NRPS genetic cluster). Therefore, one non-ribosomally synthsesized peptide can participate in the formation of different siderophores, due to the action of this later modifications (Haas 2003). Thus, the presence of an NRPS genetic cluster in a bacterial genome is an indication of the production of one or more siderophores by that specific microorganism.

It has been described that different siderophores are specific to a bacterial species or even strain. Therefore, studying the synthesis and chemical characteristics of these metabolites must be done individually for each specific bacterial strain (Miethke and Marahiel 2007), where the analysis must be performed using pure isolates, since the findings can be particular of each one. Siderophores are usually classified by the functional groups that gives them the iron-chelating activity. Figure 3 shows different siderophore types, which can be classified as catecholates, hydroxamates, carboxylates, phenolates and mixed types, which can present more than one functional group in the same molecule. As it is shown, different bacterial species produce different siderophores with specific chemical characteristics (Miethke and Marahiel 2007; Johnstone and Nolan 2015). However, independently of their chemical nature, Fe(III) uptake by siderophores can be summarized as a general process for bacteria.

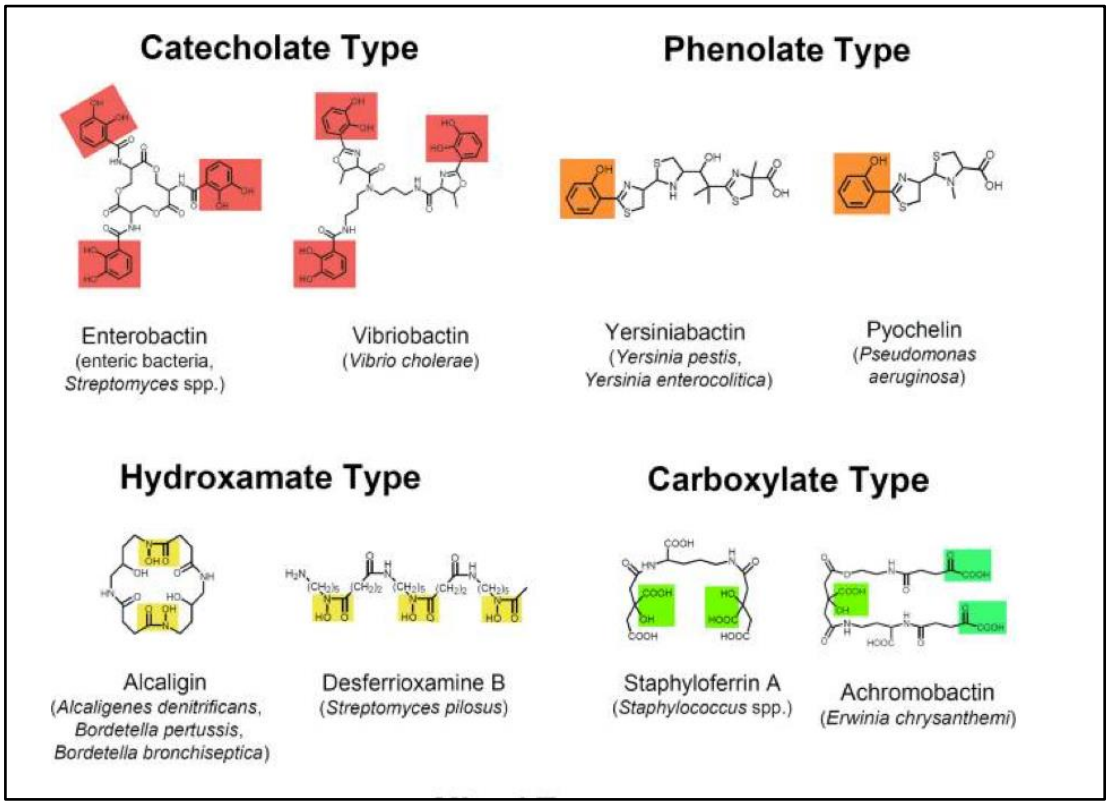

Figure 3.- Siderophore types according to their functional group with iron-chelating activity (Miethke and Marahiel, 2007).

The uptake of Fe(III) by siderophores has been identified in both Gram-negative and Gram-positive bacteria (Miethke and Marahiel 2007; Hider and Kong 2010). In Gram-negative bacteria, the outer membrane contains porins. However, these proteins only allow the passive diffusion of solutes that have a molecular weight less than 600 Da (Nikaido 2003). Most ferric-siderophore complexes exceed the molecular weight cut-off of porins. Therefore, they require specific outer membrane receptors for uptake into the periplasmic space. These iron-uptake pathways involve, in general, an outer-membrane receptor with high affinity for the iron-siderophore complex (Hider and Kong 2010), a periplasmic binding protein (PBP), and an inner-membrane ATP-binding cassette (ABC) transporter (Fig. 4). Since the outer membrane lacks an established ion gradient or ATP to provide the energy for transport, the energy requirement for the integration of the siderophore-iron complex is accomplished through the coupling of the proton motive force of the cytoplasmic membrane to the outer membrane via three proteins: TonB, ExbB, and ExbD (Fig. 4). In the case of Gram-positive bacteria, a thicker cell wall composed of murein, polysaccharides, teichoic acids and cell-wall proteins is all that separates the bacterial cytoplasm from its environment. Thus, iron uptake involves a membrane-anchored binding protein, which resembles the PBP in Gram-negative organisms, as well as an ABC transporter (Krewulak and

Vogel 2008). Recent studies have attempted to describe the molecular basis of this phenomenon in Gram-positive bacteria. However, in comparison with Gram-negative bacteria there is still relatively little information on iron transport.

Once inside the cell, iron must be released to be able to participate in bacterial metabolism. Bacteria have several mechanisms for iron release from siderophores, and can vary in different bacterial species. One of the most common mechanisms comprises the reduction of siderophore-bound Fe(III) to Fe(II), through the activity of ferrisiderophore reductases, followed by the spontaneous release or a competitive sequestration of the reduced iron species. It has been suggested that most Fe-siderophore complexes are discharged this way (Miethke and Marahiel 2007). Although, a considerable number of enzymes with ferrisiderophore reductase activity have been found, only a few possess significant specificities for their Fe-siderophore substrates, suggesting that reductive iron release is in many cases not specialized and involves already established enzymes with reductase activity. In contrast, there is another mechanism where specialized enzymes participate in iron release. This is mediated by Fe-siderophore hydrolysis, leading to a removal of the iron followed by reduction or by interaction with other cellular iron-binding components. However, hydrolytic iron release results in the destruction of the siderophore scaffold. Therefore, it is more cost-intensive to the cell than ferrisiderophore reduction that allows siderophore reutilization (Fig. 4) (Krewulak and Vogel 2008; Miethke and Marahiel 2007). In gram-positive bacteria due to a lack of outer membrane, the siderophore-iron complex is not uptaken into the cell, on the contrary, it is anchored to the TonB-machinery proteins, which allow the translocation of iron inside the cell, and the siderophore remains in the extracellular space, allowing reuse of it (Miethke and Marahiel, 2007). These are classical mechanisms of iron-uptake by siderophores with a nutritional role. However, in more recent studies, the capacity of siderophores to bind other elements besides iron has been explored, and the implications of this capacity can relate to other strategies.

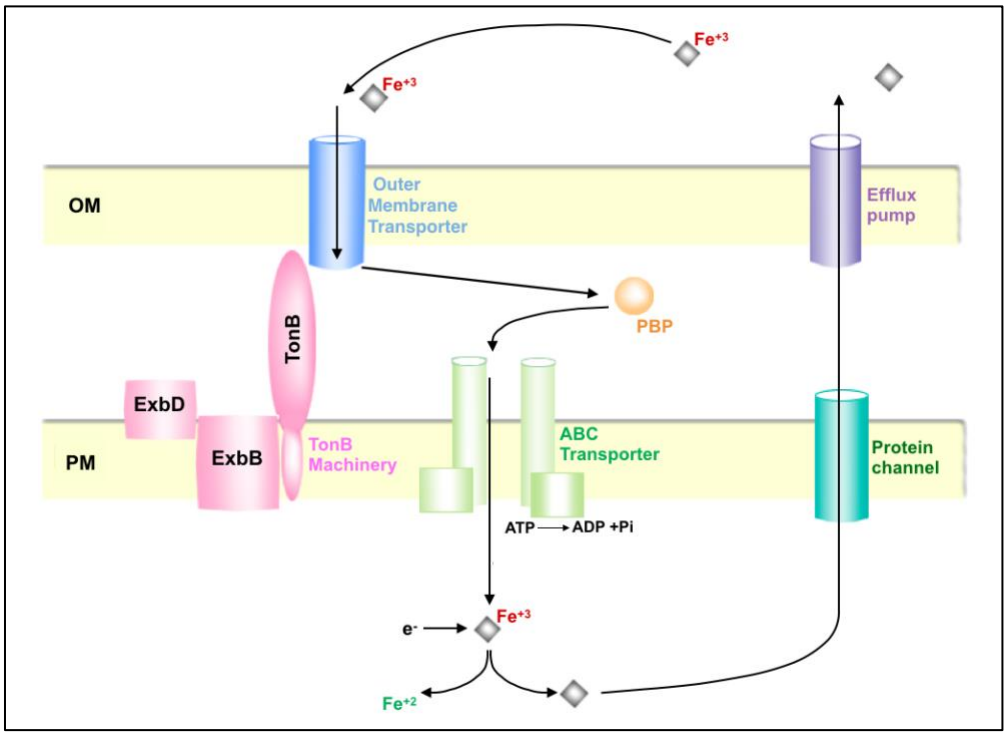

Figure 4.- Ferric iron uptake via siderophores in Gram-negative bacteria (modified from Schalk et al. 2011). The siderophore is represented by a gray diamond.

1.6. Bacterial siderophores bind several elements besides iron

Recently, several studies have reported that bacterial siderophores can have binding activity against several elements. This capacity makes siderophores extremely versatile molecules to be used in biotechnology, for example, as a carrier for antibiotics to battle the rising antimicrobial resistance developed by bacteria (Möllmann et al. 2009) or as biosensor, based on the ability of some siderophores to change their fluorescent profile when binding metals such as molybdenum (Duhme et al. 1996; Batey et al. 2007). In other applications, siderophores have been even used to chelate excess copper developed in Wilson disease, a liver related pathology (Huster 2010). Therefore, many researchers have focused their efforts to study the chelating capacity of siderophores against different metals/metalloids.

However, most of the reports explore chelating activity of siderophores against different elements from a chemical perspective, describing just the interaction between the chelators and different elements (Amin et al. 2007; Schmiederer et al. 2011; Mock et al. 2008), while their physiological role remains fairly unexplored. From a biological point of view, it has been suggested that besides their traditional role as iron scavengers for bacterial nutrition, the binding activity of

siderophores can be effective against several elements, participating in some cases in the uptake of other metals and even as a tolerance mechanism.

It has been described that bacterial siderophores are able to bind some potentially toxic elements such as copper, cobalt, cadmium and arsenic. However, in many cases, these reports only point at the binding capacity of these elements, and there is scarce information about the physiological implications of this phenomenon (Ahmed and Holmström 2014). Nevertheless, some authors have explored the capacity of siderophores to bind various compounds and also the biological implications of this interaction. For example, the Gram-negative bacterium *Azotobacter vinelandii*, produces azotochelin and azotobactin. These have the capacity of binding molybdenum and vanadium to be used as cofactor of a nitrogenase, which specifically requires these elements (Thomas et al. 2009). The role of siderophore in uptake of ligands different than iron for nutritional purposes has not been widely described, but this event sets precedent of the role of bacterial siderophores as more than just iron-chelators.

Other studies have explored the capacity of siderophores to act as a tolerance mechanism against toxic elements. It has been reported that the siderophores pyoverdine and pyochelin, produced by *Pseudomonas aeruginosa* PAO1 have the capacity of binding a wide range of toxic metals such as silver, aluminum, cadmium, cobalt, chrome, copper, europium, gallium, mercury, manganese, nickel, lead, tin, terbium, titanium and zinc, although, in this case, the metals are immobilized extracellularly and are not taken up into the bacterial cell (Fig. 5). This behavior is different from the classical Fe-siderophore uptake mechanism. Therefore, it is suggested to be a differential response, where these chelators can have a role in tolerance against toxic elements (Braud et al. 2010; Dimkpa et al. 2008; Dimkpa et al. 2009).

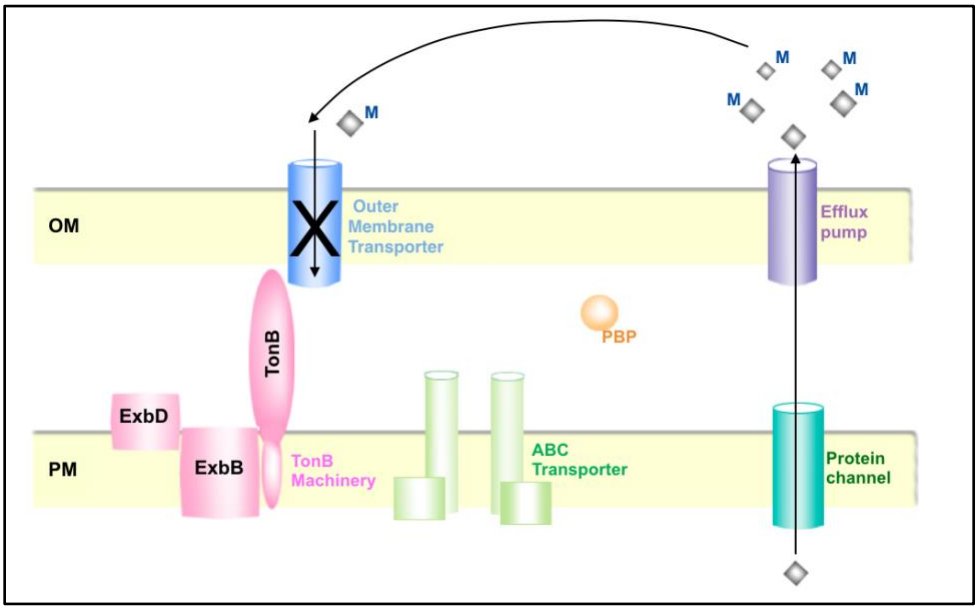

Figure 5.- Proposed arsenic tolerance mechanism by bacterial siderophores (modified from Schalk et al. 2011). The siderophore is represented by a gray diamond; M represents a toxic metal/metalloid.

Concerning the capacity of siderophores to bind arsenic, it has been described that an extracellular extract containing siderophores from *Pseudomonas azotoformans* can bind a wide range of metals, including arsenic, and can remove up to 93% of this metalloid when incubated with a contaminated soil (Nair, Juwarkar, and Singh 2007). However, the chemical nature of these arsenic chelating molecules has not been discussed in literature yet.

Other investigations have focused on the study of siderophore production by arsenic-tolerant bacteria. A correlation between siderophore production and high arsenic tolerance has been shown. This would provide siderophore producing bacteria with a competitive advantage against non-producing ones (Drewniak et al. 2008). In other studies, several bacterial strains isolated from the roots of the hyperaccumulator plant *Pteris vittata* were analyzed. It was observed that the isolates with the highest siderophore production presented also a high arsenic tolerance, in contrast with the non-producing bacteria which presented a lower tolerance level. This suggests once again that bacterial siderophores can be involved in tolerance against toxic elements, including arsenic (Ghosh et al. 2015).

Therefore, besides the current information which suggests the participation of bacterial siderophores in arsenic tolerance, there are still some unanswered questions. These include the description of chemical characteristics of the arsenic-binding compounds, which would allow to determine their similarities or differences with the traditional iron-chelating siderophores, and finally to determine their role in arsenic tolerance. From a biotechnological perspective this is

interesting, since siderophores have shown to be a useful tool in the industry (Amin et al. 2007; Schmiederer et al. 2011; Neubauer et al. 2000). In this work, it is proposed to study siderophore production and determine its relation with the classical arsenic-tolerance mechanisms. To achieve this, arsenic-tolerant bacteria were isolated from contaminated sites, then, arsenic-binding activity of siderophores was evaluated. In order to determine their structure, the compounds of interest were chemically characterized and, finally, the effect of arsenic in siderophore-production pathways was studied.

II. HYPOTHESIS AND AIMS

2.1 Hypothesis

Bacterial strains isolated from contaminated sites produce arsenic-binding siderophores as a tolerance mechanism.

2.2. Aims

2.2.1 General Aim

Evaluate the production and characterize arsenic-binding siderophores from tolerant bacteria, and determine their relation with arsenic tolerance.

2.2.2 Specific Aims

1.- Isolate arsenic tolerant bacterial strains.
2.- Setup a method to evaluate arsenic-binding activity of bacterial metabolites.
3.- Evaluate arsenic-binding activity of bacterial metabolites from arsenic-tolerant strains.
4.- Chemically characterize the arsenic-binding compound(s).
5.- Identify the effect of arsenic on the gene expression of siderophore-biosynthesis genes.

III. MATERIALS AND METHODS

3.1. Isolation of arsenic tolerant bacterial strains

3.1.1. Isolation, culture and processing of bacterial strains

Water samples used to isolate As-tolerant bacteria were collected from the mine-water purification plant Bad Schlema (Wismut GmbH), close to Aue, Germany. Total As content was in the range of 1.3–1.4 mg/L. Samples were streaked on modified ABM (2 g/L yeast extract, 5 g/L peptone, 5 g/L NaCl, 15 g/L agar) (Reddy et al. 2000), or Marine (1 g/L yeast extract, 5 g/L peptone, 0.1 g/L ferric citrate, 19.45 g/L NaCl, 8.8 g/L $MgCl_2$, 3.24 g/L Na_2SO_4, 1.8 g $CaCl_2$, 0.55 g/L KCl, 0.16 g/L $NaHCO_3$, 0.08 g/L KBr, 0.034 g/L $SrCl_2$, 0.022 g/L H_3BO_3, 0.004 g/L Na_2O_3Si, 0.0024 g/L NaF, 0.0016 g/L NH_4NO_3, 0.008 g/L Na_2HPO_4, 15 g/L Difco agar) plates supplemented with 1 mM $AsNaO_2$ at 30 °C for 48 h. Colonies were then separated individually based on morphology and cultured independently in their respective media. To narrow the tolerance range of the isolates, colonies were further selected in Lisogeny solid medium supplemented with 5 mM $NaAsO_2$ at 30 °C for 24 h.

To induce siderophore production, cells were grown in 100 mL of LB medium until reaching stationary phase. Then, cells were collected by centrifugation for 10 min at 10,000 g, washed three times with 0.9% NaCl to eliminate residual Fe, suspended in 100 mL of sterile Fe-free M9 medium, grown to an OD_{600} of 0.6 and inoculated into 1,000 mL of Fe-free M9 (Bosello et al. 2013; Vala et al. 2000) supplemented with 0.4% glucose. Cultures were incubated at 30 °C for 4 days with constant shaking at 180 rpm. Growth and siderophore production by *Rhodococcus erythropolis* S43, previously isolated and preliminarily designated "*Rhodococcus* sp. S43″ (Sultana et al. 2012), was conducted under similar conditions.

3.1.2. Determination of minimal inhibitory concentration

The minimal inhibitory concentration (MIC) of sodium arsenite $AsNaO_2$ [As(III)] and sodium arsenate Na_2HAsO_4 [As(V)] was determined for the four selected strains (here ATW) and *R. erythropolis* S43 using a micro-dilution method (Wiegand et al. 2008). Experiments were conducted in liquid Mueller-Hinton (Mueller and Hinton 1941) medium supplemented with arsenic ranging from 1 to 20 mM for As(III) and 5 to 1000 mM for As(V). Growth was evaluated by measuring turbidity of the cultures at an O.D. of 600 nm after a 24 h incubation at 30 °C with constant shaking.

3.1.3. Identification of bacterial strains

The taxonomic identification of the most tolerant strains was carried out by sequencing of the 16S rRNA gene. One colony of each isolate was directly used as a template for PCR. The 16S rRNA gene was amplified using the universal primers 27F (5′-AGAGTTTGATCCTGGCTC-3′) and 1387R (5′-GGGCGGNGTGTACAAGGC-3′) (Marchesi et al. 1998) under the conditions described by Ehinger et al. (2009). PCR products were purified and sequenced (Eurofins, Germany) by dideoxy chain termination/cycle sequencing using an ABI 3730XL sequencer. The sequences were compared with databases in GenBank using BLASTn and reference strains from Deutsche Sammlung von Mikroorganismen und Zellkulturen (DMSZ) to identify the closest matching sequences. A dendrogram based on the 16S rRNA gene sequence was constructed with the Maximum Likelihood method using bootstrap values based on 1000 replications (Sanderson 1989).

3.2. Setup of a method to evaluate arsenic-binding activity of bacterial metabolites

3.2.1. Setup of As-binding activity assay (As-$_m$CAS)

To evaluate As-binding activity of siderophore extracts, a Chrome Azurol S(CAS) assay replacing Fe(III) with As(III) was developed by modifying the concentration of the reagents and the pH used in the original CAS solution. The modified CAS solution (As-$_m$CAS) consisted of 300 µM CAS, 150 µM As(III) as $NaAsO_2$ (in 10 mM HCl), 1.5 mM HDTMA (Hexadecyltrimethylammonium bromide), and 16 mM PIPES (piperazine-N,N'-bis[2-ethanesulfonic acid]) buffer (pH 6.8). The pH of the solution was adjusted to 6.5 with HCl, and shown to be stable over the whole reaction time with methanol extracts. The As-$_m$CAS solution showed a maximum absorbance at 600 nm. The As-binding activity in siderophore extracts was therefore evaluated by measuring at this wavelength using a reference solution with methanol and a fully decolorized control using 83.3 mM EDTA (150 µL As-$_m$CAS solution + 50 µL 0.5 M EDTA and 100 µL methanol).

3.3. Evaluation of arsenic-binding activity of bacterial metabolites from arsenic-tolerant strains

3.3.1. Preparation of siderophore extracts

Siderophore extracts were prepared according to Bosello et al. (2013). To separate cells from the culture media, 1 L of a stationary-phase culture grown in M9 medium (as described in Section 4.1.1) was centrifuged for 30 min at 10,000 x g and 4 °C. The pH of each supernatant was adjusted to 6.0, and Amberlite® XAD-4 and Amberlite® XAD-7 were added to a final concentration of 5 g/L each, and a solid-phase extraction was performed. Then, the mixture was incubated for 2 h at room temperature. The Amberlite® phase was washed with Fe-free bidistilled water and eluted with 100 mL of methanol. The final extract was evaporated using a rotary evaporator at 37 °C. The completely dry extract was re-dissolved in methanol. For binding activity assays all extracts were adjusted to a final concentration of 1 mg/mL.

3.3.2. Evaluation of Fe-chelating and As-binding activity using CAS and As_m-CAS assays

Iron-chelating and As-binding activities were measured using the CAS assay (Schwyn and Neilands 1987) and As-$_m$CAS assay (as described in section 4.2.1), respectively. The traditional CAS assay uses chrome azurol S (CAS) in the presence of hexadecyltrimethylammonium bromide (HDTMA) as an indicator of chelating activity. The CAS/HDTMA complexed with ferric iron shows a blue color. When a strong iron chelator such as a siderophore removes iron from the dye complex, a decolorizing activity can be detected as a change of color from blue to orange. A quantitative estimation of siderophore activity was done by comparing the percentage of decolorization by the samples (150 µL CAS solution + 150 µL sample) versus a fully decolorized control using 16.7 mM EDTA (Titriplex ® III, Merck KGaA) (150 µL CAS solution + 10 µL EDTA 0.5 M and 140 µL methanol). Decolorization was measured at 630 nm against a fully colored reference (150 µL CAS solution + 150 µL methanol). If the extracts reached 100% decolorization, dilutions of them were made using methanol as solvent. Then, the true decolorization percentage was calculated by multiplying with the dilution factor. All reactions were measured in a microtiter plate after a 4 h incubation at room temperature. Fe-chelating activity was determined by calculating the percentage of CAS decolorization as compared to the calibration curve using the commercially available desferrioxamine B (DFOB) from 4 to 500 µM

(expressing the results in µM Eq of DFOB) (Alexander and Zuberer 1991). To evaluate arsenic-binding activity of the extracts the procedure was carried as explained in section 4.2.1. A DFOB calibration curve could not be made for As-$_m$CAS, due to the inability of DFOB to bind arsenic and thereby decolorize As-$_m$CAS.

The isolate which produced the extract with the highest arsenic-binding activity was selected for further studies comprising the chemical characterization of the binding compounds and the transcriptomic analysis.

3.3.3. Detection of siderophore-As(III) complex formation

To detect the interaction between siderophores and As(III) and to corroborate that As-$_m$CAS decolorization was the result of such interaction and not an effect of pH or unspecific decolorization of CAS, a modified version of the method was used to identify the absorbance spectra of the siderophore-metalloid complex (Shenker et al. 1995). Siderophore extracts (100 µL siderophore extract + 100 µL distilled water), As(III)-siderophore solution (100 µL siderophore extract + 100 µL 0.015mM $AsNaO_2$) and As(III) solution (100 µL 0.015mM $AsNaO_2$ + 100 µL bi-distilled water) were used to record the fluorescence spectra for the extracts at neutral pH. Emission spectra were obtained using an excitation wavelength of 275 nm and emission wavelengths ranging from 300 to 500 nm with a sequential increase of 5 nm. As a control for chelating activity, the siderophore-Fe spectra with the same siderophore extracts were recorded (100 µL siderophore extract + 100 µL 0.015mM $FeCl_3$) with an excitation wavelength of 248 nm and emission wavelengths ranging from 300 to 500 nm and a sequential increase of 5 nm. Photon detection was performed using an 80% of light recovery (Lee 2009).

3.4. Chemical characterization of arsenic-binding compounds

3.4.1.- Separation of compounds through thin layer chromatography (TLC)

Once the strain that produced the extracts with the highest arsenic-binding activity had been selected, a separation of the compounds via TLC was performed. The assays were carried out based on the method described by Memon (2005). Two TLC assays were made, the first one was revealed with 10% H_2SO_4 to observe all organic compounds present in the extract,

meanwhile, a second assay was revealed using 10% $FeCl_3$ to detect Fe(III) chelating compounds and identify, if one or more compounds showed siderophore-like activity.

Once the complexity of the extract had been determined, the Fe-chelating compound was isolated by mechanical removal of the silica band containing the compound and elution with 100% methanol. It was then submitted to infrared spectroscopy (IR).

3.4.2. IR spectroscopy of the TLC-isolated compound

The IR spectrum analysis of the isolated Fe-chelating compound was carried out using an FT-IR Spectometer equipment (PerkinElmer, USA). The isolated compound was dissolved in methanol and analyzed directly.

3.4.3. Purification of bacterial siderophores by column fractionation

In order to perform the chemical analysis of the Fe-chelating and As-binding molecules, an optimization of the culture conditions was performed. Cells were incubated using a 3 L bioreactor for 7 days under two different conditions, a first condition in M9 Fe-depleted medium, a traditional medium to obtain siderophore production, and a second condition in M9 Fe-depleted medium with addition of sodium arsenite in a concentration of 1/8 MIC for the selected isolate, to trigger production of As-binding metabolites, if these were different molecules. Siderophore extraction from supernatant was performed using a modified version of the protocol explained in section 4.3.1, switching the use of Amberlite® XAD-7 for Amberlite® XAD-16, since the latter showed a better yield of siderophore recovery. To purify siderophores from the other compounds contained in the extract, a fractionation protocol using a C18 reversed-phase Hypersep column (Thermo Scientific, Rockford, IL, USA) was performed. Each extract was dissolved in an aqueous solution of 20% methanol and then was pumped onto the fractionation column to allow siderophore binding. Six fractions of 10 mL volume each were eluted, with increasing methanol concentrations between 20 and 100%, representing 20%, 40%, 50%, 60%, 80% and 100% methanol fractions. Each one was centrifuged for 10 min at 10,000 g to sediment possible particles and then analyzed by HPLC. In parallel, all fractions were evaluated for Fe-chelating and As-binding activities using the CAS and As-$_m$CAS assays, respectively.

3.4.4. High performance liquid chromatography (HPLC) analysis of Amberlite fractions

To evaluate the purity of the fractions obtained from Amberlite, an HPLC analysis was performed for each one of them. HPLC runs were made by injecting 10 µL of each fraction into an U-HPLC Ultimate 3000-2015 chromatograph (ThermoFischer), equipped with a C18 Polaris 5 reversed-phase column from Agilent (5 µm; 25 x 4.6 cm), using an elution gradient of 20% to 95% methanol and 80% to 5% of 0.1% trifluoroacetic acid in deionized water (Fig. 6). Detection of absorbance peaks was performed using a Waters 2996 photodiode array detector (DAD). Chromatograms and absorbance spectra were recorded in all wavelengths between 200 - 800 nm, and results registered at 250 nm were used for the evaluation. Recovery of the liquid from absorbance peaks was possible using an automatic fractionation system Frac920. The As-binding and Fe-chelating activities of these recovered peaks was also evaluated using the As-$_m$CAS and the CAS assay, respectively. The peaks with As-$_m$CAS/CAS activity were used for the following chemical characterization studies.

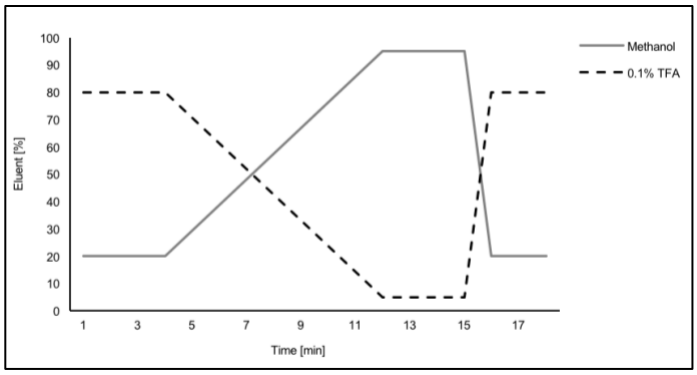

Figure 6.- Elution gradient of HPLC runs for evaluation of Amberlite fractions.

3.4.5. Nuclear magnetic resonance spectroscopy (NMR) and mass spectrometry (LC-MS) analyses of As-binding compounds

To determine the chemical structure of the As-binding compounds identified in the HPLC runs, NMR and LC-MS studies were performed. After HPLC analysis and determination of which fractions contained the purified (or most pure) siderophore with As-binding and Fe-chelating activity, all fractions were dried at 37ºC at reduced pressure using a rotary evaporator and

dissolved in deuterated dimethyl sulfoxide (d-DMSO) for the NMR analysis. An ^{1}H-NMR spectrum was performed for the most pure fraction of each culture condition. The analysis was made using a 500-MHz Bruker Advance III equipment.

To obtain the mass spectra, HPLC peaks with As-$_{m}$CAS and CAS activity were isolated in a separate run with injection of 100 µL of the most pure fraction of each culture condition. The isolated peaks were analyzed by Christoph Senges in the Chemistry department of Ruhr-Universität Bochum as a part of a collaborative work. Separation of the compounds present in the isolated peaks was performed in an elution gradient of water/acetonitrile/0.1% formic acid, using a C18 column. Mass spectra was obtained in positive mode in a Synapt G2-S HFMS equipment with an ESI source and TOF detector (Senges et al. 2018).

3.5. Identification of the effect of arsenic on gene expression of siderophore biosynthesis on a tolerant strain

To elucidate if arsenic-binding siderophores relate with classic arsenic tolerance mechanisms in the selected strain, a study of gene expression of the siderophore biosynthesis genes and arsenic-tolerance determinants was performed in absence and presence of arsenic stress.

3.5.1. Genome sequencing of arsenic-tolerant strain

After the arsenic-tolerant strain able to produce arsenic-binding siderophores with the best activity had been selected, genomic DNA was isolated for genome sequencing as described in Sambrook and Russel (2001). Protein-free, RNA-free, whole genomic DNA was used for the generation of genomic libraries. Paired-end libraries were sequenced using v3-v4 chemistry (Illumina) on the Illumina MiSeq sequencing platform, available in the Institute of Biosciences in TU-Freibeg, Germany. Then, genome assembly was performed using Edena (Hernandez et al. 2008). Identification of protein encoding sequences, as well as of tRNA and rRNA genes was made by automatic annotation using RAST 4.0 (http://rast.nmpdr.org/).

With the draft genome assembled and annotated, a metabolic reconstruction using the bioinformatic platforms Artemis Bioinformatics (http://www.sanger.ac.uk/science/tools/artemis), Metacyc (https://metacyc.org/), Kegg (http://www.genome.jp/kegg/) and SnapGene (http://snapgene.com) was made. In order to determine the arsenic-tolerance mechanisms and siderophore-production potential encoded in the bacterial genome, a search for classic arsenic

tolerance mechanisms (reductases, oxidases, methylases, etc.) and siderophore production pathways (NRPS) was performed.

3.5.2 Determination of expression of siderophore biosynthesis genes under arsenic stress

As a first step to the determination of the changes in the mRNA levels of arsenic-tolerance and siderophore biosynthesis genes in iron-depleting conditions, a RT-PCR of these determinants was performed in presence of iron, in order to know if iron-depletion was a necessary factor to trigger the translation of siderophore biosynthesis genes. RNA extraction was performed as indicated by Sambrook and Russel (2001) in cells cultured in 100 mL of M9 medium with addition of 40 µM of $FeCl_3$, and later stressed in presence of As(III) and As(V) for 1 h, 1.5 h and 2h, in a concentration of 1/8 of MIC which corresponds to 937 µM for As(III) and 31.35 mM for As(V). Retro-transcription was performed using the specific primers for the genes *htbG* (NRPS for heterobactin synthesis), *arsC* (arsenate reductase) and *16s rRNA* gene (Table S2) with the kit M-MuLV Reverse Transcriptase, by New England BioLabs. RT-PCR was carried out using GoTaq, Green Master Mix by PROMEGA. PCR cycle was performed in the following conditions: 30 s at 95°C and 30 cycles of 3 s at 95°C and 30 s at 60°C. Amplification of PCR products was evaluated by visualization in a 2% agarose gel with ethidium bromide (10 µL of Et-Br per 100 mL of agarose) and the relative level of transcripts was evaluated measuring the digital pixels of the electrophoresis bands, using the software My Image Analysis by Thermo Scientific.

To detect the effect of arsenic on the mRNA levels of siderophore biosynthesis genes and to elucidate whether these can be upregulated in a condition of arsenic stress, a transcriptomic study by RT-qPCR was performed. Cells were cultured in 100 mL of culture media as explained in 4.1.1. Three culture conditions were used for total RNA extraction, a control condition (M9 medium supplemented with $FeCl_3$ 40 µM), an iron-depleted condition to allow siderophore production (M9 iron-depleted medium) and an iron-depleted condition in presence of arsenic, to evaluate the effect of the metalloid on siderophore production (M9 iron-depleted medium with $NaAsO_2$ 937 µM). This last condition was also meant to allow to determine, if arsenic tolerance genes are transcriptionally active.

Total RNA extraction was performed using the commercial kit RNeasy® mini (Qiagen) and later quantified through photometric analysis. Quality and integrity were evaluated using an Agilent Bioanalyzer 2100 and a RNA 600 Nano kit (Agilent Techinologies), where the samples of total RNA with a RIN (RNA Integrity Number) above 7 were approved to be used in the study.

The synthesis of cDNA was performed using an AffinityScript qPCR cDNA Synthesis Kit (Agilent Technologies). Gene expression of *arsC* (arsenate reductase) as an arsenic-stress

marker, and *htbG* (NRPS for heterobactin production) were analyzed by quantitative reverse-transcriptase polymerase chain reaction (qRT-PCR) using a Kapa SYBR Green qPCR reaction kit (Kapa Biosystems). For details of specific primers used in each qRT-PCR experiment, see Table S2. All primer sets exhibited suitable efficiency as required for the comparative Ct(ΔΔCt) method (Table S3). Reactions were performed in 20 µL reaction volumes containing 10 µL of KAPA SYBR Fast qRT-PCR Master Mix 2X (Kapa Biosystems), 0.4 µL of each primer (at a concentration of 10 µM each), 0.4 µL of 50X ROX High, 7.8 µL of nuclease-free water, and 1 µL of cDNA. Quantification was carried out with a StepOne Real-Time PCR System (Applied Biosystems) using the following conditions: 30 s at 95°C and 40 cycles of 3 s at 95°C and 30 s at 60°C. Appropriate negative controls were included. For each gene expression analysis, three replicates were performed. The data were analyzed according to the comparative Ct(ΔΔCt) method and were normalized to the 16S rRNA (*R. erythropolis* S43) gene expression for each sample.

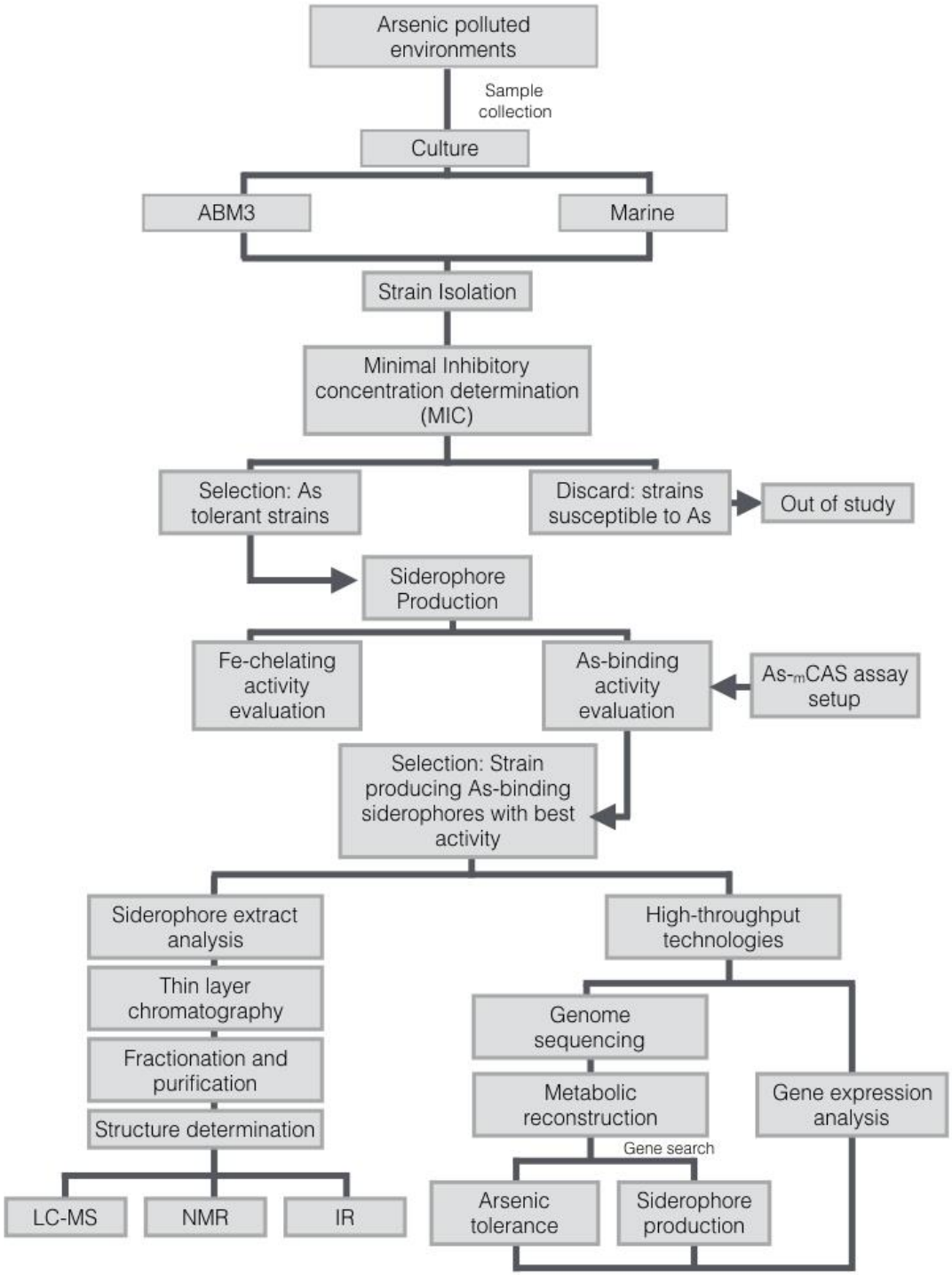

Figure 7.-Summary pipeline of Materials and Methods.

IV. RESULTS

4.1. Isolation of arsenic-tolerant bacterial strains

Most bacterial strains used in this study were isolated from arsenic-contaminated water obtained from a water-purification plant (Bad Schlema Wismut GmbH) close to Aue, Germany, where the total content of As in the water sample ranged from 1.3 to 1.4 mg/L at the moment of collection. After cultivation, and based on the morphological differences of the obtained colonies, 40 different strains were isolated. Of this total, based on their level of As tolerance 14 strains were selected and received the designation ATW (Arsenic Tolerant from Water) plus a number from 1 to 14 (Table S3, Supplementary Material).

The identification of the 14 isolates was carried out by amplification and sequencing of the 16S rRNA gene. The obtained nucleotide sequences were compared with the ones available in the NCBI database using BLASTn. Species assignments were made according to which type strain in the BLASTn search showed the most similar 16S rRNA gene. Of the 14 strain 4 were selected for more detailed analyses. For these, the queries were also compared with strains of the reference database DMSZ (Table S4, Supplementary Material) and used to performed a dendrogram to corroborate the classification (Figure S2, Supplementary Material). All 4 were identified as belonging to the phylum Actinobacteria, specifically ATW1 to *Rhodococcus erythropolis* (K5476725.1), ATW2 and ATW3 to *Arthrobacter oxydans* (NR_026236.1) and ATW4 to *Kocuria rosea* (NR_044871.1). In addition, this analysis included the strain *Rhodococcus erythropolis* S43 (KM047507.1), a partially characterized strain which had previously been isolated from an upper-soil horizon sample with high arsenic content taken at the “Rauchblöße”, Muldenhütten, an old smelting site close to Freiberg, Germany (Sultana et al. 2012).

The arsenic tolerance level of these five strains was determined experimentally by determination of the minimum inhibitory concentration (MIC) for As(III) as $NaAsO_2$, and As(V) as Na_3AsO_4 (Table 3). This study revealed that the isolated strains possess a moderate level of arsenic tolerance, with exception of the strain *A. oxydans* ATW3, which according to the nomenclature of Pandey and Bhatt (2015) has a high tolerance level to arsenite.

Table 3.- Minimal inhibitory concentration (MIC) values of five of the environmental strains against arsenite and arsenate. The selected strains for siderophore production are highlited in bold.

Isolate	Microorganism	MIC AsIII (mM)	MIC AsV (mM)	Isolation medium	Genbank accession number
ATW1	***Rhodococcus erythropolis***	**7.5**	**250**	**ABM**	**MH029266**
ATW2	***Arthrobacter oxydans***	**6.0**	**500**	**Marine**	**MH028755**
ATW3	***Arthrobacter oxydans***	**10.0**	**500**	**Marine**	**MH028873**
ATW4	***Kocuria rosea***	**5.0**	**500**	**Marine**	**MH028608**
ATW5	*Arthrobacter sulfureus*	5.0	500	ABM	MH031276
ATW6	*Arthrobacter sulfureus*	5.0	500	ABM	MH037148
ATW7	*Rhodococcus erythropolis*	5.0	500	ABM	MH029273
ATW8	*Acinetobacter radioresistens*	5.0	250	ABM	MH028636
ATW9*	*Microbacterium foliorum*	15.0	500	ABM	MH029158
ATW10*	*Microbacterium foliorum*	15.0	500	ABM	MH029237
ATW11	*Chryseobacterium koreense*	7.5	125	ABM	MH029144
ATW12	*Alcaligenes* sp.	7.5	250	ABM	MH029897
ATW13	*Rhodococcus* sp.	7.5	500	Marine	MH029274
ATW14	*Chryseobacterium* sp.	5.0	500	ABM	MH029145
S43	***Rhodococcus erythropolis***	**7.5**	**250**	**-**	**-**

* Bacteria not selected due to insufficient growth after 48 h.

4.2. Setup of an As-binding activity assay (As-$_m$CAS)

In order to develop an assay to evaluate the As-binding capacity of bacterial siderophores, modifications to an existent colorimetric assay had to be made. A modified version of the CAS assay (Schwyn and Neilands 1987) replacing Fe (III) with As (III) was set up. To achieve the new protocol which was named As-$_m$CAS, it was necessary to modify the concentrations of the reagents and the pH of the original CAS solution. The modified solution contained the following reagents, 300 µM Chrome azurol S, 150 µM As(III) in the form of $NaAsO_2$ (in 10 mM HCl), 1.5 mM HDTMA and 16 mM PIPES buffer (pH = 6.8). The pH of the solution was adjusted to 6.5 with HCl.

This method was used to measure As-binding activity of siderophore extracts using methanol as eluent. To perform the assay, the conditions described by Schwyn and Neilands (1987) were also modified. In this case, methanol without siderophore was used as fully colorized reference for 0% of As-binding activity (150 µL As-$_m$CAS solution + 150 µL methanol). For a fully decolorized reference, 83.3 mM EDTA (150 µL As-$_m$CAS + 50 µL 0.5 M EDTA and 100 µL methanol) was used as a complete decolorization control of 100% As-binding activity. To

determine the best photometric measurement condition, absorbance spectra were studied for both controls. The fully colorized As-$_m$CAS solution showed a maximum absorbance at 600 nm, while the fully decolorized solution showed its minimum absorbance at the same wavelength. This generates a range adequate for measurements for sample screening, this spectra and an image of the fully-colorized and fully-decolorized Asm-CAS solutions are available in Figure S3, (Supplementary Material). The solution showed stability through an incubation time of 4h, so the decolorization obtained at the end of such a period is a product of the As-binding activity of the extracts (or of the EDTA for the controls) and not of a spontaneous discoloration of the CAS dye.

This method has shown to be reproducible, economical and fast to screen As-binding activity of siderophores. The protocol of As-$_m$CAS and other results from this work have recently been published (Retamal-Morales et al. 2018).

4.3. Evaluation of arsenic-binding activity of siderophores from arsenic-tolerant strains

4.3.1. Evaluation of Fe(III)-chelating and As(III)-binding activity of bacterial siderophores

To evaluate Fe(III)-chelating and As-binding activity of the siderophores contained in methanol extracts obtained from the arsenic-tolerant isolates, the CAS and the As-$_m$CAS assays were used as screening methods. The Fe(III)-chelating activity of each of the extracts is shown in Figure 8. It is observed that all the extracts presented Fe(III)-chelating activity. However, the activity on ferric iron was characteristic for each tested strain. In this assay two groups are recognizable, one with high chelating capacity showing a percentage of activity over 100% (103-118%) (*Rhodococcus erythropolis* ATW1, *K. rosea* ATW4, and *A. oxydans* ATW2), and a group of intermediate Fe(III)-chelating capacity with decolorization percentages between 39 and 65% (*A. oxydans* ATW3 and *Rhodococcus erythropolis*, S43), compared with the decolorization obtained by EDTA.

Regarding the As(III)-binding capacity, all evaluated strains showed a high activity against the metalloid in a range from 82 to 123% (Fig. 9). Among all the tested strains, *A. oxydans* ATW3 and *R. erythropolis* S43 showed the highest As(III)-binding activity, reaching above 100% of activity compared to the decolorization obtained with EDTA and differing from their Fe(III)-chelating activity which was intermediate.

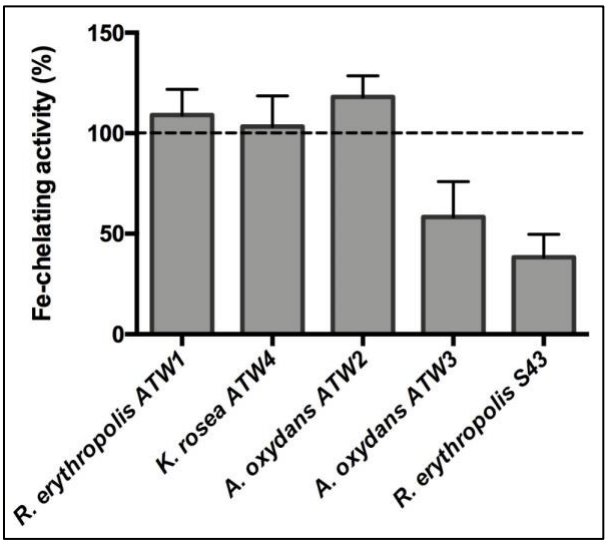

Figure 8.-Evaluation of iron-chelating activity in siderophore extracts. The iron-chelating activity was determined for siderophore extracts from the isolated actinobacterial strains grown under iron-limiting conditions. Data represent the average and standard deviation of three independent experiments. Bars represent percentages of CAS decolorization. EDTA was used as a reference for decolorization (100% chelating activity).

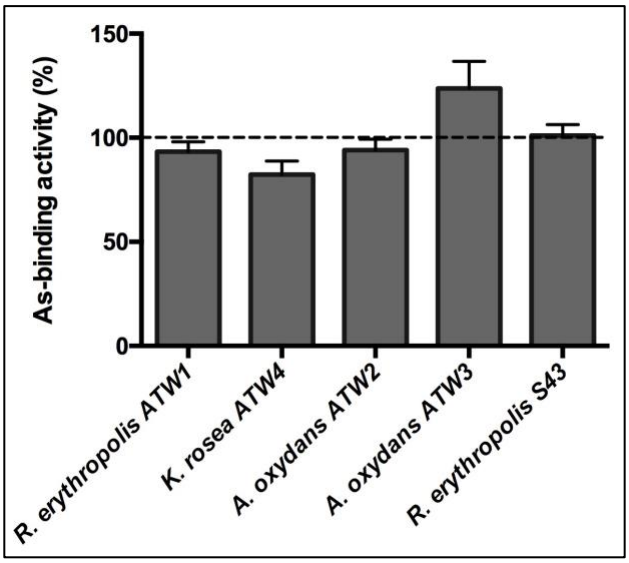

Figure 9.- Evaluation of arsenic-binding activity in siderophore extracts**.** The same extracts used for iron chelating activity (as shown in Fig. 8) were used to determine also arsenic-binding activity. Data represent the average and standard deviation of three independent experiments. Bars represent percentages of As-$_m$CAS decolorization. EDTA was used as a reference for decolorization (100% binding activity).

Since the final aim of this work was to determine the chemical nature of the As(III)-binding siderophores and to elucidate how these are related to metalloid tolerance, chemical characterization and genetic expression studies were performed using the strain with the best As(III)-binding activity. At this point in the study it was unknown if the Fe(III)-chelating and As(III)-binding activities were performed by the same compound or not. Since the strains *A. oxydans* ATW3 and *R. erythropolis* S43 showed the highest As-binding activity, a way to select only one of them, was to calculate the ratio between the As(III)-binding and Fe(III)-chelating activity, to prioritize the first one in case this phenomenon is mediated by the same molecule. *A. oxydans* ATW3 has a ratio of 2.32; while the strain *Rhodococcus erythropolis* S43 has a ratio of 2.58. Thus, the strain selected for the following analyses of chemical characterization of siderophores and subsequent transcriptomic analysis was *Rhodococcus erythropolis* S43.

4.3.2. Detection of siderophore-As(III) complex formation

In parallel, to determine if the As(III)-binding activity of siderophores, measured through the As-$_m$CAS assay is a product of the siderophore-As(III) interaction and not of a non-specific decolorization of CAS, an assay based on the capacity of the siderophores to emit fluorescence was performed. The fluorescence spectrum of the extracted siderophores in the presence of As(III) was compared to a siderophore solution without As and to an As(III) solution, in the form of sodium arsenite (Del Olmo et al. 2003). As a positive control, a fluorescence spectrum of the siderophore-Fe(III) complex was recorded by using the same siderophore extracts obtained from the strains under study.

In Figure 10 and Figure 11, the emission spectra of the extracts from each arsenic-tolerant strain are shown, in comparison with the fluorescence emission spectra of the siderophore-arsenic and siderophore-iron complex, respectively. In presence of arsenic an increase in the fluorescence peak at the maximum emission wavelength was observed for all analyzed siderophore extracts, compared with the fluorescence emitted by the siderophores without addition of the metalloid, similarly as it happens with iron. Interestingly, for the strains *R. erythropolis* ATW1 and *A. oxydans* ATW3, the fluorescence spectrum of the free siderophore presented an almost imperceptible maximum. In addition, it can be observed that for the strain *A. oxydans* ATW2, the intensity of the fluorescence of the siderophore-As complex is approximately ten times higher than for the other isolates. These results show that the fluorescence emission spectrum of the siderophores is particular for each strain and in this sense, a useful method to determine that there is interaction between extracted siderophores and As (III).

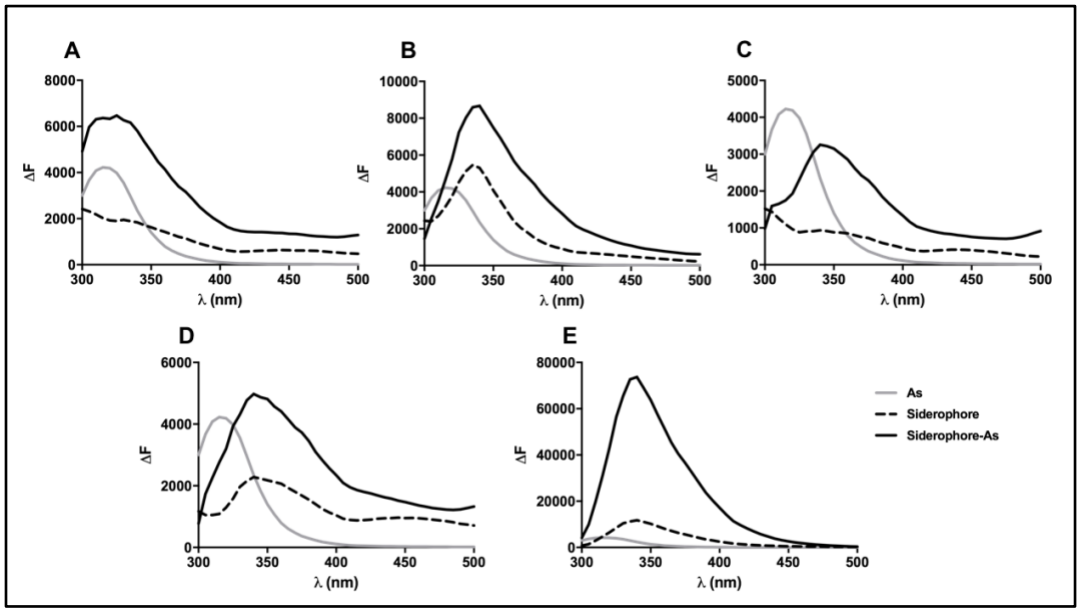

Figure 10.- Detection of siderophore-As(III) complexes by fluorescence emission spectra. The graphs show the fluorescence emission spectra of the siderophore-As(III) complex (black line), of the siderophore alone (black dashed line), and of As(III) (grey line) for each actinobacterial strain. A) *Rhodococcus erythropolis* ATW1, B) *Kocuria rosea* ATW4, C) *Arthrobacter oxydans* ATW3, D) *Rhodococcus erythropolis* S43 and E) *Arthrobacter oxydans* ATW2.

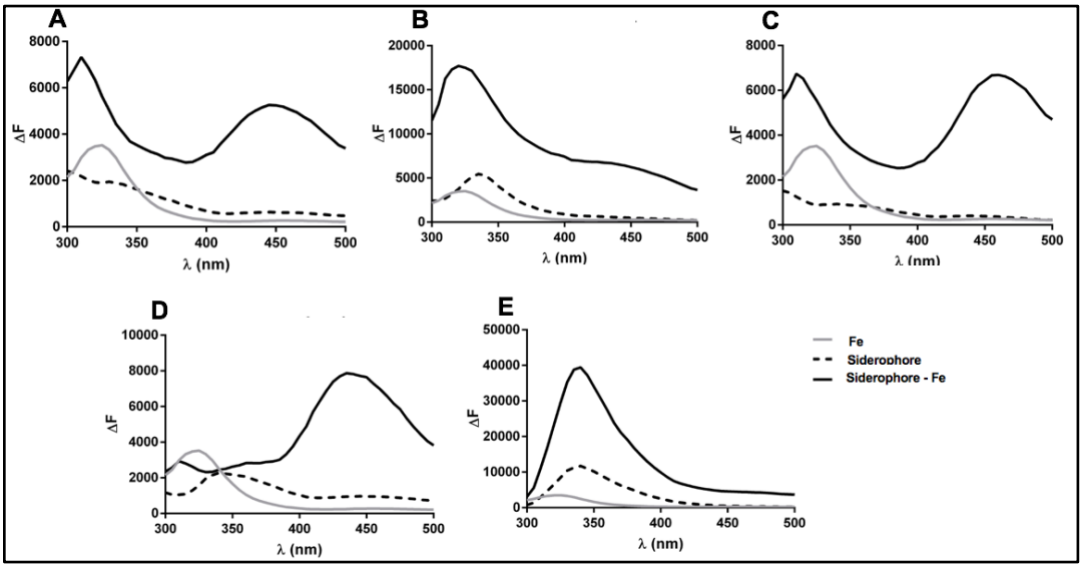

Figure 11.- Detection of siderophore-Fe(III) complex by fluorescence emission spectra. Graphs show the fluorescence emission spectrum of siderophore-Fe(III) complex (black line), siderophore alone (black dashed line) and Fe(III) (grey line) for each actinobacterial strain. A) Rhodococcus erythropolis ATW1, B) Kocuria rosea ATW4, C) Athrobacter oxydans ATW3, D) Rhodococcus erythropolis S43, E) Arthrobacter oxydans ATW2.

4.4. Chemical characterization of arsenic-binding siderophores

4.4.1. Extract separation using thin-layer chromatography (TLC)

In order to determine the complexity of the extract of *R. erythropolis* S43 which contained the Fe(III)/As(III) binding siderophores, and to separate the components of it, a thin-layer chromatography was carried out using silica sheets and elution with dichloromethane-methanol in a ratio 9:1 on 1 mg of dry weight of siderophore extract dissolved in methanol. After the chromatographic separation process the compounds were observed by illumination with UV light at 254 nm and 365 nm and subsequently a development with 10% H_2SO_4 was performed to visualize all the compounds present in the extract. Finally, a different plate was developed with 10% $FeCl_3$, which was used as an indicator of Fe(III)-chelating activity. As seen in Figure 12, a single band with Fe(III)-chelating activity was obtained, which showed a retention factor (R_f) of 0.436 and blue fluorescence in both wavelengths observed.

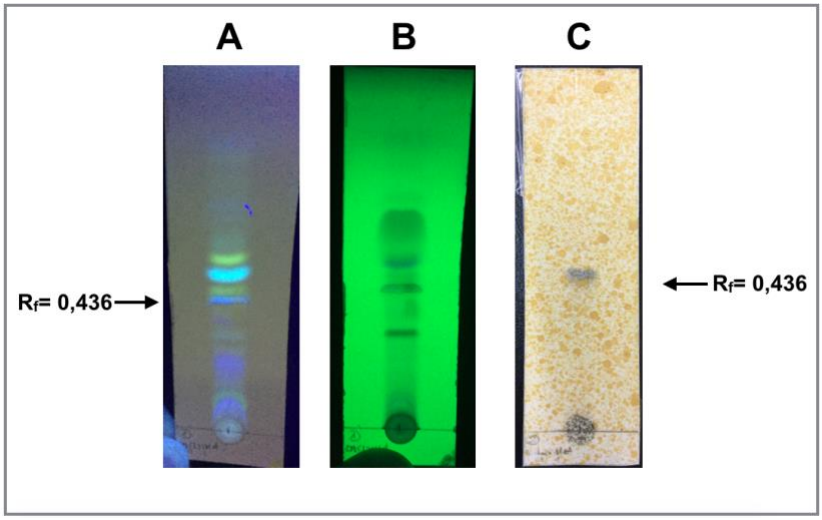

Figure 12.- Thin layer chromatography (TLC) of siderophore extract from *R. erythropolis* S43. 1 mg of siderophore extract was deposited on an aluminum-based silica plate. The band indicated with an R_f value of 0.436 corresponds to the compound(s) with Fe(III)-chelating activity. A) Visualization with fluorescence displayed with excitation at 365 nm. B) Visualization with fluorescence displayed with excitation at 254 nm. C) Development with 10% $FeCl_3$.

4.4.2. IR spectroscopy of the TLC-isolated compound

To elucidate the functional groups that are present in the compound(s) with Fe(III)-chelating activity observed through TLC (Section 4.4.1), an infrared-spectral analysis of the band of interest was carried out. In order to perform this, a new TLC plate was run and the silica of the band containing the compound with an R_f value of 0.436 was removed. Then, the chelating compound was eluted with methanol and used directly to determine its IR profile. This analysis (Fig. 13) suggested the presence of some of the classical groups found in siderophores (Miethke and Marahiel 2007). A wide zone of low intensity at 3400 cm^{-1} indicated the presence of hydroxyl groups (-OH), which could be indicative of the catechol or phenol groups, classical functional groups with Fe(III)-chelating capacity in siderophores. This interpretation is consistent with a peak observed at a wave number of 1600 cm^{-1}, which is an indicator of aromatic rings. Finally, a peak of transmittance at 2900 cm^{-1} indicates the presence of alkyl chains, which could correspond to the hydrocarbon skeleton of the siderophore.

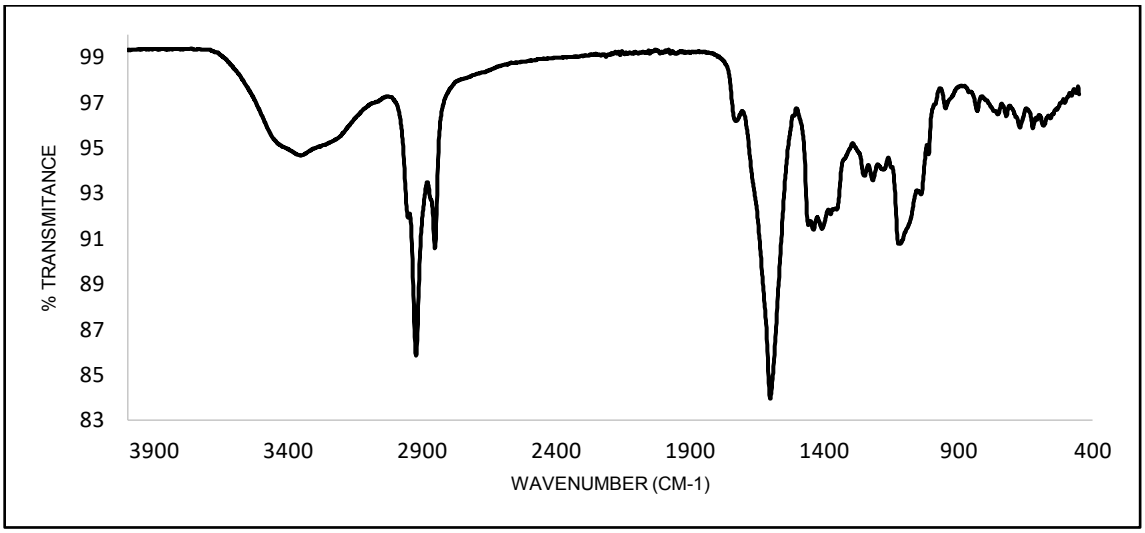

Figure 13.- Infrared spectrum of the Fe(III)-chelating compound with Rf value of 0.436 during purification by TLC, after elution with methanol.

4.4.3. High performance liquid chromatography (HPLC) analysis of extract fractions

According to the results obtained in 4.4.1 and 4.4.2, the compound of interest was contained in a complex extract, and its quantity proved to be insufficient to perform more specific chemical characterization assays, rising the necessity of improving the siderophore recovery. In order to optimize the yield and purification of the chelating metabolites and to be able to perform structure analyses of the compound(s) of interest, a new culture method was established using a bioreactor with continuous stirring and air injection. Also, a fractionation protocol for the extracts was set up. These methods were carried out with new cultures in Fe-free M9 medium (control condition) and Fe-free M9 medium supplemented with 937 µM sodium arsenite. The latter corresponded to 1/8 of the MIC and was added in order to determine if the addition of As (III) triggers the production of As-binding siderophores with different chemical characteristics compared with those detected under the control condition.

The siderophore extracts were fractionated using a C18 Hypersep column (Thermo Scientific) as indicated in Materials and Methods. Tables 4 and 5 show the purification steps and the CAS and As-$_m$CAS activities of the extraction and fractionation process. For the fractions obtained from Fe-free M9 medium, the best Fe-chelating and As-binding activity was observed in the fraction eluted in 80% of methanol, while for the fractions obtained from Fe-free M9 medium supplemented with As(III) the best Fe-chelating and As-binding activity was obtained at a concentration of 60 % methanol. Later, HPLC analyses with linear gradients were carried out in all the fractions. However, when choosing the fractions for the chemical analyzes, only those with the highest CAS and As-$_m$CAS activity were used. Therefore, the selected fractions used for the following chemical characterization were the ones obtained at 80% for the extract obtained from culture in M9 medium and 60% methanol for the extract obtained from a culture carried out in M9 medium with As (III) (Fig. 14).

Table 4.- Fractionation of siderophore extracts obtained from *R. erythropolis* S43 in iron-free M9 medium. Extracts were obtained from a seven-day incubation using a 3 L bioreactor. Stepwise fractionation was obtained with fixed 10 mL volume of methanol from 20% to 100%. Fold increase evaluated in comparison with 100% decolorization achieved with EDTA. All activity, concentration and yield values are average values of two replicates of 3-L extractions. Values for Mm DFOB Eq were calculated using a DFOB calibration curve (Figure S3).

Siderophore extract in Fe-free M9						
Purification step	**Fraction**	**Fraction volume (mL)**	**CAS activity (fold)**	**As-$_m$CAS activity (fold)**	**Concentration (mM [DFOB]Eq)**	**Yield (%)**
Supernatant collection	**Crude extract**	3000	1.1	85	160.9	100
XAD Extraction with MeOH elution	**XAD Extract**	300	57	705	6.5	405
HyperSep C18 Fractionation	**20% MeOH**	10	0	0	0	0
	40% MeOH	10	0.23	0.49	1.1	2.2
	50% MeOH	10	3.5	0.95	1.2	2.5
	60% MeOH	10	5.9	10.1	4.5	9.3
	80% MeOH	10	44	10.8	10.4	21.6
	100% MeOH	10	7.2	0.90	2.1	4.3

Table 5.- Fractionation of siderophore extracts obtained from *R. erythropolis* S43 in iron-free M9 medium supplemented with As(III) as sodium arsenite. Extracts were obtained from a seven-day incubation using a 3 L bioreactor. Stepwise fractionation was obtained with fixed 10 mL volume of methanol from 20% to 100%. Fold increase evaluated in comparison with 100% decolorization achieved with EDTA. All activity, concentration and yield values are average values of two replicates of 3-L extractions. Values for Mm DFOB Eq were calculated using a DFOB calibration curve (Figure S3).

Siderophore Extract M9 +As(III) 937µM						
Procedure	**Step**	**Fraction volume (mL)**	**CAS Activity (fold)**	**As-$_m$CAS Activity (fold)**	**Concentration (mM [DFOB]Eq**	**Yield (%)**
Supernatant collection	**Crude Extract**	3000	0.90	100	0.09	100
XAD Extraction with MeOH elution	**XAD Extract**	300	33.6	80.9	4	401.7
HyperSep C18 Fractionation	**20% MeOH**	10	0.99	0.94	14.5	4.9
	40% MeOH	10	12	2.52	15.3	5.1
	50% MeOH	10	13	14	19.8	6.6
	60% MeOH	10	38	8.4	24	7.9
	80% MeOH	10	16.1	1.8	10.1	16.2
	100% MeOH	10	19	0.41	12	0.074

The chromatograms obtained by HPLC of the fractions are shown in Figure 14. Regarding the fractions obtained from Fe-free M9 medium, Figure 14A shows the chromatogram of the compounds obtained in 60% methanol elution. The analysis shows multiple absorbance peaks, but one principal peak at retention time 9.6 min, that when tested for Fe(III)-chelating activity and As(III)-binding activity using CAS and As-$_m$CAS assay, respectively, turned out to have no chelating capacity, therefore did not contain siderophores. A group of peaks observed around 12 min retention time was isolated and tested using CAS and As-$_m$CAS assay as well, these peaks presented both arsenic and iron-chelating activities. Therefore, it is suggested that the siderophore(s) of interest must be contained in this retention time. Figure 14B corresponds to the HPLC run of the compounds obtained in the fraction eluted at 80% methanol. Here, only one principal peak was found at retention time 11.8 min, which showed Fe(III)-chelating and As(III)-binding activity (Table 6). Therefore, it is suggested that in the extract obtained from Fe-free M9 medium the siderophore(s) of interest is(are) contained in this single peak.

Meanwhile, Figure 14C shows the chromatogram of the 60% methanol fraction for the extract obtained from Fe-free M9 medium supplemented with 937 µM of As(III). Just as in the previous condition a high intensity absorbance peak was observed at the retention time 11.8 min. However, a new peak with lower intensity was recorded at retention time 10.5 min, which was not observed in the culture in Fe-free M9 medium without As(III). Both peaks were recovered and their chelating capacity of iron and arsenic was evaluated. As indicated in Figure 14C and summarized in Table 6, the absorbance peak at 10.5 min did not show chelating activity, while the one obtained at retention time 11.8 min presented Fe(III)-chelating and As(III)-binding activity. Figure 14D shows the HPLC run of the compounds obtained in the fraction eluted at 80% methanol where the same principal peak at retention time 11.8 min is the one with the activity of interest. Nevertheless, in this fraction the intensity of this peak is lower, which correlates with the Fe(III)-chelating and As(III)-binding activity values presented previously in Table 5. Finally, as observed in the control condition, the compound(s) contained in the absorbance peak which eluted at 11.8 min seem(s) to be the one(s) containing the siderophore(s) of interest.

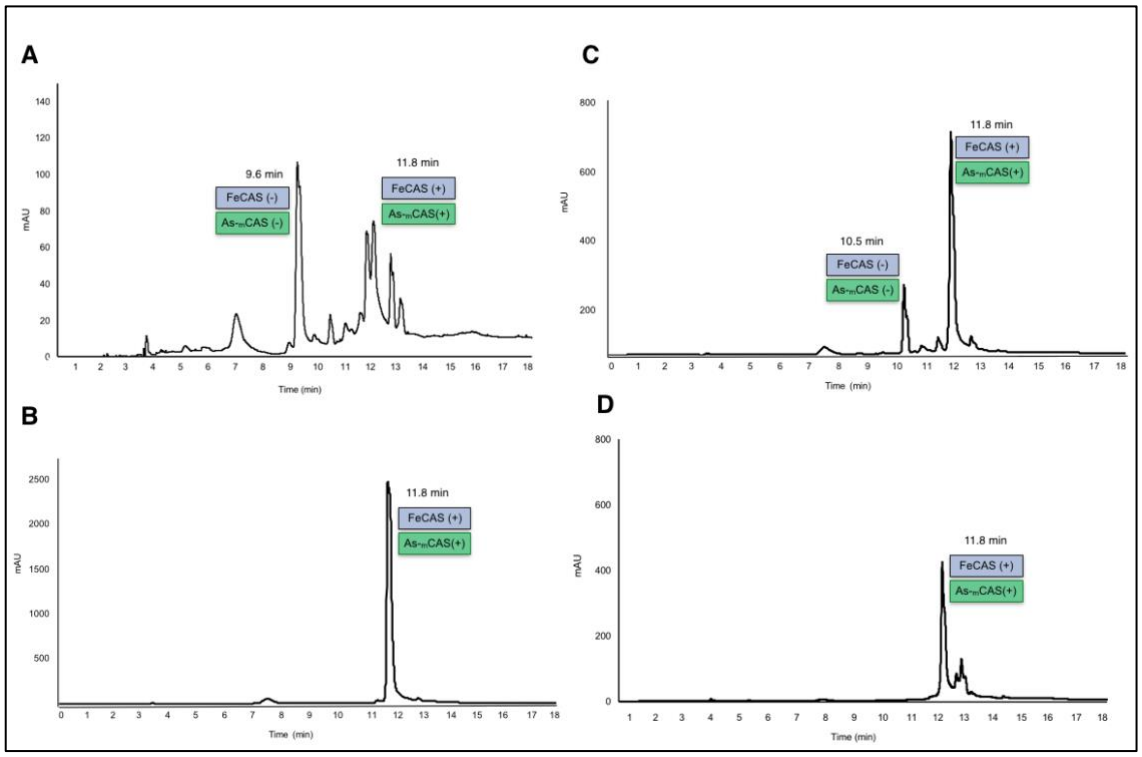

Figure 14.- HPLC analyses of fractions with highest CAS /As-$_m$CAS activity. Blue squares with a black "+" indicate Fe-chelating activity detected on the peaks and with a black "-" indicate that the activity test was performed, but was negative, Green squares with a black "+" indicate As-binding activity detected on the peaks and with a black "-" indicate that the activity test was performed, but was negative. Analyses were performed with a linear methanol gradient as shown in Figure 6 for the following fractions of the preparative C18 HyperSep runs shown in Tables 2 and 3: (A) 60% methanol fraction from culture obtained from Fe-free M9 medium, (B) 80% methanol fraction from culture obtained from Fe-free M9 medium, (C) 60% methanol fraction from culture obtained from Fe-free M9 medium and sodium arsenite, (D) 80% methanol from culture obtained from Fe-free M9 medium and sodium arsenite.

Once the elution profile of the Fe(III)-chelating and As(III)-binding siderophores had been detected by HPLC, a study of the absorbance spectra of the compounds of interest was carried out, so the absorption properties of these compounds could be compared. The spectra of the peaks obtained at retention time of 11.8 min for the iron-depleted (M9 medium) and the iron-depleted and arsenic-augmented (M9 + As(III)) conditions were analyzed. Figure 15 shows a comparison between the absorbance spectra of these peaks and previously reported absorbance spectra of the siderophore heterobactin (in its A and S1 forms). The absorbance spectrum of heterobactin has been described previously (Bosello et al. 2013) and shows a single maximum absorbance around 300 nm. For both conditions, a single maximum of absorbance was observed. The similarity between the absorbance spectra described for heterobactin and those obtained in the extracts under study strongly suggests that these could contain this type of siderophore.

Table 6.- Evaluation of Fe(III)-chelating and As(III)-binding activity of absorbance peaks obtained by HPLC.

Condition	Fraction	Retention Time (min)	CAS activity	As-$_m$CAS activity
Fe-free M9	60% methanol	9.6	-	-
		11.8	+	+
	80% methanol	11.8	+	+
Fe-free M9 + As(III) 937 µM	60% methanol	10.5	-	-
		11.8	+	+
	80% methanol	11.8	+	+

After the HPLC analysis, the peaks of interest that showed Fe(III)-chelating and As(III)-binding activity were recovered, and used for the next stage of chemical characterization by LC-MS. In parallel, the fractions with the best activity (80% methanol from Fe-free M9 medium and 60% methanol from Fe-free M9 medium supplemented with sodium arsenite) were dried and dissolved in d-DMSO for NMR analysis.

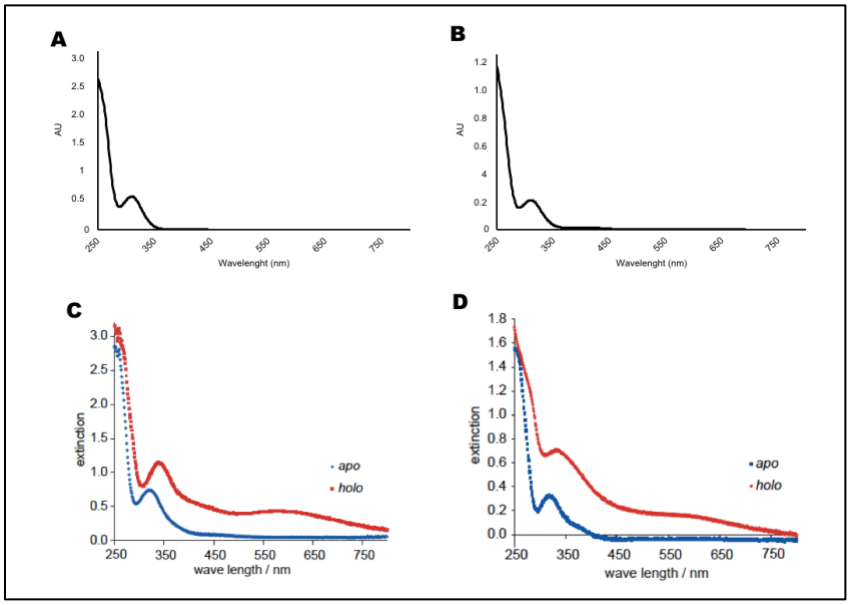

Figure 15.- Comparison of absorbance spectra of CAS/As-$_m$CAS active peaks obtained from HPLC and heterobactins absorbance spectra. (A) Absorbance spectrum of the principal peak with retention time 11.8 min obtained from the culture in Fe-free M9 medium. (B) Absorbance spectrum of the principal peak with retention time 11.8 min obtained from Fe-free M9 medium supplemented with sodium arsenite. (C) Absorbance spectrum of the siderophore heterobactin A, with red line representing the siderophore with bound Fe(III) and blue line representing the siderophore alone (Bosello et al. 2013). (D) Absorbance spectrum of siderophore heterobactin S1 with red line representing the siderophore with bound Fe(III) and blue line representing the siderophore alone (Bosello et al. 2013).

4.4.4. Nuclear magnetic resonance spectroscopic (NMR) and mass spectrometric (LC-MS) analyses of As-binding compounds

To determine the structure of the compounds with Fe(III)-chelating and As(III)-binding activity contained in the HPLC peaks, ^{1}H-NMR spectroscopic and mass spectrometric (MS) studies were performed for the fractions with the highest activity from both culture conditions. The ^{1}H-NMR analysis was made at the Central Analysis Unit of the University of Freiberg, Germany; while the MS analysis was carried out in the Institute of Applied Microbiology of the University of Bochum, Germany.

To this date, the ^{1}H-NMR spectra of heterobactin A and B have been previously reported and described (Bosello et al. 2013; Carrano et al. 2001), and in these studies the proton signals have been assigned to the amino acids and acids fragments that conform with the heterobactin structure. The ^{1}H-NMR spectroscopic analysis performed for the fractions with the best activity showed high similarity for both culture conditions (Fe-free M9 medium and Fe-free M9 medium

supplemented with $NaAsO_2$), suggesting the presence of the same principal compound, regardless of the additional presence of arsenic stress. The NMR spectrum of this principal compound from the arsenic-supplemented culture can be seen in Figure 16.

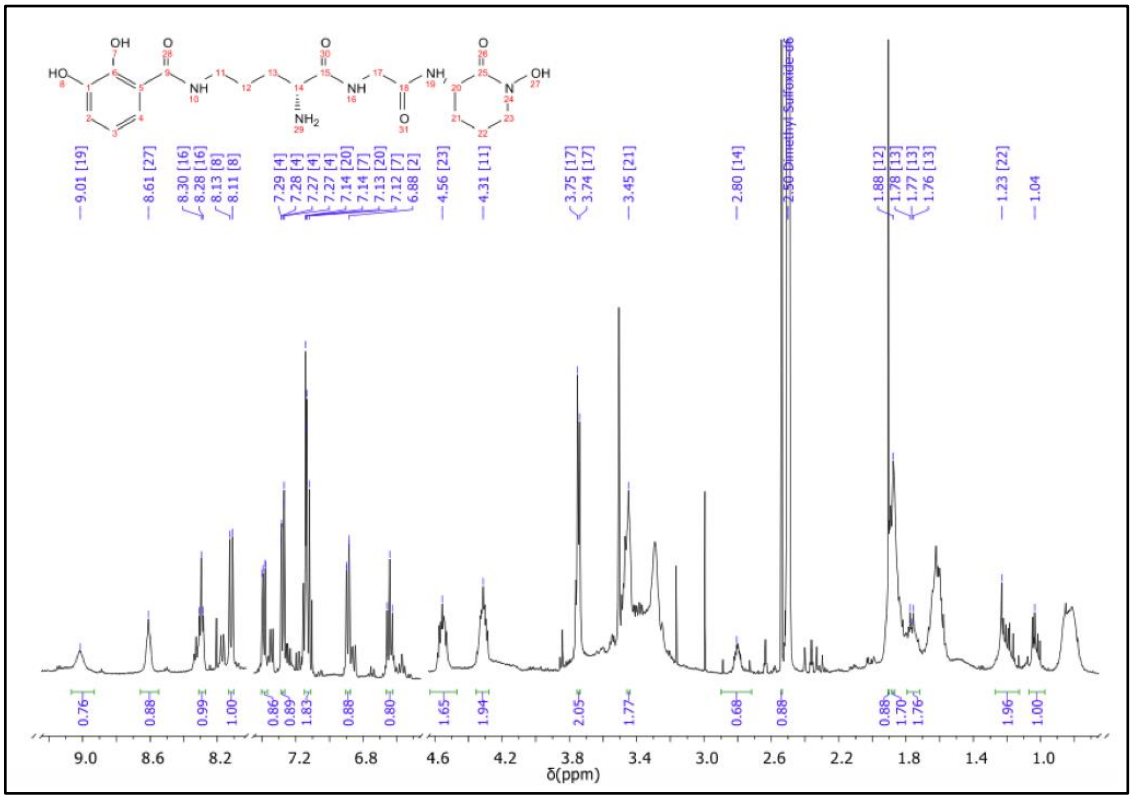

Figure 16.- ^{1}H-NMR spectrum in d6-DMSO of the 60% methanol extract fraction with CAS / As-$_{m}$CAS activity. The spectrum was obtained from the culture in Fe-free M9 medium with 937 µM sodium arsenite. The ^{1}H-NMR spectrum of the 80% methanol fraction from normal Fe-free M9 medium (without arsenic) turned out to be highly similar (Figure S4, Supplementary material).

In order to maintain the data interpretation consistent with the currently published studies, the analysis of the sample was performed by segmenting the molecule into amino acids and acids (ornithine, glycine, and 2,3-dihydroxybenzoic acid) that comprise the siderophore structure. Table 7 shows the signal assignment for the presented NMR spectrum used for the final elucidation of the siderophore. The samples show proton signals chemical shifts of 7.27, 6.89 and 6.64 ppm that indicate the presence of an aromatic ring corresponding to 2,3-dihydroxybenzoic acid, which gives a catechol group to the siderophore (Carrano et al. 2001). The signals at δH = 8.12 ppm and δH = 7.13 ppm correspond to the hydroxyl groups of this compound. Regarding the presence of the amino acid ornithine, proton signals belonging to an amide group (δH = 7.39 ppm) and an amino group (δH = 1.23 ppm) were identified, as well as the aliphatic protons corresponding to the δH = 4.31 ppm, δH = 1.88 ppm and δH = 1.77 ppm signals. In relation to the amino acid glycine, it is

represented by the presence of a signal at δH = 8.30 ppm, that suggests the presence of a proton belonging to an amide group and an aliphatic proton at δH = 3.74 ppm. Finally, a signal at δH = 9.01 ppm would indicate the presence of a proton belonging to an amide group, together with an aliphatic ring of 6 atoms (δH = 7.14 ppm, δH = 3.45 ppm, δH = 1.23 ppm, δH = 4.56 ppm) and a hydroxyl group (δH = 8.61 ppm). It was not possible to calculate the coupling constants (*J*) for all hydrogen signals, because, although the described compound was the main one, some mix signals happened specially in the signals arranged in multiplets. Figure 17 shows the signal assignment together with the structure of the principal siderophore present in the studied fractions, which after these analyses was determined to be the mixed-type siderophore heterobactin B. Similar results have been reported by other authors studying siderophores from *R. erythropolis* (Bosello et al. 2013; Carrano et al. 2001). To corroborate this structure analysis, MS analyses were performed with the purified HPLC peaks of the active fractions from both culture conditions.

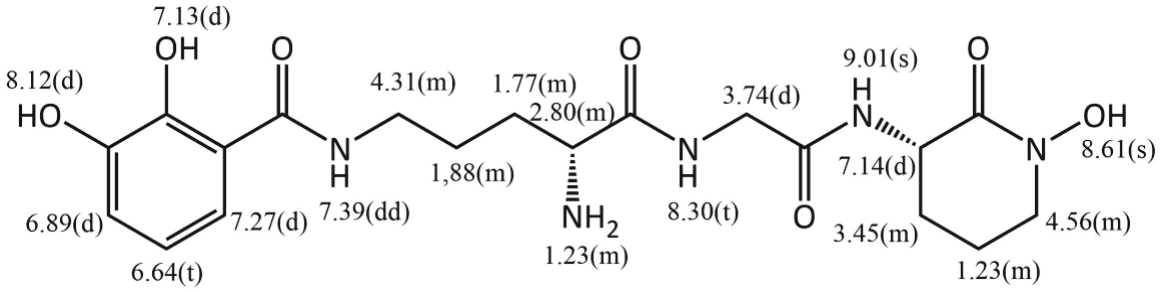

Figure 17.- Structure of heterobactin B elucidated by ^{1}H-NMR signal assignment. Numbers represent chemical shifts (ppm) in the ^{1}H-NMR spectrum, while letters in parentheses represent the type of multiplicity of each hydrogen signal, s (singlet), d (doublet), t (triplet), m (multiplet).

Table 7- Assignments (ppm) of the ^{1}H-NMR spectrum in d6-DMSO of the CAS/As-CAS active HPLC peak from Fe-free M9 with 937 µM sodium arsenite culture.

Signal	Integration (I)	Multiplicity (m)	Coupling Constant (*J*)		Segment
7.13	1	d	7,14-7,12	10	DHBA
8.12	1	d	8,13-8,11	10	
6.89	1	d	6,90-6,88	10	
6.64	1	t	6,66-6,64-6,63	10-5	
7.27	1	d	7,29-7,28-7,27-7,27	5-5	
7.39	1	dd	7,40-7,40-7,38-7,38	10	Orn
4.31	2	m	-		
1.88	2	m	-		
1.77	2	m	1,78-1,77-1,76	5-5	
2.80	1	m	-		
1.23	2	m	-		
8.3	1	t	8,31-8,30-8,28	5-10	Gly
3.74	2	d	3,75-3,74	5	
9.01	1	s	-		Orn
7.14	1	d	7,14-7,13	5	
3.45	2	m	-		
1.23	2	m	-		
4.56	2	m	-		
8.61	1	s	-		

To corroborate the elucidation of the structure obtained by the NMR analyses, mass spectrometry of the purified peaks obtained from HPLC (peaks at retention time 11.8 min of Table 6) with Fe(III)-chelating and As(III)-binding activities was carried out. The mass spectra of heterobactin A and B have previously been studied (Bosello et al. 2013) and could be used as a model to compare signal assignment. The fragments were analyzed using as reference the heterobactin B molecule obtained from the ^{1}H-NMR analysis. The fragment assignment is shown in Figure 18, and was performed by Dr. Christoph Senges at the Institute of Applied Microbiology of the University of Bochum. One principal compound was found to be present in both fractions, and it was determined to have the same structure, and the molecular mass of the siderophore heterobactin B (PubChem ID 53261294) which is 437,453 g/mol, while the molecular mass of the isolated compound was determined to be 437,191 g/mol.

In summary, the combined analyses by ^{1}H-NMR and mass spectrometry strongly suggest that the CAS/As-$_{m}$CAS activity detected in the extracts obtained from *R. erythropolis* S43, is due to the activity of heterobactin B.

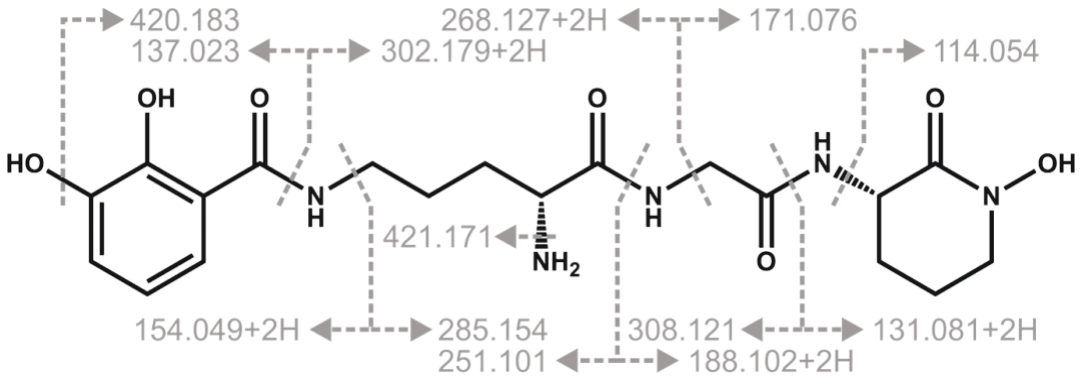

Figure 18.- Structure of heterobactin B with mass spectrometry signal assignment. Gray arrows represent the fragments found in the mass spectrum, numbers represent the mass of each segment.

4.5. Identification of arsenic effect on the transcriptomic profile of *R. erythropolis* S43

4.5.1. Genome sequencing of the arsenic-tolerant bacterium *R. erythropolis* S43

In order to obtain the genetic information related to arsenic tolerance and siderophore production encoded in the genome of the selected arsenic-tolerant bacterium, the genomic DNA of the strain *R. erythropolis* S43 was sequenced using the Illumina MiSeq massive sequencing technology in the laboratory of the Interdisciplinary Ecology Center at the University of Freiberg, Germany. A genome of 6,152,541 bp was obtained, assembled in 264 scaffolds and 848 contigs (Table 8). Using various bioinformatic platforms, a search for arsenic-tolerance mechanisms described in the literature and genes involved in the production of siderophores (NRPS clusters) was performed. The main results are mentioned below.

Table 8.- Genome overview for *R. erythropolis* strain S43, predicted with Artemis Bioinformatics and RAST 4.0.

Feature	Value
Sum of contig length (bp)	6,152,541
Number of contigs	848
N50	8361
L50	848
Protein coding genes	6,040
% G + C	62.5
tRNA	49
rRNA*	55

*rRNA number was estimated using Artemis Bioinformatics.

4.5.2. Genetic determinants of arsenic tolerance and siderophore production in *R. erythropolis* S43

Based on the information in the sequenced genome, a search for classical determinants of arsenic tolerance and siderophore production was performed, using as guideline the genomic annotation obtained by RAST 4.0.

Using Artemis, Metacyc and BLASTp, a putative *ars* operon was found in the genome of *R. erythropolis* S43. This cluster was compared with the genetic determinants of the *ars* operons of 5 other strains of the same species, *R. erythropolis* DN1 (Genbank Accesion: AUZK01000000), *R. erythropolis* CCM2595 (Genbank Accesion: CP003761), *R. erythropolis* P27 (Genbank Accesion: AVCO01000000), *R. erythropolis* XP (Genbank Accesion: AGCF00000000), *R. erythropolis* PR4 (Genbank Accesion: AP008931.1). It is important to mention that not all strains showed the predicted arsenic resistance genes in the classical disposition of an *ars* operon. Although their genomes do code for arsenic resistance determinants, the strains *R. erythropolis* DN1, *R. erythropolis* CCM2595 and *R. erythropolis* P27, have these coding sequences spread across the different contigs and do not present the classical operon disposition. Figure 19 shows a comparison between strain S43 and the two strains that do have their predicted arsenic resistance genes in a putative operon, *R. erythropolis* XP and the plasmid pREL1 of R. *erythropolis* PR4. Figure 19A shows the *ars* gene cluster found in strain S43 (*arsCRCRCODA*), containing the coding sequences for the ArsA protein (efflux pump ATPase), *ArsC* (arsenate reductase), ArsD (transcriptional regulator), ArsO (flavin-dependent monooxygenase) and ArsR (transcriptional

regulator). Figure 19B and 19C show the structure of arsenic tolerance operons predicted for the strains XP and PR4. In comparison, the presence of the putative *ars* operon found in *R. erythropolis* S43 correlates not only with what is found in other stains of the same species, but also may be responsible of the arsenic-tolerant phenotype of *R. erythropolis* S43, since other tolerance mechanisms as arsenite oxidases, methylases and dissimilatory reductases were not detected.

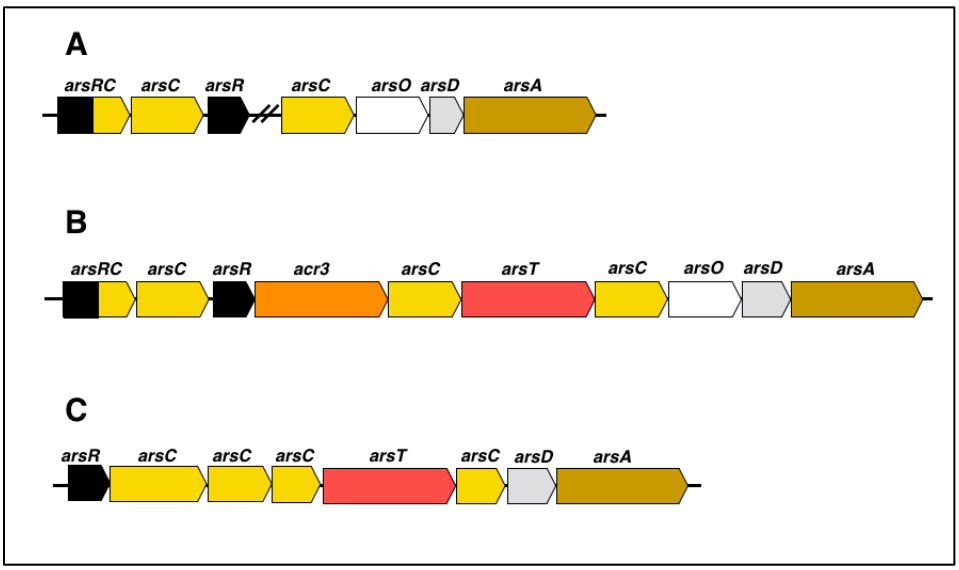

Figure 19.- Bioinformatic reconstruction of ars operons in different strains of *R. erythropolis*. The genes represented correspond to arsO (in white, flavin binding monooxygenase), arsC (in yellow, arsenate reductase), arsD (in grey, transcriptional regulator ArsD), arsA (in gold, extrusion pump and ATPase), arsR (in black, transcriptional regulator ArsR), arsT (in red, thioredoxin reductase) and acr3 (in orange, arsenic resistance protein). A) *R. erythropolis* S43. B) *R. erythropolis* PR4, pREL1 (NC_007491.1). C) *R. erythropolis* XP (NZ_AGCF00000000.1).

In order to predict which secondary metabolites are produced by *R. erythropolis* S43, a study using the bioinformatics platform anti-SMASH was carried out on the whole draft genome (Fig. 20). According to this analysis, strain S43 has 100% of the elements for an NRPS cluster to produce the siderophore heterobactin. A predicted NRPS cluster for heterobactin production has previously been found in the strain *R. erythropolis* PR4 (Bosello et al. 2013).

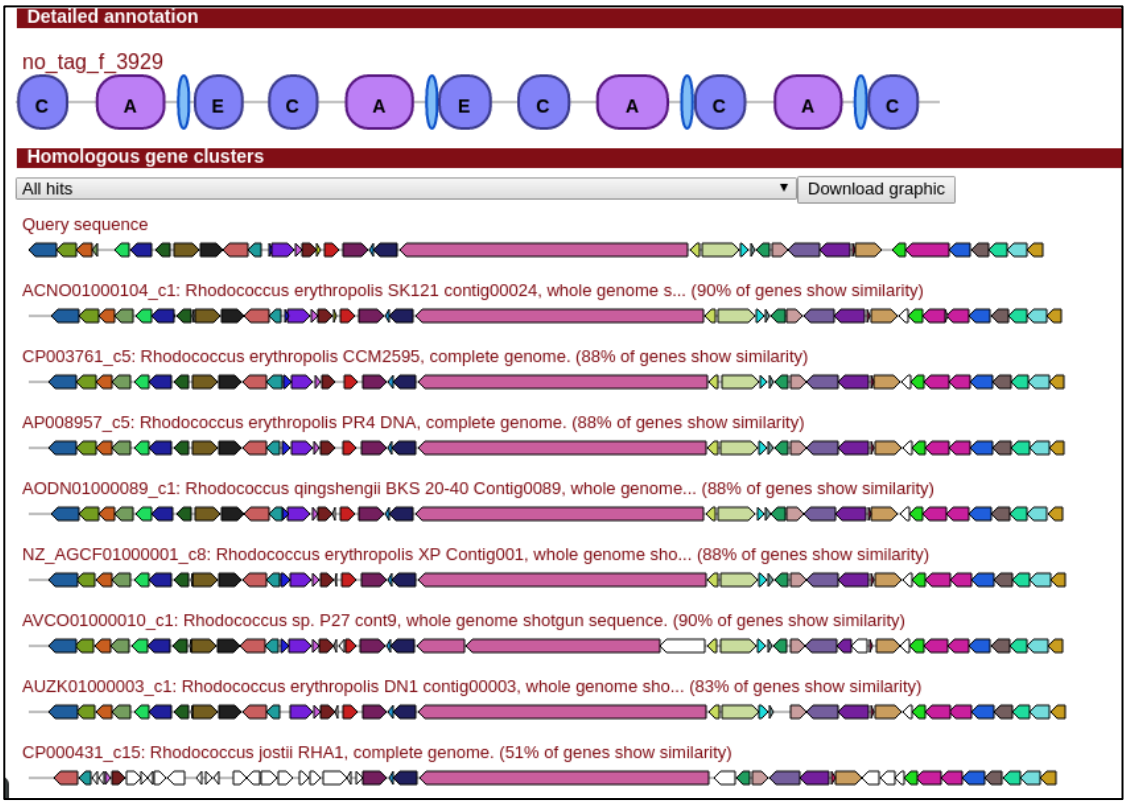

Figure 20.- Analysis of secondary-metabolite-production clusters by anti-SMASH. Diagram of homologous clusters in different *R. erythropolis* strains for the production of the siderophore heterobactin, compared with the cluster found in the draft genome of *R. erythropolis* S43 and shown on top as “Query sequence”.

The predicted cluster that codes for the proteins required for heterobactin synthesis in *R. erythropolis* PR4 has been designated as the "*htbABCDEFGHIJK*" cluster (Bosello et al. 2013) (Fig. 21). Within this sequence, the gene *htbG* has been predicted to encode for an NRPS that synthesizes a tripeptide arginine-glycine-ornithine which is the structural base of the final siderophore in the strain PR4. Also, the *htbABC* genes encode the proteins involved in the formation of 2,3-dihydroxybenzoic acid, which is the main precursor of a catechol group, and one of the responsible groups for the chelating activity in the siderophore (Miethke and Marahiel 2007). Finally, the *htbHIJK* genes encode proteins related to siderophore export.

To locate the putative cluster for the synthesis of heterobactin in the genome of *R. erythropolis* S43, an additional bioinformatic search was performed using a local alignment (BLAST) between the predicted sequence of strain PR4 and the complete genome of strain S43. The alignment results showed 100% identity and 100% coverage (in BLASTp) with a sequence encoded in a single contig, the query was contained in the CDS between the nucleotides 1,211,118 and 1,231,390. Here, the arrangement of the genes in S43 (Fig. 21B) turned out to be identical to the one found in strain PR4 (Fig. 21A), suggesting some level of conservation in this

cluster among some strains of *R. erythropolis*. Additionally, a bioinformatic prediction on the substrate specificity of the adenylation-domains (A-domains) from the genes *htbE* and *htbG*, from to the NRPS for the synthesis of heterobactin was carried out. Differently as found in the strain PR4, the first adenylation-domain of the gene *htbG* has specificity for the amino acid ornithine instead of arginine (Table 9), which is consistent with the results obtained in the chemical characterization. The different substrate specificities of this adenylation-domain will be commented more in depth in the discussion chapter.

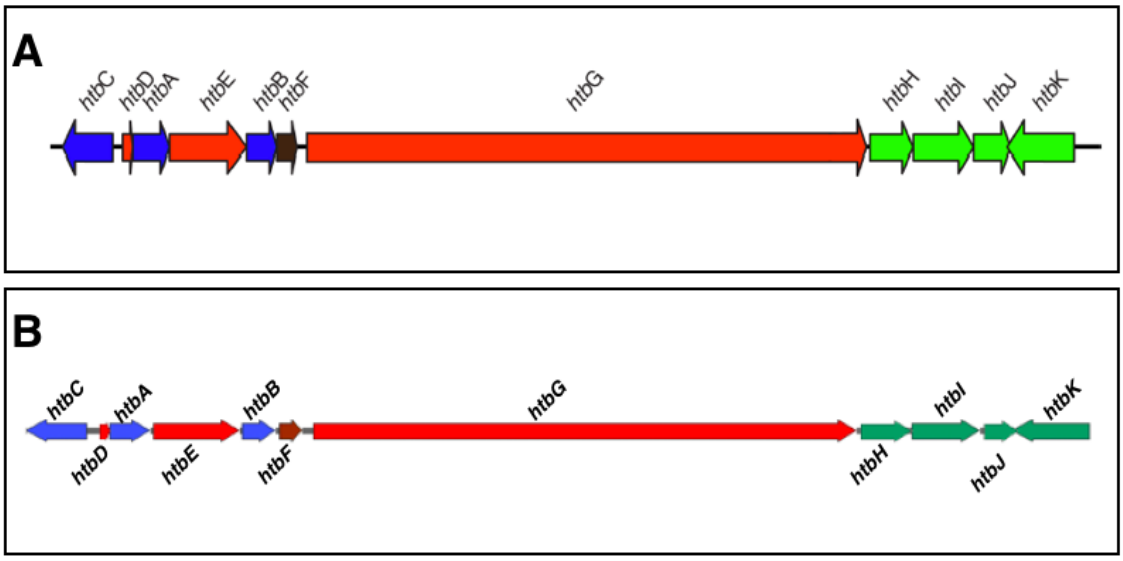

Figure 21.- Comparison of gene clusters for heterobactin production in *R. erythropolis* PR4 and *R. erythropolis* S43. A) Putative heterobactin cluster in *R. erythropolis* PR4 taken from the paper (Bosello et al. 2013). B) Putative heterobactin cluster found in the genome of *R. erythropolis* S43 as drawn with the SnapGene Bioinformatic tool. Siderophore export and iron release genes are shown in green, NRPS related genes in red, 2,3 dihydroxibenzoic acid byosinthesis genes in blue and NADPH-dependent FMN reductase in brown.

Table 9.- Adenylation substrate specificity prediction of the *htb*-cluster A-domains performed with the NRPSsp Bioinformatic platform (Prieto, 2016).

Adenylation Domain	Substrate Prediction	Score (HMMER bit-score)	Prediction-conditioned fallout
htbE	2,3 dihydroxibenzoic acid	914	0.0037
htbG A1	Ornithine	329.6	0.1438
htbG A2	Glycine	495.9	0.1303
htbG A3	Ornithine	499.6	0.1303

4.5.3. Determination of gene expression of siderophore biosynthesis determinants under arsenic stress

Before the determination of the changes in the mRNA levels in the genes *htbG* and *arsC* in siderophore-production conditions, a determination of the transcription of these genes in iron-supplemented conditions was carried out, to determine if iron-depletion is a necessary requirement, as it is indicated in literature (Miethke and Marahiel, 2007; Bosello et al. 2013, Johnstone and Nolan, 2015). In Figure 22 a 2% agarose electrophoresis with the RT-PCR products of the genes *htbG*, *arsC* and *16srRNA*, obtained from *R. erythropolis* S43 are shown, cells were cultured in presence of iron and arsenic stress, against a control condition without arsenic (marked as C in the figure). The cultures stressed with arsenic for time periods from 1 h to 2 h showed an increase in the mRNA levels of the gene *arsC* in presence of arsenic stress (for both arsenite and arsenate) in comparison with the control condition, which does not show detectable presence of the transcripts for this gene. Meanwhile, the gene *htbG*, for siderophore synthesis, did not show an increase in the transcript levels in comparison with the control, being not detectable via this method. This indicates that the presence of arsenic by itself it is not enough to trigger synthesis of siderophores, and an iron-depletion condition must be present. Therefore, this condition with arsenic stress and presence of iron was not included in the following RT-qPCR studies.

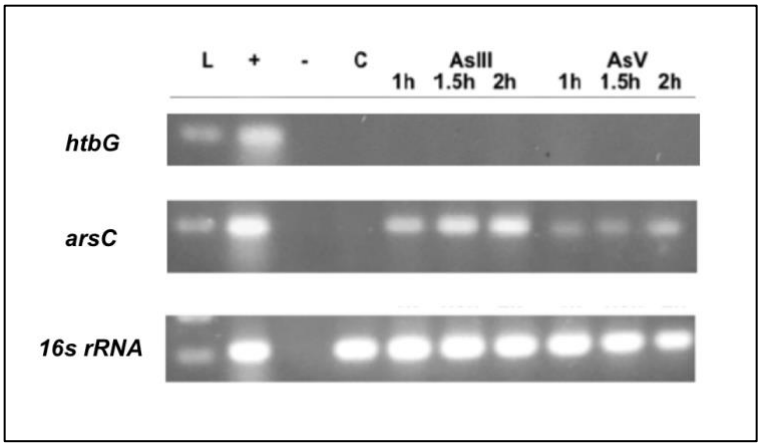

Figure 22.- 2% Agarose gel with RT-PCR products of *arsC* and *htbG* genes. Electrophoresis shows the presence of fluorescent bands that indicate amplification of cDNA from the studied genes. L :100 bp marker, "+" : positive control with genomic DNA of *R. erythropolis* S43, "-": negative control without cDNA, C: control condition with presence of iron and without arsenic stress.

To determine the effect of arsenic on the siderophore biosynthesis genes, specifically on the NRPS gene *htbG* of *R. erythropolis* S43 in iron-depletion conditions, an RTq-PCR was performed. Also, the gene *arsC* for an arsenate reductase was used as an arsenic-tolerance marker. Three culture conditions, a control condition (M9 medium supplemented with 40 μM

$FeCl_3$), a condition of iron deficiency (Fe-free M9 medium) and a condition of iron deficiency and arsenic stress at 1/8 of the MIC (M9 medium with 937 µM As (III)) was carried out. The total (protein-free and DNA-free) extracted RNA is shown in Table 10. The degradation in the samples was monitored by the 23S/16S ratio, while the RNA Integrity Number (RIN) was used to select the samples. All samples that showed a RIN above 7 were selected for cDNA synthesis and later for study of gene expression.

Table 10.- Total RNA values of transcriptomic samples of *R. erythropolis* S43 incubated under conditions of Fe-depletion and arsenic stress.

Condition	Sample	Replicate	RNA conc. (ng/µL)	23S/16S ratio	RNA Integrity Number (RIN)	Selected
Control	M9+Fe Glucose 0.4%	1	260	1.73	10	Yes
		2	143	1.75	10	Yes
		3	175	1.94	10	Yes
		4	122	1.95	N/A	No
Fe depleted	M9 Glucose 0.4%	1	386	1.45	9.5	Yes
		2	448	1.44	9.6	Yes
		3	374	1.51	9.6	Yes
		4	225	1.52	9.6	Yes
Fe depleted As stress	M9+As Glucose 0.4%	1	420	1.4	9.5	Yes
		2	240	1.42	9.2	Yes
		3	543	1.99	7.6	Yes
		4	504	1.2	8.5	Yes

In Figure 23A, gene expression of *arsC* (arsenate reductase) and *htbG* (NRPS for heterobactin synthesis) evaluated by RTq-PCR are shown. The arsenate reductase gene showed a seven-fold rise in its expression in the culture condition with arsenic stress (M9 + As condition) compared with the control without arsenic (M9 + Fe condition) and the siderophore production condition (M9), indicating a genetic response against arsenic-stress in the studied condition.

Figure 23B shows the gene expression of *htbG*, the NRPS for the biosynthesis of heterobactin. As expected, a rise in expression was found in the iron-depleted siderophore production condition (M9) with an increase of 5.9 times in total mRNA. In the condition of iron-depletion and arsenic stress an increase of 5.3 times was found. Thus, there was no statistically significant difference between the total mRNA levels of these two conditions.

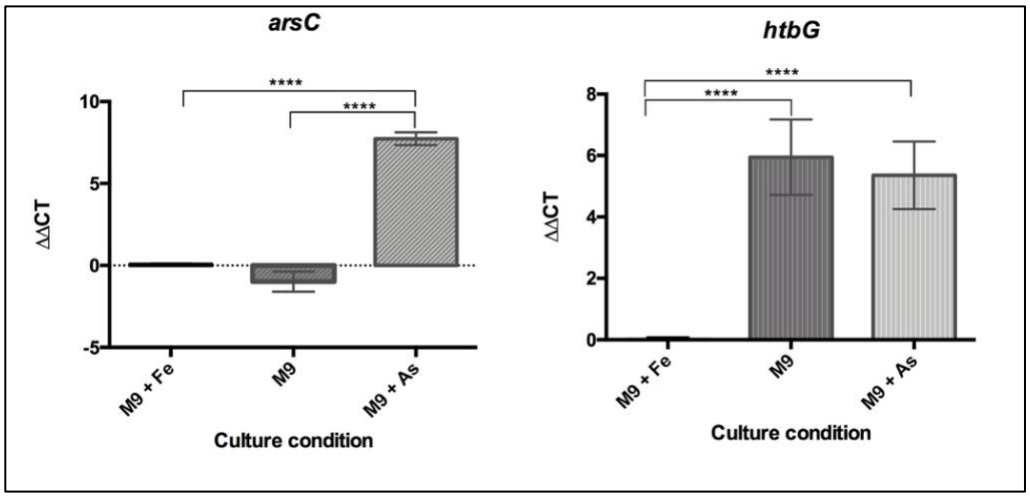

Figure 23.- Total mRNA level fold-change of arsenic-tolerance and heterobactin-biosynthesis marker genes in *R. erythropolis* S43 investigated by RTq-PCR. (A) Differential expression profile of gene arsC (arsenate reductase). (B) Differential expression profile of gene htbG (non-ribosomal peptide synthetase). Expression of both genes was evaluated in three culture conditions, control (M9 + Fe), iron-depleted condition (M9) and iron depletion with arsenic stress (M9 + As). Stars (****) represent statistical significance calculated using the t-test (p-value >0.001).

V. DISCUSSION

During this chapter the main results obtained during this thesis will be discussed, starting with the use and implications of the isolated arsenic-tolerant bacteria and their capacity to produce arsenic-interacting molecules, including the limitations and applications of the assays performed to screen said activity. Additionally, the characterization of heterobactin and their biosynthesis genes in *R. erythropolis* S43 will be discussed and compared with the current literature, where the presence and functioning of the siderophore-production cluster and arsenic-tolerance genes will be discussed. Also, the implications of arsenic-binding siderophores in arsenic tolerance will be commented, taking in consideration the results obtained during this thesis and what has been described by other authors. Finally, the biotechnological applications and projections of the results obtained in this work will be commented.

In this work, forty strains were isolated from arsenic-contaminated mining water from Bad Schlema purification plant (Aue, Germany). Of these forty strains, fourteen were identified and later, four arsenic-tolerant Actinobacteria from the genera *Rhodococcus*, *Arthrobacter,* and *Kocuria* were selected for further studies, due to their ability to grow in traditional culture media and possessing the highest tolerance to arsenic. In addition, the previously isolated *R. erythropolis* S43 (Sultana et al. 2012) was included in the further analysis. All the selected isolates, according to the parameters described by Pandey and Bhatt (2015), showed a moderate level of arsenic tolerance, with the exception of *A. oxydans* ATW3 which proved to be highly tolerant to As(III). The extracellular extracts obtained from a culture in Fe-free M9 medium contained siderophore-like molecules able to bind iron and also arsenic as trivalent arsenite, properties that were evaluated using the CAS assay to detect the iron-chelating activity (Schwyn and Neilands 1987) and the As-$_m$CAS assay, a modified version of the first (Retamal-Morales et al. 2018), developed during this thesis work. A screening test to detect arsenic-binding activity has previously been used to evaluate the capacity of siderophores produced by *P. azotoformans* to bind the metalloid (Nair et al. 2007). However, the changes required to perform this assay had not been described, turning it into a methodology impossible to reproduce. In the current work, the As-$_m$CAS assay has been developed carrying out specific modifications to the traditional method, considering pH, concentration of the CAS dye and element to chelate, which have allowed its reproducibility and publication. Also, the effectiveness of this methodology has been proven by studying the spectra of fluorescence emission of the arsenic chelating siderophores, corroborating the effectiveness of the As-$_m$CAS assay for detection of As-binding siderophores.

The five selected strains in this study are members of the phylum Actinobacteria, typically described as mostly free-living microorganisms that are widely distributed and abundant in both terrestrial and aquatic ecosystems, although they are mostly found in soil (Barka et al. 2016).

Several reports have highlighted the importance of Actinobacteria as a source of novel secondary bioactive metabolites (Barka et al. 2016), including siderophores with traditional iron-chelating activity (Emmanuel et al. 2012; Solecka et al. 2012; Bosello et al. 2013). However, the ability of these iron-chelating siderophores to bind arsenic remained understudied in members of this lineage. Therefore, in this study the capacity of the five selected isolates to produce As-binding siderophores has been addressed and studied with more depth. It is noteworthy that the Fe-chelating and As-binding activity of the tested extract do not seem to correlate between the isolates. Thus strains that presented intermediate Fe-chelating activity showed a high activity As-binding activity. For example, *A. oxydans* ATW3 and *R. erythropolis* S43 showed a comparatively high arsenic-binding activity, while their iron-chelating activity was relatively low, while the opposite behavior was observed in other strains. This may be due to the fact that the two screening methods used in this study, CAS and As-$_m$CAS assay, are different and that their pH conditions, dye concentrations and element-to-chelate concentrations are not the same. Therefore, in this case it is not possible to directly compare the activities of Fe(III)-chelating and As(III)-binding among the isolates, and the results must be interpreted separately. Nevertheless, the lacking correlation of the Fe-chelating and As-binding activities between the strains also indicates that the strains may, to some extent, be equipped with different siderophores.

Regarding the study of fluorescence emission spectra from siderophores, this has been shown to be useful to detect the interaction between siderophores and a particular element. For example, this method has previously been used to identify the ability of pyoverdine, a siderophore produced by *P. aeruginosa,* which has the capacity to interact with Al(III). For this species a change in the fluorescence profile of the metabolite was observed when $AlCl_3$ was added to a siderophore extract (Del Olmo et al. 2003). In the present study, the fluorescence emission spectra for *A. oxydans* ATW3 and *R. erythropolis* ATW1 (Figs. 10 and 11) showed that their iron- and arsenic-siderophore spectra had a different profile in terms of the wavelength of maximum emission and number of peaks, suggesting the occurrence of different chemical characteristics of the siderophores produced by these two isolates, which would result in their different binding profiles. These findings suggest that the binding activity of a siderophore (or a siderophore extract) can happen against different ligands, this has been described before in literature, where it has been reported that the activity of siderophores against different elements can be modified when manipulating the pH (Neubauer et al. 2000), or in *Azotobacter vinelandii*, where azotobactin and azotochelin have different affinities for different metals (Thomas et al. 2009). Also, in *P. aeruginosa*, the siderophores pyoverdine and pyochelin are implicated in iron uptake, but they can also bind other metals with different affinities (Braud et al. 2009a; Braud, et al. 2009b). Since in this case, the physical-chemical characteristics of the media were not modified, it could indicate a double-specificity of one molecule.

However, if only this assay is taken in consideration, and since it was performed with a complex extract (which can contain more than one molecule with binding activity), it could also suggest the co-occurrence of different compounds able to bind different elements, being this a possible explanation of the variation in the binding activity. In this sense, there are several non-exclusive mechanisms that could explain the observed differences in iron-chelating and arsenic-binding activities for a given extracellular extract, and they must be explored studying more in depth each siderophore extract for each strain.

Regarding the relation with tolerance, how widely this presumed tolerance mechanism is spread in the bacterial domain and how the mechanistic works is not yet clear in the current literature. While the findings of Drewniak et al. (2008) and Ghosh et al. (2015) indicate a correlation of siderophore formation and arsenic tolerance, but did not show binding, Nair et al. (2007) showed binding, but no association to arsenic tolerance. In this work, was shown that compounds formed by arsenic-tolerant Actinobacteria do, in fact, interact with arsenic. However, the possible implication in tolerance of these chelators had to be studied using an interdisciplinary approach, which not only took in consideration the production of arsenic-binding compounds, but also the gene expression of the siderophore biosynthesis genes in response to arsenic stress, which will be discussed further in this chapter.

The finding of arsenic-tolerant Actinobacteria able to produce As(III)-binding (or interacting) siderophores opens interesting perspectives for application. Due to their high abundance and their ability to produce secondary metabolites, it is possible to suggest that Actinobacteria might represent an interesting source of arsenic-binding compounds which can be further studied, and when overproduced or in association with plants (Braud et al. 2009a) may be used to decontaminate soil or water and for other potential biotechnological applications.

When studying the chemical characteristics to determine the structure of these chelating compound(s), it was necessary to select the isolate with the highest As(III)-binding activity. Since *A. oxydans* ATW3 and *R. erythropolis* S43 showed a high As(III)-binding activity, reaching above 100% of decolorization (in comparison with EDTA), a way to select only one of them was to calculate the ratio between the As(III)-binding and Fe(III)-chelating activity. This was made to prioritize the As(III)-binding activity in case this phenomenon was mediated by the same compound. This possibility had to be evaluated with the results later obtained by the chemical and mRNA level of siderophore biosynthesis gene studies.

To be able to perform the chemical analyzes, it was necessary to obtain an amount of extract equivalent to 10 mg of dry weight. However, it is important to mention that siderophore production is a phenomenon that happens under nutrient depletion conditions (Miethke and

Marahiel, 2007). Thus, these molecules are produced in small amounts, but present high activity. Therefore, obtaining a sufficient quantity of rapidly purified siderophores for chemical characterization poses a challenge that still needs to be resolved. To face this problem, the culture of strain S43 was improved and scaled up from a traditional flask method to a bioreactor with constant agitation and air injection, which allowed a higher siderophore production than previously. The extracts obtained by this method were sufficient to perform the chemical characterization via ^{1}H-NRM and LC-MS for structure elucidation of the siderophore(s).

After the evaluation with analytical HPLC, the absorbance spectra of the HPLC peaks of potential siderophores were compared with the absorbance spectra of previously isolated siderophores. It was found that they had high similarity with the spectrum of the previously described siderophore heterobactin, a mixed-type siderophore (that presents catechol and hydroxamate functional groups). The siderophore produced by the strain S43, as well as heterobactin (Bosello et al. 2013), showed an absorbance spectrum with only one maximum of absorbance around 320 nm when evaluated in a range of 250 - 800 nm.

From these results, it is possible to suggest that, under both culture conditions with and without arsenic stress, the obtained siderophores have similar chemical characteristics, since they have a similar HPLC profile and similar absorbance spectra. However, this interpretation is not definitive, since it has been described that some siderophores can undergo modifications and despite having differences in their structure, possess the same chromatographic profile by HPLC (Boiteau et al. 2016). To address this issue, a protocol for the separation of siderophores by HPLC, that allows to differentiate isoforms has recently been published (Heine et al. 2017). With this in mind, it is possible that the analyzed peaks contain more than one type of heterobactin. It has been reported that heterobactin can occur in four isoforms, heterobactin B, heterobactin A, heterobactin S1 and heterobactin S2. Heterobactin S1 and S2 are sulfonated forms of heterobactin A (Bosello et al. 2013). While heterobactin B has a hydrogen on the alpha-amino group of the amino acid, the forms A, S1 and S2 present a 2,3-dihydroxybenzoyl rest in this position, which is probably added after the peptide synthesis in the siderophore production process (Bosello et al. 2013; Carrano et al. 2001).

When elucidating the structure of the As(III)-binding compounds obtained under both culture conditions, the analyzes by ^{1}H-NMR and MS indicated that these corresponded to heterobactin B. At the moment of the development of this manuscript, the siderophore heterobactin has been characterized by NMR and MS twice in literature, a first approach was carried out by Carrano et al. (2001) studying the ^{1}H-NMR, ^{13}C-NMR for heterobactin A and B, with an additional mass spectra for heterobactin A, both isolated from *R. erythropolis* IGTS8. In that work, the coupling constants of said NRM analyses were not disclosed, so it was not possible to

compare them with the ones obtained in the studied compound produced by the strain S43, however, a similarity in the amino acid and acid composition of the siderophore heterobactin B has to be highlighted. In this thesis, the amino acids and acids that form heterobactin B are DHBA-Ornithine-Glycine-Ornithine, similarly to what was found by Carrano et al.

A second approach on elucidation of heterobactin produced by *R. erythropolis* PR4 was carried out by Bosello et al. (2013) where a Heteronuclear Multiple Bond Correlation (HMBC) NMR for C and H was carried out, in addition with the study of the mass spectra of the isolated heterobactin siderophores. Also, siderophores produced by the strain IGTS8 (the same used by Carrano et al.) were studied to compare if the siderophores produced by both strains had different chemical characteristics. In that work, it was determined that under iron-limiting conditions both *R. erythropolis* PR4 and *R. erythropolis* IGTS8 produce three iron-binding compounds, whereas two of them are modified by sulfonation. The authors determined that the most lipophilic compound was identical as one described previously, and it was corroborated to be heterobactin A, whereas the two other sulfonated forms were named heterobactin S1 and S2. In this study, the form heterobactin B was not found neither by MS or NMR, showing a discrepancy in the current literature, regarding the reports of heterobactin. In this thesis, the independent structure elucidation via MS give more evidence to think that *R. erythropolis* S43 produces heterobactin B, however, a bi-dimensional NMR could be the solution to characterized more detailed the obitained arsenic-binding molecule.

As it was discussed further up, siderophores can occur in different forms, so the presence of the form heterobactin B in the studied extracts it is possible and does not rule out the presence (in lower concentration) of heterobactin A, S1 or S2, although the additional presence of a 2,3-dihydroxybenzoayl group could be expected to been visible in the analytical HPLC if present in enough concentration. Thus, the Fe(III)-chelating and As(III)-binding capacity of the extracts obtained from strain S43 can be attributed mostly, but not necessarily exclusively, to heterobactin B.

The finding of heterobactin as the isolated siderophore from the strain S43 is consistent with the presence of the heterobactin production cluster *htbABCDEFGHIJK,* and the substrate prediction that indicated Adenylation-domains for DHBA, ornithine, glycine and a second ornithine, which corresponds with the obtained chemical characterization. However, this is not similar to the findings by Bosello et al. (2013), which reported that heterobactin not only includes a 2,3-dihydroxybenzoayl, but also that the substrates adenylation-domains are DHBA, ornithine, glycine and arginine, which was predicted bioinformatically and also carried out using a ATP/$^{32}PP_i$ exchange assay, where the adenylation-domain from the dissected initiation module of the protein HtbG was highly specific for arginine, so in order to bring some light into this, it would be possible to perform a substrate specificity test as the one described by Bosello et al., and determine if the

Adenylation-domaing of HtbG of the strain S43 does in fact has activity over ornithine. For now, the bioinformatic approach seems consistent with the chemical characterization by NMR and MS, but the limitations of these predictions cannot be ignored, since using different platforms, it is possible to obtains different results depending on the internal algorithm of the specific bioinformatic tool. Specifically, if different platforms are used to predict the substrates of the adenylation-domains of HtbG in the strains S43 and PR4, both show a prediction for ornithine using the platform *NRPSsp* (Prieto, 2016), and for glutamic acid when using the platform *LSI A-domain function predictor* (Baranasic et al. 2014), which can be observed in Figure S6 (Supplementary Material). Therefore, an experimental approach is necessary to clarify if the NRPS present in *R. erythropolis* S43 can use either ornithine or arginine, or both.

When evaluating the potential of *R. erythropolis* S43 to tolerate arsenic and to produce As(III)-binding siderophores, the bioinformatic reconstruction showed interesting findings regarding the presence of arsenic tolerance determinants, where a putative *ars* gene-cluster regulated by ArsR was found as the only determinant related to tolerance. Putative sequences for an *ars* operon regulated by ArsR have been found in a variety of bacterial species and this seems to be the classical way of regulation (Prithivirajsingh et al. 2001). For example, in *Campylobacter jejuni*, the activation of the operon genes has been described to happen when the concentration of extracellular arsenic increases, in both oxidation states: As (III) and As (V) (Wang et al. 2009). ArsR is a repressor protein, member of the metal-responsive transcriptional regulator ArsR/SmtB family (Shi et al. 2004), which has been extensively reviewed in recent years (Busenlehner et al. 2003; Pennella and Giedroc 2005; Qin et al. 2006; Murphy and Saltikov 2009; Osman and Cavet 2010; Antonucci et al. 2017). The DNA binding motif consists of a homodimeric 'winged' helix-turn-helix structure. The homodimeric ArsR has generally only a single metalloid binding site per monomer, coordinating As(III), As(V) or Sb(III). This protein is normally inhibiting the expression of the *ars* operon by binding as a homodimer to an imperfect inverted repeat sequence proximal to, or overlapping, the -35 element of the *ars* promoter, thus blocking the initiation of transcription. However, the binding As(III) or As(V), induces a conformational change leading to DNA release and to the initiation of transcription. This model has been described as a response mechanism to arsenic in different species (Yang et al. 2005, Rosen and Tamas 2010) and, consequently, it is expected to be found also in a strain isolated from an arsenic-contaminated environment. The presence of this operon as the only mechanism of tolerance in the genome of strain S43 allows us to postulate that its arsenic-tolerant phenotype is mainly due to the presence and functionality of this operon.

Before the beginning of this work, *R. erythropolis* S43 was characterized as an arsenic-tolerant Actinobacteria with the capacity of oxidize arsenite through dissimilatory oxidation, based in a growth curve carried out in presence of arsenite, in which after the incubation time, a decrease

in the concentration of As(III) was found (Sultana et al. 2012), However, as it was stated before, when looking into the genome of this strain, no arsenite oxidase genes were found, therefore, an experimental assay was performed in parallel of this thesis, to determine if the arsenic-oxidation capacity of this bacteria was in fact accurate. A measurement of a growth curve and oxidation of arsenite was carried out (Fig. S7, Supplementary Material), and it was found that although As(III) concentration decreased about 20% during the measurement time, there was no generation of As(V). It is possible that this decrease of arsenite concentration in the culture media is due to a minor accumulation in the dead biomass, which is removed previous to the measurement of arsenic species via ICP-MS, which is carried out in the culture supernatant. Regarding the presence of an arsenite oxidase marker gene, Sultana et al. reported that there was no PCR amplification with the AOXI primers in *R. erythropolis* S43, therefore, the lack of this gene in the now sequenced genome is consistent with was determined experimentally during this work.

When the structure of the *ars* operon of S43 was compared with others found in strains of the same species, the results is that, first, not all evaluated genomes of *R. erythro*polis show the arsenic determinants in a cluster fashion, even though the arsenic-tolerance genes classically described as *ars* operon determinants are present. Second, for the strains that do present an organized operon containing the arsenic tolerance genes, a common pattern was found, where all the operons start with an *arsR* gene, followed by *arsC* and finishing with *arsD*, followed by *arsA*. Third, this general pattern in the *Rhodococcus* strains is highly modified by occurrence of additional genes, like *arsRC* plus *arsC* preceding *arsR* in S43 and PR4, additional copies of *arsC* especially pronounced in strain XP, but also in PR4, *arsT* in PR4 and XP, ARC3 in PR4, and *arsO* in S43 and PR4 (Fig. 19). These patterns could be common in the strains of *R. erythropolis* that possesses an *ars* gene-cluster (Fig. 19). Regarding this, the characterization of the *ars* cluster in these strains has shown the presence of a specific arrangement of the genes for each strain. This has been reported before after studying *ars* gene-cluster of Gram-positive bacteria, where the organization of the genes seems to be specific for each bacterial species studied (Achour-Rokbani et al. 2010). It is necessary to mention that since the sequenced genome of *R. erythropolis* S43 is not yet complete, and the analyses were performed in an assembly of several contigs, a better sequencing effort must be carried out to complete the sequencing of the genome and have a better characterization of this ars cluster, since as it is shown in Figure 19, a gap between arsR and arsC is present, since these sequences are in different contigs, so the distance between them can not be easily determined. To solve this issue, a PacBio sequencing of the complete genome is being planned at the moment, this way the already existing sequences can be complemented with a more accurate method of sequencing.

Regarding the implications of the synthesis of heterobactin in arsenic-tolerance, the physiological implications of this arsenic-binding siderophore are still unclear. Nowadays, only few

studies describe in depth the biological role of siderophores chelating elements different from Fe(III) in bacteria. Some of them have focused in the capacity of these chelators to recover elements with nutritional value for the microorganism, for example, the production of azotochelin and azotobactin by *A. vinelandii*, which can chelate and uptake molybdenum and vanadium to be used as cofactors for a nitrogenase enzyme (Thomas et al. 2009). In other studies, the capacity of siderophores to bind potentially toxic elements as a tolerance mechanism has been suggested. In some approaches, based on the detection of radioactive isotopes of these toxic elements bound to siderophores, it was determined that in contrast to Fe(III) uptake, some elements are chelated, but not internalized into the cell biomass (Braud et al. 2009a; Braud et al. 2009b; Dimkpa et al. 2009; Dimkpa et al. 2008).

However, when studying the transcript levels of *htbG* under arsenic stress, a stress-related response resulting in tolerance does not seem to be clear for *R. erythropolis* S43. As it could be expected, an increase in the expression of *htbG* was found when strain S43 was cultured in Fe-free M9 medium, since iron depletion has been broadly described as the triggering factor for siderophore production (Miethke and Marahiel 2007). But, when the strain was cultured in additional presence of arsenic stress, no significant difference in the expression of *htbG* was observed. From a physiological perspective, if only this result is taken into consideration, it suggests that arsenic stress does not trigger the expression of the NRPS for heterobactin B production. Therefore, in *R. erythropolis* S43 the production of this siderophore may not be a tolerance mechanism in response to arsenic. Nevertheless, this is only argued from the perspective that tolerance can be regulated by the over-expression of biosynthesis-related genes, which is not necessarily accurate. This consideration can be explained using the example of some *P. aeruginosa* strains that produce siderophores. These strains seem to be more resistant to metals than strains that do not produce siderophores (Braud et al. 2010). In *P. aeruginosa*, pyochelin production reduced the intracellular accumulation of Al(III), Co(III), Cu(II), Zn(II) by more than 80%, and pyoverdine decreased the uptake of Al(III) and Cu(II) by 80% and that of several other metals by 40%. Although it is not clear yet, how this mechanism is regulated for each toxic metal/metalloid, it has been shown that pyoverdine binds a number of different metals, and several of these metal-pyoverdine complexes also bind to the outer-membrane siderophore transporter (FpvAI), but only when siderophores are bound to Fe(III), the complex can efficiently be transported into the cell by the TonB system (Braud et al. 2009b).

Therefore, tolerance can be related to the specificity of the uptake mechanisms, which depends on the transport system and not just on the biosynthesis of the siderophore itself. This fits to the observation that in *P. aeruginosa,* copper exposure increases siderophore production by upregulating the expression of genes required for pyoverdine synthesis, while the expression of *fpvA*, encoding a pyoverdine-Fe transporter, is downregulated, increasing siderophore

production, but decreasing the uptake of the siderophore-metal complex (Schalk et al. 2011). Siderophores from *S. acidiscabies* and *S. tendae* can bind nickel or cadmium, respectively, thus protecting the bacteria from metal toxicity (Dimkpa et al. 2009). These findings suggest that in the presence of certain toxic metals/metalloids, cells respond by inducing siderophore production, chelating the free-metals by forming a metal-siderophore complex, which would not be transported into the cell. In this context, to elucidate the specific interaction between siderophore biosynthesis and transport pathways, and arsenic stress, a global transcriptomic study may be expected to bring more light into this process that seems to be very specific for different bacterial species.

Overall, this study has highlighted possible novel biotechnological applications of bacterial siderophores against arsenic, including the characterization of several actinobacterial strains as a potential tool for discovering new interesting metabolites. Additionally, the characterization of heterobactin B as an arsenic-binding molecule, which had not been described before, and the development of a screening method for arsenic-binding molecules as a useful method for detecting different metabolites, all are oriented to face the environmental and public health problem that arsenic still is.

Biotechnological implications and projections of this work

The presented thesis work has allowed to isolate and identify fourteen arsenic-tolerant bacteria from contaminates sites, which comprehend an interesting niche of biotechnological capacities that remain to be studied. The study of tolerance to different metals and metalloids among these isolates can be recommended to discover the new tolerance mechanisms against toxic elements, which can be very useful to understand the metabolic pathways involved in tolerance to several toxic elements, a base for fundamental research and then, find new bacterial products of industrial interest. Additionally, the capacity of the studied Actinobacteria to produce arsenic-binding siderophores, although being not fully characterized molecules, makes them interesting organisms to be used in bioremediation when coupled with other biological technologies of decontamination.

It is important to mention that during the development of this work, it was noticed that the production and purification of siderophores in enough quantity to develop any type of technological prototype (for example, filters containing siderophores) is a process with high costs, which not necessarily relates with the requirements of the industry, specially in contaminated sites with low income and low technology-input communities, which are many around the world (Ferrechio and Sancha, 2006; Sancha, 2003). Therefore, since arsenic-free (or with concentrations below the limit) drinking water is a necessity for human health, we should emphasize that the purification of water should be researched looking for the most effective, economically achievable. This way, the

chemical characterization of heterobactin B as an arsenic-binding siderophore is an interesting contribution to the research in the field, but not a technology possible to apply broadly in a short-period of time. Considering the economical limitations in the application of this technology, it is possible to propose the use of this bacterial species producing of arsenic-binding molecules instead of an isolated compound. A plausible way to do this is to study the interaction of these bacteria with the rhizosphere of vegetal species used in bioremediation, where the production of these metabolites can give these plants a higher chance of survival in the inhospitable environments they are put in (Mesa et al. 2017; Oller et al. 2013). Also, rise the possibility of only apply not only the isolates described in this work, but to use environmental Actinobacteria present in soil and water of the same contaminated sites, since these are a dominant phylum in many environments (Tekaya et al. 2012).

A suitable method to apply the products of this work, instead of the decontamination industry, is the biomedical field, where purified siderophores have been previously used to treat diseases, based on their capacity to chelate iron (Saha et al. 2016). Here, these arsenic-binding molecules could be potentially immobilized and used to develop arsenic-capturing displays, a novel technology that it has been recently improved for heavy metals (Peng et al. 2018). It would be interesting also to test the chelating activities of the isolated siderophores against different metals of economic interest such as gold, gallium, or indium, and apply this technology in fields where a highly technical approach is more suitable.

Finally, the fluorescent properties of the studied siderophores (seen in figs. 10 and 11) allows them to be tried as biosensors. Methods based in the capacity of emission of fluorescence by siderophores (Del Olmo, Caramelo, and SanJose 2003) have been developed using these chelators as sensors in environmental samples. One example is the use of the siderophore parabactin, a chelator produced by *Paracoccus denitrificans* that can be used to determine iron concentration in sea water, with a sensitivity in a pM range (Lam et al. 2006). Although the use of siderophores as biosensors is mainly focused on iron, they are not limited to it, since they have been reported to be able to bind other elements selectively, such as molybdenum (Duhme et al. 1996). In the case of arsenic, the fluorescent properties of siderophores remain to be an interesting characteristic which can be perfected and standardized to measure arsenic in water, at least for research purposes.

VI.- CONCLUSIONS

The arsenic-tolerant Actinobacteria isolated from contaminated environments produce arsenic-binding siderophores, activity of which was measured with a method developed during this work, the arsenic-binding and iron-chelating activity relative values cannot be compared between themselves, since the screening methods work in different conditions and the chemical interactions between arsenic and the isolated siderophores is not yet clear.

.

In the arsenic-tolerant Actinobacteria *R. erythropolis* S43, the arsenic-binding and iron-chelating activity of the extracellular extract is carried out by the mixed-type siderophore heterobactin B.

The biosynthesis of heterobactin B in *R. erythropolis* S43 does not seem to be related with arsenic tolerance, when studying the transcript levels of the siderophore synthesis gene *htbG*

REFERENCES

Ahmed, E., Holmström, S. (2014). Siderophores in environmental research: roles and applications. *Microbial Biotechnology,* 7 (3):196–208. https://doi.org/10.1111/1751-7915.12117.

AIDIS. (2014). Capítulo chileno de la asociación interamericana de ingeniería sanitaria y ambiental. 48, Santiago, Chile.

Al-Abed, S. Jegadeesan, G., Purandare, J., Allen, D. (2007). Arsenic release from iron rich mineral processing waste: Influence of pH and redox potential. *Chemosphere*, 66 (4):775-82. https://doi.org/10.1016/j.chemosphere.2006.07.045.

Albarracín, V., Amoroso, M., Abate, C. (2005). Isolation and characterization of indigenous copper-resistant actinomycete strains. *Chemie der Erde,* 65 (SUPPL. 1):145–56. https://doi.org/10.1016/j.chemer.2005.06.004.

Alexander, D., Zuberer, D. (1991). Use of chrome azurol S reagents to evaluate siderophore production by rhizosphere bacteria. *Biology and Fertility of Soils,* 12 (1):39–45. https://doi.org/10.1007/BF00369386.

Achour-Rokbani, A., Cordi, A., Poupin, P., Bauda, P., Billard, P. (2010). Characterization of the *ars* gene cluster from extremely arsenic-resistant *Mycobacterium* sp. strain A33. *Applied Environmental Microbiology*, 76(3): 948-955. https://doi:10.1128/AEM.01738-09.

Amin, S., Küpper, F., Green, D., Harris, W., Carrano, C. (2007). Boron binding by a siderophore isolated from Marine Bacteria associated with the toxic dinoflagellate *Gymnodinium Catenatum*. *Journal of the American Chemical Society,* 129 (3):478–79. https://doi.org/10.1021/ja067369u.

Anjum, S., Gautam, D., Gupta, B., Ikram, S. (2014). The Environmental Geochemistry of Arsenic -An Overview-. *Reviews in Mineralogy and Geochemistry*, 79 (1):1–16. https://doi.org/10.2138/rmg.2014.79.1

Antonucci, I., Giovanni, G., Limauro, D., P Contursi, P., Ribeiro, A., Blesa, A., Berenguer, J., Bartolucci, S., Fiorentino, G. (2017). An ArsR/SmtB family member regulates arsenic resistance genes unusually arranged in *Thermus thermophilus* HB27. *Microbial Biotechnology*, 10 (6):1690-1701. https://doi.org/10.1111/1751-7915.12761.

Ayangbenro, A., Olanrewaj, O., Babalola, O. (2018). Sulfate-Reducing Bacteria as an Effective Tool for Sustainable Acid Mine Bioremediation. *Frontiers in Microbiology*, 9:1986. https://doi.org/10.3389/fmicb.2018.01986.

Baranašić, D., Zucko, J., Diminic, J., Gacesa, R., Long, P., Cullum, J., Hranueli, D., Starcevic, A.(2014). Predicting substrate specificity of adenylation domains of nonribosomal peptide synthetases and other protein properties by latent semantic indexing. *Journal of Industrial Microbiology and Biotechnology*, 41 (2): 461-467. https://doi.org/10.1007/s10295-013-1322-2.

Barka, E., Parul, V., Sanchez, L., Gaveau-Vaillant, N., Jacquard, C., Klenk, H., Clément, C., Ouhdouch, Y., van Wezel, G. (2016). Taxonomy, physiology, and natural products of Actinobacteria. *Microbiology and Molecular Biology Reviews,* 80 (1):1–43. https://doi.org/10.1128/MMBR.00019-15.

Basha, C., Ahmed, S., Selvi, J., Ramasamy, E., Chellammal, S. (2008). Removal of Arsenic and Sulphate from the Copper Smelting Industrial Effluent. *Chemical Engineering Journal*, 4: 313-23. https://doi.org/10.1016/j.cej.2007.10.027.

Batey, H., Whitwood, A., Duhme-Klair, A. (2007). Synthesis, characterization, solid-state structures, and spectroscopic properties of two catechol-based luminescent chemosensors for biologically relevant oxometalates. *Inorganic Chemistry,* 46 (16):6516–28. https://doi.org/10.1021/ic700554n.

Battaglia-Brunet, F., Morin, D., Coulon, S., Joulian, C. (2009). Bioprecipitation of arsenic sulphide at low pH. *Biohydrometallurgy: A Meeting Point Between Microbial Ecology, Metal Recovery Processes and Environmental Remediation,* 71–73:581–84. https://doi.org/10.4028/www.scientific.net/AMR.71-73.581.

Bhattacharjee, H., Mukhopadhyay, R., Saravanamuthu, T., Rosen, B. (2008). Aquaglyceroporins: ancient channels for metalloids. *Journal of Biology,* 7 (9). https://doi.org/10.1186/jbiol91.

Boiteau, R., Mende, D., Hawco, J., McIlvin, R., Fitzsimmons, J., Saito, M., Sedwick, P., DeLong, E., Repeta, D. (2016). Siderophore-based microbial adaptations to iron scarcity across the eastern Pacific ocean. *Proceedings of the National Academy of Sciences*, https://doi.org/10.1073/pnas.1608594113.

Bosello, M., Zeyadi, M., Kraas, F., Linne, U., Xie, X., Marahiel, M. (2013). Structural characterization of the heterobactin siderophores from *Rhodococcus erythropolis* PR4 and elucidation of their biosynthetic machinery. *Journal of Natural Products,* 76 (12):2282–90. https://doi.org/10.1021/np4006579.

Bowell, R., Alpers, C., Jamieson, H., Nordstrom, D., Majzlan, J. (2014). The environmental geochemistry of arsenic -- An Overview --. *Reviews in Mineralogy and Geochemistry*, 79 (1):1–16. https://doi.org/10.2138/rmg.2014.79.1.

Braud, A., Geoffroy, V., Hoegy, F., Mislin, G., Schalk, I. (2010). Presence of the siderophores pyoverdine and pyochelin in the extracellular medium reduces toxic metal accumulation in *Pseudomonas aeruginosa* and increases bacterial metal tolerance. *Environmental Microbiology Reports,* 2 (3):419–25. https://doi.org/10.1111/j.1758-2229.2009.00126.x.

Braud, A., Hannauer, M., Mislin, G., Schalk, I. (2009a). The *Pseudomonas aeruginosa* pyochelin-iron uptake pathway and its metal specificity. *Journal of Bacteriology*, 191 (11):3517–25. https://doi.org/10.1128/JB.00010-09.

Braud, A., Hoegy, F., Jezequel, K., Lebeau, T., Schalk, I. (2009b). New insights into the metal specificity of the *Pseudomonas aeruginosa* pyoverdine-iron uptake pathway. *Environmental Microbiology,* 11 (5):1079–91. https://doi.org/10.1111/j.1462-2920.2008.01838.x.

Busenlehner, L., Pennella, M., Giedroc, D. (2003). The SmtB/ArsR family of metalloregulatory transcriptional repressors: structural insights into prokaryotic metal resistance. *FEMS Microbiology Reviews,* 23 (2-3):131-143 . https://doi.org/10.1016/S0168-6445(03)00054-8.

Campbell, K., Nordstrom, D. (2014). Arsenic speciation and sorption in natural environments. *Reviews in Mineralogy and Geochemistry*, 79 (1):185-216. https://doi.org/10.2138/rmg.2014.79.3.

Carrano, C., Jordan, M., Drechsel, M., Schmid, D., Winkelmann, G. (2001). Heterobactins: a new class of siderophores from *Rhodococcus erythropolis* IGTS8 containing both hydroxamate and catecholate donor groups. *BioMetals,* 14 (2):119–25. https://doi.org/10.1023/A:1016633529461.

Chen, W., Shi, Y., Wu, S., Zhu, Y. (2016). Anthropogenic arsenic cycles: a research framework and Ffatures. *Journal of Cleaner Production*, 139: 328-336 https://doi.org/10.1016/j.jclepro.2016.08.050.

Cullen, W., Reimer, K. (1989). Arsenic speciation in the environment. *Chemical Reviews,* 89 (4):713–64. https://doi.org/10.1021/cr00094a002.

Dambies, L., Roze, A., Guibal, E. (2000). As(V) sorption on molybdate impregnated chitosan gel beads (MICB). *Advanced Chitin Sciences*, 4: 302-309. https://doi.org/ 10.1016/j.biortech.2008.02.015

Del Olmo, A., Caramelo, C., SanJose, C. (2003). Fluorescent complex of pyoverdin with aluminum. *Journal of Inorganic Biochemistry,* 97 (4):384–87. https://doi.org/10.1016/S0162-0134(03)00316-7.

Deschamps E. (2011) Chapter 4: Technology options for arsenic removal and immobilization. *In: Arsenic: Natural and Anthropogenic* (pages 49-56). Arsenic in the Environment, Vol. 4 Deschamps, E., Matschullat, J. (eds) CRC Press, Balkema.

Dimkpa, C., Merten, D., Svatoš, A., Büchel, G., Kothe, E. (2009). Siderophores mediate reduced and increased uptake of cadmium by *Streptomyces tendae* F4 and sunflower (*Helianthus annuus*), respectively. *Journal of Applied Microbiology*, 107 (5):1687–96. https://doi.org/10.1111/j.1365-2672.2009.04355.x.

Dimkpa, C., Svatoš, A., Merten, D., Büchel, G., Kothe, E. (2008). Hydroxamate siderophores produced by *Streptomyces acidiscabies* E13 bind nickel and promote growth in cowpea (*Vigna unguiculata* L.) under nickel stress. *Canadian Journal of Microbiology*, 54 (3):163–72. https://doi.org/10.1139/w07-130.

Drewniak, L., Styczek, A., Majder-Lopatka, M., Sklodowska, A. (2008). Bacteria hypertolerant to arsenic in the rocks of an ancient gold mine, and their potential role in dissemination of arsenic pollution. *Environmental Pollution,* 156 (3):1069–74. https://doi.org/10.1016/j.envpol.2008.04.019.

Drewniak, L., Rajpert, L., Mantur, A., Sklodowska, A. (2014). Dissolution of arsenic minerals mediated by dissimilatory arsenate reducing bacteria: estimation of the physiological potential for arsenic mobilization. *BioMed Research International,* 2014. https://doi.org/10.1155/2014/841892.

Duhme, A., Dauter, Z., Hider, R., Pohl, S. (1996). Complexation of molybdenum by siderophores: synthesis and structure of the double-helical cis-dioxomolybdenum(VI) complex of a bis(catecholamide) siderophore analogue. *Inorganic Chemistry,* 35 (10):3059–61. https://doi.org/10.1021/ic9512183.

Duval, S., Santini, J., Nitschke, W., Hille, R., Schoepp-Cothenet, B. (2010). The small subunit AroB of arsenite oxidase: lessons on the [2Fe-2S] rieske protein superfamily. *Journal of Biological Chemistry,* 285 (27):20442–51. https://doi.org/10.1074/jbc.M110.113811.

Ellis, D., Gumaelius, L., Indriolo, E., Pickering, I., Banks, J., Salt, D. (2006). A novel arsenate reductase from the arsenic hyperaccumulating fern *Pteris vittata*. *Plant Physiology,* 141 (4):1544–54. https://doi.org/10.1104/pp.106.084079.

Elson, C., Davies, D., Hayes, E. (1980). Removal of Arsenic from Contaminated Drinking Water by a Chitosan/Chitin Mixture. *Water Resources*, 14 (9):1307-1311. https://doi.org/10.1016/0043-1354(80)90190-6

Emmanuel, E., Ananthi, T., Anandkumar, B., Maruthamuthu, S. (2012). Accumulation of rare earth elements by siderophore-forming *Arthrobacter luteolus* isolated from rare earth environment of chavara, India. *Journal of Biosciences,* 37 (1):25–31. https://doi.org/10.1007/s12038-011-9173-3.

EPA. (2003). Minor clarification of the national primary drinking water regulation for arsenic. Fe Register 40 CFR Part 141. *US Environmental Protection Agency*. Available at http://www.epa.gov/ fedrgstr/EPA-WATER/2003/March/day-25/w7048.htm.

Ferreccio, C., Sancha, A. (2006). Arsenic exposure and its impact on health in Chile. *Journal of Health, Population and Nutrition*, 24 (2):164–75. https://doi.org/10.2307/23499354.

Fançois, F., Lombard, C., Guigner, J., Soreau, P., Brian-Jaisson, F., Martino, G., Vandervennet, M., Garcia, D., Molinier, A., Pignol, D., Peduzzi, J., Zirah, S., Rebuffat, S. (2012). Isolation and characterization of environmental bacteria capable of extracellular biosorption of mercury. Applied and Environmental Microbiology, 78 (4):1097–1106. https://doi.org/10.1128/AEM.06522-11.

Ghosh, P., Rathinasabapathi, B., Teplitski, M., Ma, L. (2015). Bacterial ability in AsIII oxidation and AsV reduction: relation to arsenic rolerance, P uptake, and siderophore production. *Chemosphere,* 138:995–1000. https://doi.org/10.1016/j.chemosphere.2014.12.046.

Gomez-Caminero, A., Howe, P., Hughes, M., Kenyon, E., Lewis, D., Moore, M., Ng, J., Aitio, A., Becking, G. (2001). Environmental health criteria 224 arsenic and arsenic compounds. *United Nations Environment Programme*. https://doi.org/NLM Classification: QV 294.

Gorchev, H., Ozolins, G. (2011). WHO guidelines for drinking-water quality. WHO Chronicle. Geneva, Switzerland : WHO Press, World Health Organization.

Goyer, R. (2001). Toxic effects of metals. *In: Doull's toxicology: the basic science of poisons* (pages 811-867). Casarett, L., Doull, J., Klaassen. 6th ed. New York, NY.

Haas, H. (2003). Molecular genetics of fungal siderophore biosynthesis and uptake: the role of siderophores in iron uptake and storage. *Applied Microbiology and Biotechnology,* 62 (4):316–30. https://doi.org/10.1007/s00253-003-1335-2.

Harrison, J., Ceri, H., Turner, R. (2007). Multimetal resistance and tolerance in microbial biofilms. *Nature Reviews Microbiology,* 5:928-938. https://doi.org/10.1038/nrmicro1774.

Heine, T., Mehnert, M., Schwabe, R., Tischler, D. (2017). Siderophore purification via immobilized metal affinity chromatography. *Solid State Phenomena,* 262 :505–8. https://doi.org/10.4028/www.scientific.net/SSP.262.505.

Hernandez, D., François, P., Farinelli, L., Østerås, M., Schrenzel, J. (2008). De novo bacterial genome sequencing: millions of very short reads assembled on a desktop computer. *Genome Research,* 18 (5):802–9. https://doi.org/10.1101/gr.072033.107.

Hider, R., Kong, X. (2010). Chemistry and biology of siderophores. *Natural Product Reports,* 27 (5):637. https://doi.org/10.1039/b906679a.

Höll, W., Deschamps, E. (2011). Chapter 3: Arsenic removal from water *In: Arsenic: Natural and Anthropogenic* (pages 39-47). Arsenic in the Environment, Vol. 4. Deschamps, E., Matschullat, J. (eds) CRC Press, Balkema.

Hong, Y., Song, K., Chung, J. (2016). Health effects of chronic arsenic exposure. *Journal of Preventive Medicine and Public Health*, 47 (5):245–252. https://doi.org/10.3961/jpmph.14.035.

Hughes, M. (2002). Arsenic toxicity and potential mechanisms of action. *Toxicology Letters*, 133(1):1-16. https://doi.org/10.1016/S0378-4274(02)00084-X.

Huster, D. (2010). Wilson Disease. *Best practice & research clinical gastroenterology,* 24 (5):531–39. https://doi.org/10.1016/j.bpg.2010.07.014.

Johnstone, R., Nolan, E. (2015). Beyond iron: non-classical biological functions of bacterial siderophores. *Dalton Transactions,* 44 (14):6320–39. https://doi.org/10.1039/c4dt03559c.

Jomova, K., Jenisova, Z., Feszterova, M., Baros, S., Liska, J., Hudecova, D., Rhodes, C., Valko, M. (2011). Arsenic: toxicity, oxidative stress and human disease. *Journal of Applied Toxicology,* 31 (2):95–107. https://doi.org/10.1002/jat.1649.

Kaur, T., Singh, A., Kumar-Goel, R. (2011). Mechanisms pertaining to arsenic toxicity. *Toxicology International*, 18 (2):87-93. https://doi.org/10.4103/0971-6580.84258.

Kraemer, S. (2004). Iron oxide dissolution and solubility in the presence of siderophores. *Aquatic Sciences,* 66 (1):3–18. https://doi.org/10.1007/s00027-003-0690-5.

Krewulak, K., Vogel, H. (2008). Structural biology of bacterial iron uptake. *Biochimica et Biophysica Acta – Biomembranes,* 1778 (9):1781–1804. https://doi.org/10.1016/j.bbamem.2007.07.026.

Kumar Kaushal, R. 2007. Arsenic removal from water/wastewater using adsorbents - a critical review. *Journal of Hazardous Materials,* 142 (1–2):1–53. https://doi.org/10.1016/j.jhazmat.2007.01.006.

Lam, C., Chun, C., Jickells, T., Richardson, D., Russell, D. (2006). Fluorescence-based siderophore biosensor for the determination of bioavailable iron in oceanic waters. *Analytical Chemistry*, 78 (14):5040–45. https://doi.org/10.1021/ac060223t.

Lee, C. (2009). Fluorescence spectroscopy. *Current Protocols Essential Laboratory Techniques*, 2 (1):241-249. https://doi.org/10.1002/9780470089941.et0204s02.

Litter, M., Sancha, A., Ingallinella, A. (2010). ancha, A., Ingallinella, A., Eds. (2010). Tecnologías económicas para el abatimiento de arsénico en aguas. Argentina:CYTED.

Mcafee, B., Gould, W., Nedeau, J., da Costa, A. (2001). Biosorption of Metal Ions Using Chitosan, Chitin, and Biomass of Rhizopus oryzae. *Separation Science and Technology*, 36 (14):3207-3222. https://doi.org/ 10.1081/SS-100107768

Magalhães, C. (2002). Arsenic. An environmental problem limited by solubility. *Pure and Applied Chemistry*, 74 (10): 1843-1850. https://doi.org/10.1351/pac200274101843.

Mandal, B., Suzuki, K. (2002). Arsenic round the world: a review. *Talanta,* 58 (1):201–35. https://doi.org/10.1016/S0039-9140(02)00268-0.

Marchesi, J., Sato, T., Weightman, A., Martin, T., Fry, J., Hiom, S., Wade, W. (1998). Design and evaluation of useful bacterium-specific PCR primers that amplify genes coding for bacterial 16S rRNA. *Applied and Environmental Microbiology,* 64 (2):795–99.

Marshall, G., Ferreccio, C., Yuan, Y., Bates, M., Steinmaus, C., Selvin, S., Liaw, J., Smith, A. (2007). Fifty-year study of lung and bladder cancer mortality in Chile related to arsenic in drinking water. *Journal of the National Cancer Institute,* 99 (12):920–28. https://doi.org/10.1093/jnci/djm004.

Matschullat, J. (2000). Arsenic in the geosphere - A review. *Science of the Total Environment*, 249 (1-3):297-312. https://doi.org/10.1016/S0048-9697(99)00524-0.

Mello de Capetani, E. (2011). Chapter 2: Arsenic toxicology – A review. I*n : Arsenic: Natural and Anthropogenic* (pages 27-37). Arsenic in the Environment, Vol 4. Deschamps, E., Matschullat, J. (eds) CRC Press, Balkema.

Memon, B. (2005). Detection of siderophores by thin layer chromatography. *Journal of Chemistry Society of Pakistan*, 27(6): 658-61.

Mesa, V., Navazas, A., González-Gil, R., González, A., Weyens, N., Lauga, B., Gallego, J., Sánchez, J., Peláez, A. (2017). Use of endophytic and rhizosphere bacteria to improve phytoremediation of arsenic-contaminated industrial soils by autochthonous *Betula celtiberica*. *Applied and Environmental Microbiology*, 83 (8): e03411-16. https://doi.org/10.1128/AEM.03411-16.

Miethke, M., Marahiel, M. (2007). Siderophore-based iron acquisition and pathogen control. *Microbiology and Molecular Biology Reviews,* 71 (3):413–51. https://doi.org/10.1128/MMBR.00012-07.

Mkandawire, M., Lyubun, Y., Kosterin, P., Dudel, E. (2004). Toxicity of arsenic species to *Lemna gibba L*. and influence of phosphate on arsenic bioavailability. *Environmental Toxicology*, 19 (1):26–35. https://doi.org/ 10.1002/tox.10148

Mkandawire, M., Dudel, E. (2005). Accumulation of arsenic in *Lemna gibba L*. (duckweed) in tailing waters of two abandoned uranium mining sites in Saxony, Germany. Sc*ience of Total Environment*, 336 (1-3) :81-89. https://doi.org/ 10.1016/j.scitotenv.2004.06.002

Mock, T., Samanta, M., Iverson, V., Berthiaume, C., Robison, M., Holtermann, K., Durkin, C., BonDurant, S., Richmond, K., Rodesch, M., Kallas, T., Huttlin, E., Cerrina, F., Sussman, M., Armbrust, V. (2008). Whole-genome expression profiling of the marine diatom *Thalassiosira pseudonana* identifies genes involved in silicon bioprocesses. *Proceedings of the National Academy of Sciences of the United States of America,* 105 (5):1579–84. https://doi.org/10.1073/pnas.0707946105.

Möllmann, U., Heinisch, L., Bauernfeind, A., Köhler, T., Ankel-Fuchs, D. (2009). Siderophores as drug delivery agents: application of the 'trojan horse' strategy. *BioMetals,* 22 (4):615–24. https://doi.org/10.1007/s10534-009-9219-2.

Mootz, H., Schwarzer, D., Marahiel, M. (2002). Ways of assembling complex natural products on modular nonribosomal peptide synthetases. *ChemBioChem,* 3 (6):490. https://doi.org/10.1002/1439-7633(20020603)3:6<490::AID-CBIC490>3.0.CO;2-N.

Mueller, J., Hinton, J. (1941). A protein-free medium for primary isolation of the Gonococcus and Meningococcus. *Experimental Biology and Medicine,* 48 (1):330–33. https://doi.org/10.3181/00379727-48-13311.

Murphy, J., Saltikov, C. (2009). The ArsR repressor mediates arsenite-dependent regulation of arsenate respiration and detoxification operons of *Shewanella* sp. strain ANA-3. *Journal of Bacteriology,* 91 (21):6722-31. https://doi.org/10.1128/JB.00801-09.

Murugesan, G., Sathishkumar, M., Swaminathan, K. (2006). Arsenic removal from groundwater by pretreated waste tea fungal biomass. *Bioresource Technology*, 97 (3):483-87. https://doi.org/ 10.1016/j.biortech.2005.03.008

Nair, A., Juwarkar, A., Singh, S. (2007). Production and characterization of siderophores and its application in arsenic removal from contaminated soil. *Water, Air, and Soil Pollution,* 180 (1–4):199–212. https://doi.org/10.1007/s11270-006-9263-2.

Neubauer, U., Furrer, G., Kayser, A., Schulin, R. (2000). Siderophores, NTA, and citrate: potential soil amendments to enhance heavy metal mobility in phytoremediation. *International Journal of Phytoremediation*, 2 (4):353–68. https://doi.org/10.1080/15226510008500044.

Nikaido, H. (2003). Molecular basis of bacterial outer membrane permeability revisited. *Microbiology and Molecular Biology Reviews,* 67 (4):593–656. https://doi.org/10.1128/MMBR.67.4.593.

Nitzsche, K., Lan, V., Trang, P., Viet, P., Berg, M., Voegelin, A., Planer-Friedrich, B., Zahoransky, J., Müller, S., Byrne, J., Schröder, C., Behrens, S., Kappler, A. (2015). Arsenic removal from drinking water by a household sand filter in Vietnam - effect of filter usage practices on arsenic removal efficiency and microbiological water quality. *Science of the Total Environment*, 502: 526-36. doi:10.1016/j.scitotenv.2014.09.055

Oller, W., Talano, M., Agostini, E. (2013). Screening of plant growth-promoting traits in arsenic-resistant bacteria isolated from the rhizosphere of soybean plants from Argentinean agricultural soil. *Plant and Soil*, 369 (1-2):93-102. https://doi.org/10.1007/s11104-012-1543-6.

Oremland, R., Saltikov, C., Wolfe-Simon, F., Stolz, J. (2009). Arsenic in the evolution of earth and extraterrestrial ecosystems. *Geomicrobiology Journal,* 26 (7):522–36. https://doi.org/10.1080/01490450903102525.

Oremland, R. S,Stolz. J.F. (2003). The ecology of arsenic. *Science,* 300 :939–44. https://doi.org/10.1126/science.1081903.

Osman, D., Cavet, J. (2010). Bacterial metal-sensing proteins exemplified by ArsR-SmtB family repressors. *Natural Product Reports*, 27:669-680. https://doi.org/10.1039/b906682a.

Pavez, O., Palacios, J., Aguilar, C. (2009). Arsenic removal by using colloidal adsorption flotation utilizing $Fe(OH)_3$ floc in a dissolved air flotation system. *Revista de Metalurgia,* 45 (2):85–91. https://doi.org/10.3989/revmetalm.0724.

Peng, Y., Huang, H., Zhang, Y., Kang, C., Chen, S., Song, L., Liu, D., Zhong, C. (2018). A versatile MOF-based trap for heavy metal ion capture and dispersion. *Nature Communications*, 9:187. https://doi.org/10.1038/s41467-017-02600-2.

Pennella, M., Giedroc, D. (2005). Structural determinants of metal selectivity in prokaryotic metal-responsive transcriptional regulators. *BioMetals*, 18 (4):413-28. https://doi.org/10.1007/s10534-005-3716-8.

Pokhrel, D., Viraraghavan, T. (2006), Arsenic removal from an aqueous solution by a modified fungal biomass. *Water Resources*, 40 (3):549-52. https://doi.org/10.1016/j.watres.2005.11.040

Prieto C. (2016). Characterization of nonribosomal peptide synthetases with NRPSsp. *In: Nonribosomal peptide and polyketide biosynthesis* (pages 273-8). Methods in Molecular Biology, Vol. 1401. Humana Press, New York, NY.

Prithivirajsingh, S., Mishra, S., Mahadevan, A. (2001). Functional analysis of a chromosomal arsenic resistance operon in *Pseudomonas fluorescens* strain MSP3. *Molecular Biology Reports* 28 (2):63–72. https://doi.org/10.1023/A:1017950207981.

Qin, J., Rosen, B., Zhang, Y., Wang, G., Franke, S., Rensing, C. (2006). Arsenic detoxification and evolution of trimethylarsine gas by a microbial arsenite s-adenosylmethionine methyltransferase. *Proceedings of the National Academy of Sciences*, 103 (7):2075-80. https://doi.org/10.1073/pnas.0506836103.

Ranjan, D., Mishra, D., Hasan, S. (2011). Bioadsorption of arsenic: an artificial neural networks and response surface methodological approach. *Industrial and Engineering Chemistry Research,* 50 (17):9852–63. https://doi.org/10.1021/ie200612f.

Reddy, G., Aggarwal, R., Matsumoto, G., Shivaji, S. (2000). *Arthrobacter flavus* sp. nov., a psychrophilic bacterium isolated from a pond in McMurdo Dry Valley, Antarctica. *International Journal of Systematic and Evolutionary Microbiology,* 50 (4):1553–61. https://doi.org/10.1099/00207713-50-4-1553.

Renshaw, J., Robson, G., Trinci, A., Wiebe, M., Livens, F., Collison, D., Taylor, R. (2002). Fungal siderophores: structures, functions and applications. *Mycological Research,* 106 (10):1123–42. https://doi.org/10.1017/S0953756202006548.

Retamal-Morales, G., Mehnert, M., Schwabe, R., Tischler, D., Zapata, C., Chávez, R., Schlömann, M., Levicán, G. (2018). Detection of arsenic-binding siderophores in arsenic-tolerating actinobacteria by a modified CAS assay. *Ecotoxicology and Environmental Safety,* 157:176-81. https://doi.org/10.1016/j.ecoenv.2018.03.087.

Retamal-Morales, G., Heine, T., Tischler, J., Erler, B., Gröning, J., Kaschabek, S., Schlömann, M., Levicán, G., Tischler, D. (2018). Draft genome sequence of *Rhodococcus erythropolis* B7g, a biosurfactant producing Actinobacterium. Jo*urnal of Biotechnology* 280:38–41. https://doi.org/10.1016/j.jbiotec.2018.06.001.

Robins, R. (2001). Some chemical aspects relating to arsenic remedial technologies. Procedures US EPA workshop on managing arsenic risks to the environment. Denver, CO, (1–3 May 2001). http://www.epa.gov/ ttbnrmrl/ArsenicPres/78.pdf

Rosen, B., Liu, Z. (2009). Transport pathways for arsenic and selenium: A minireview. *Environment International*, 35 (3):512-15. https://doi.org/10.1016/j.envint.2008.07.023.

Rosen, B., Tamas, M. (2010) Arsenic transport in prokaryotes and eukaryotic microbes. *Advances in Experimental Medicine and Biology*, 679: 47-55. https://doi.org/10.1007/978-1-4419-6315-4_4.

Roussel, C., Néel, C., Bril, H. (2000). Minerals controlling arsenic and lead solubility in an abandoned gold mine tailings. *Science of the Total Environment*, 263(1-3):209-19. https://doi.org/10.1016/S0048-9697(00)00707-5.

Saha, M., Sarkar, S., Sarkar, B., Sharma, B., Bhattacharjee, S., Tribedi, P. (2016). Microbial siderophores and their potential applications: A review. *Environmental Science and Pollution Research,* 23 (5):3984–99. https://doi.org/10.1007/s11356-015-4294-0.

Sancha, A. (2003). Removing arsenic from drinking water. A brief review of some lessons learned and Gaps arisen in chilean water utilities. In: Arsenic Exposure and Health Effects V (Pages 471-481). Proceedings of the Fifth International Conference on Arsenic Exposure and Health Effects, July 14–18, 2002, San Diego, California.

Sanderson, M. (1989). Confidence limits on phylogenesis: The boostrap revisited. *Cladistics*, 5 (2):113-29. https://doi.org/10.1111/j.1096-0031.1989.tb00559.x.

Schalk, I., Hannauer, M., Braud, A. (2011). New roles for bacterial siderophores in metal transport and tolerance. *Environmental Microbiology*, 13 (11):2844-2080. https://doi.org/10.1111/j.1462-2920.2011.02556.x.

Schmiederer, T., Rausch, S., Valdebenito, M., Mantri, Y., Mösker, E., Baramov, T., Stelmaszyk, K., Schmieder, P., Butz, D., Müller, S., Schneider, K. Baik, M., Hantke, K., Süssmuth, R.

(2011). The *E. coli* siderophores enterobactin and salmochelin form six-coordinate silicon complexes at physiological pH. *Angewandte Chemie - International Edition,* 50 (18):4230–33. https://doi.org/10.1002/anie.201005792.

Schwyn, D., Neilands, J. (1987). Universal chemical assay for the detection and determination of siderophores. *Analytical Biochemistry*, 160 (1):47–56. https://doi.org/10.1016/0003-2697(87)90612-9.

Sekine, M., Tanikawa, S., Omata, S., Saito, M., Fujisawa, T., Tsukatani, N., Tajima, T., Sekigawa, T., Kosugi, H., Matsuo, Y., Nishiko, R., Imamura, K., Ito, M., Narita, H., Tago, S., Fujita, N., Harayama, S. (2006). Sequence analysis of three plasmids harboured in *Rhodococcus erythropolis* strain PR4. *Environmental Microbiology,* 8 (2):334–46. https://doi.org/10.1111/j.1462-2920.2005.00899.x.

Sen, M., Manna, A., Pal, P. (2010). Removal of arsenic from contaminated groundwater by membrane-integrated hybrid treatment system. *Journal of Membrane Science,* 354 (1–2):108–13. https://doi.org/10.1016/j.memsci.2010.02.063.

Senges, C., Al-Dilaimi, A., Marchbank, D., Wibberg, D., Winkler, A., Haltli, B., Nowrousian, M., Kalinowski, Russell, J., Kerr, G., Bandow, J. (2018). The secreted metabolome of *Streptomyces chartreusis* and implications for bacterial chemistry. *Proceedings of the National Academy of Sciences*, 115 (10):2490-2495. https://doi.org/10.1073/pnas.1715713115.

Shenker, M., Chen, Y., Hadar, Y. (1995). Rapid method for accurate determination of colorless siderophores and synthetic chelates. *Soil Science Society of America Journal,* 59 (6):1612. https://doi.org/10.2136/sssaj1995.03615995005900060015x.

Shevtsov, A., Tarlykov, P., Zholdybayeva, E., Momynkulov, D., Sarsenova, A., Moldagulova, N., Momynaliev, K. (2013). Draft genome sequence of *Rhodococcus erythropolis* DN1, a crude oil biodegrader. *Genome Announcement*, 1: 1-5. doi:10.1128/genomeA.00846-13

Shi, H., Xianglin, S., Liu, K. (2004). Oxidative mechanism of arsenic toxicity and carcinogenesis. *Molecular and Cellular Biochemistry,* 255 (1–2):67–78. https://doi.org/10.1023/B:MCBI.0000007262.26044.e8.

Smith, A., Hopenhayn-Rich, C., Bates, M., Goeden, H., Hertz-Picciotto, I., Duggan, H., Wood, R., Kosnett, M., Smith, M. (1992). Cancer risks from arsenic in drinking water. *Environmental Health Perspectives,* 97:259–67. https://doi.org/10.1289/ehp.9297259.

Smith, A., Ercumen, A., Yuan, Y., Steinmaus, C. (2009). Increased lung cancer risks are similar whether arsenic is ingested or inhaled. *Journal of Exposure Science and Environmental Epidemiology,* 19 (4):343–48. https://doi.org/10.1038/jes.2008.73.

Solecka, J., Zajko, J., Postek, M., Rajnisz, A. (2012). Biologically active secondary metabolites from Actinomycetes. *Open Life Sciences,* 7 (3). https://doi.org/10.2478/s11535-012-0036-1.

Srivastava, S., Verma, P., Singh, A., Mishra, M., Singh, N., Sharma, N., Singh, N. (2012). Isolation and characterization of *Staphylococcus* sp. strain NBRIEAG-8 from arsenic contaminated site of west Bengal. *Applied Microbiology and Biotechnology* 95 (5):1275–91. https://doi.org/10.1007/s00253-012-3976-5.

Stolz, J., Basu, P., Santini, J., Oremland, R. (2006). Arsenic and selenium in microbial metabolism. *Annual Review of Microbiology,* 60 (1):107–30. https://doi.org/10.1146/annurev.micro.60.080805.142053.

Strnad, H., Patek, M., Fousek, J., Szokol, J., Ulbrich, P., Nesvera, J., Paces, V., Vlcek, C. (2014). Genome sequence of *Rhodococcus erythropolis* strain CCM2595, a phenol derivative-degrading bacterium. *Genome Announcements,* 2 (2):e00208-14-e00208-14. https://doi.org/10.1128/genomeA.00208-14.

Sultana, M., Vogler, S., Zargar, K., Schmidt, A., Saltikov, C., Seifert, J., Schlömann, M. (2012). New clusters of arsenite oxidase and unusual bacterial groups in enrichments from arsenic-contaminated soil. *Archives of Microbiology,* 194 (7):623–35. https://doi.org/10.1007/s00203-011-0777-7.

Swash, P., Monhemius, A. (1998). The scorodite process: a technology for the disposal of arsenic in the 21st century. *In: Effluent treatment in the mining industry* (pages 119-61). Castro, S., Vergara, F., Sanchez, M. Concepción, Chile.

Taketani, R., Zucchi, T., Melo, I., Mendes, R. (2013). Whole-genome shotgun sequencing of *Rhodococcus erythropolis* strain P27, a highly radiation-resistant actinomycete from Antarctica. *Genome Announcement*, e00763-13. doi:10.1128/genomeA.00763-13.

Tao, F., Zhao, P., Li, Q., Su, F., Yu, B., Ma, C., Tang, H., Tai, C., Wu, G., Xu, P. (2011). Genome sequence of *Rhodococcus erythropolis* XP, a biodesulfurizing bacterium with industrial potential. *Journal of Bacteriology*, 193: 6422–6423. doi:10.1128/JB.06154-11

Tekaya, B., Sherlyn, T., Murugesan, C., Woojong, Y., Tongmin, S. (2012). Actinobacteria isolation from metal contaminated soils for assessment of their metal resistance and plant growth promoting (PGP) characteristics. *Korean Journal Soil Science and Fertilizer*, 45(4): 593-601. http://dx.doi.org/10.7745/KJSSF.2012.45.4.593

Vogels, C., Johnson, M. (1998). Arsenic remediation in drinking waters using ferrate and ferrous ions, Technical Completion Report, Account No. 01-4-23922, New Mexico Resources Research Institute.

Wichard, T., Bellenger, J., Morel, F., Kraepiel, A. (2009). Role of the siderophore azotobactin in the bacterial acquisition of nitrogenase metal cofactors. *Environmental Science and Technology,* 43 (19):7218–24. https://doi.org/10.1021/es8037214.

Ueno, A., Ito, Y., Yumoto, I., Okuyama, H. (2007). Isolation and characterization of bacteria from soil contaminated with diesel oil, and the possible use of these in autochthonous bioaugmentation. *World Journal of Microbiology and Biotechnology,* 23 (12):1739–45. https://doi.org/10.1007/s11274-007-9423-6.

Vala, A., Vaidya, S., Dube, H. (2000). Siderophore production by facultative marine fungi. *Indian Journal of Marine Sciences,* 29 (4):339–40.

Wang, L., Jeon, B., Sahin, O., Zhang, Q. (2009). Identification of an arsenic resistance and arsenic-sensing system in *Campylobacter jejuni*. *Applied Environmental Microbiology*, 75: 5064-73. https://10.1128/AEM.00149-09

Welch, A., Westjohn, D., Helsel, D., Wanty, R. (2000). Arsenic in ground water of the United States: occurrence and geochemistry. *Ground Water,* 38 (4):589–604. https://doi.org/10.1111/j.1745-6584.2000.tb00251.x.

Wiegand, I., Hilpert, K., Hancock, R. (2008). Agar and broth dilution methods to determine the minimal inhibitory concentration (MIC) of antimicrobial substances. *Nature Protocols,* 3 (2):163–75. https://doi.org/10.1038/nprot.2007.521.

Yang, H., Cheng, J., Finan, T., Rosen, B., Bhattacharjee, H. (2005) Novel pathway for arsenic detoxification in the legume symbiont *Sinorhizobium meliloti*. *Journal of Bacteriology*, 187: 6991-97. https://10.1128/JB.187.20.6991-6997.2005

Yang, J., Rawat, S., Stemmler, T., Rosen, B. (2010). Arsenic binding and transfer by the ArsD as (III) metallochaperone. *Biochemistry,* 49 (17):3658–66. https://doi.org/10.1021/bi100026a.

SUPPLEMENTARY MATERIAL

Table S1.- Arsenic content of water rivers in Chile (obtained and translated from Aidis Chile, 2014)

Service	Plant	Source	Pollutants	Flow (L/s)	Total As (mg/L)
Iquique- Alto Hospicio	Santa Rosa	Groundwater	Arsenic	240	60-80
Calama	Cerro Topater	Superficial Water	Arsenic, turbidity	500	400-450
Antofagasta	Salar del Carmen	Superficial Water	Arsenic, turbidity	1000	400-450
Taltal	Taltal	Groundwater	Arsenic	30	60-80
Diego de Almagro	Diego de Almagro	Superficial Water	Arsenic, chloride, sulfates	35	100-500
Santiago Oriente	El Gallo	Mixed Ground and superficial water	Arsenic, chloride, iron, manganese	650	100-500
Lampa	Alto Lampa	Groundwater	Arsenic	50	60
Qulicura	Quilicura	Groundwater	Arsenic	100	60
Rancagua	Nogales	Superficial Water	Arsenic, turbidity	500	100-500

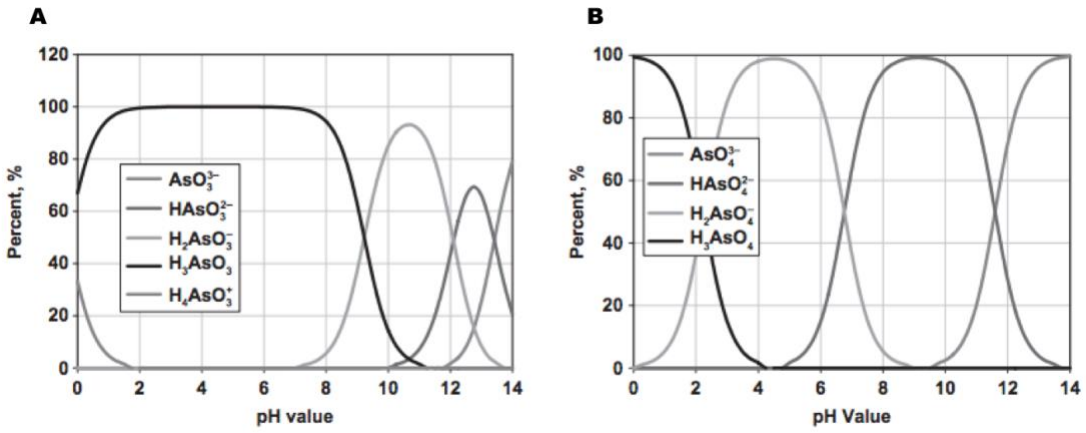

Figure S1.- Concentrations of the arsenic species in groundwater at different pH values, with total As concentration of 100 µg/L (Obtained from Höll and Deschamps, 2011) . (A) Concentration of As(III) species, (B) Concentration of the As(V) species. Shaded area indicates the pH range of most groundwater.

Table S2.- RTq-PCR primer sequences used in this study

Name	Sequence (5'-3')	Tm
RES43_arsC_fw	ATC CAC ACC CAT CTC ACC TC	60 ºC
RES43_arsC_rv	CAC GTC CTT GGT GAG TGC	60 ºC
RES43_htbG_fw	GTA CCA CCT GCT CGG CTA CT	60 ºC
RES43_htbG_rv	GAT CAG ACC GGC GAA CTC	60 ºC
RES43_16s_fw	CAG AAG AAG CAC CGG CTA AC	60 ºC
RES43_16s_rv	GAC AAA CCG CCT ACG AAC TC	60 ºC

Table S3.- Primer efficiency values for RTq-PCR

Primer set	Intercept	R^2	%Efficiency
RES43_arsC	0.792	0.996	93.754
RES43_htbG	0.948	0.995	96.453
RES43_16s	0.98	0.993	92.034

Table S4.- Sequence Alignment via BLASTn of 16s rDNA for the selected arsenic tolerant isolated strains.

Isolate Code	Reference Strain	Q. cover (%)	Identity (%)	Query Length (bp)	E-value	NCBI Access number
S43	*Rhodococcus erythropolis* DSM 25948	100	99	1502	0.0	KM047507.1
ATW1	*Rhodococcus erythropolis* DSM 43066	99	99	892	0.0	K5476725.1
ATW2	*Arthrobacter oxydans* DSM 20119	99	99	876	0.0	NR_026236.1
ATW3	*Arthrobacter oxydans* DSM 20119	98	99	896	0.0	NR_026236.1
ATW4	*Kocuria rosea* DSM 20447	99	100	892	0.0	NR_044871.1

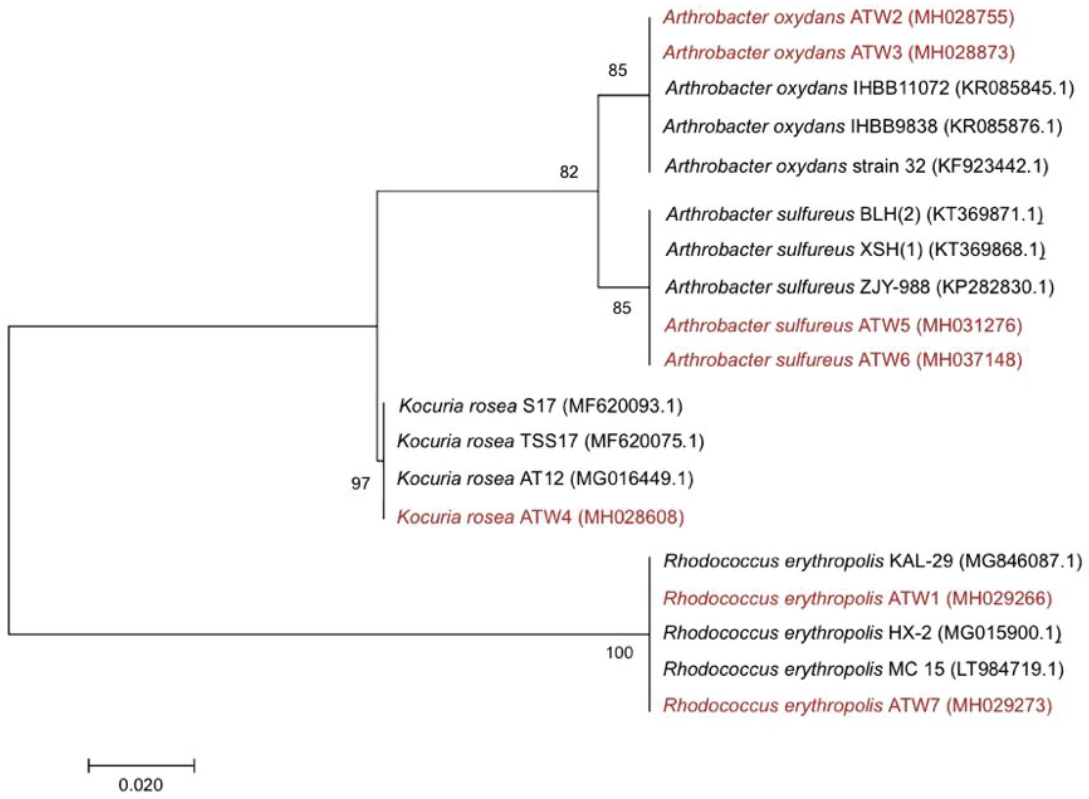

Figure S2.- Dendrogram of arsenic tolerant actinobacterial strains. Dendrogram performed using a Maximum-likelyhood method with Boostrap of 1000 replications. Bars represent 2 substitutions per 100 nucleotides .Clades show bacterial strains and their Genbank Accession number in parenthesis.

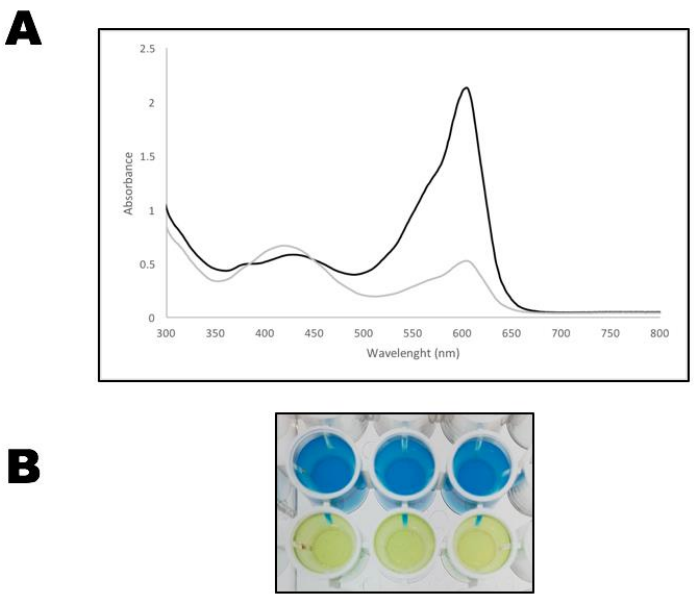

Figure S3.- Absorbance spectra of the As-$_m$CAS solution and image of fully-colorized and fully-decolorized As$_m$-CAS. (A) The grey line represents a fully decolorized solution (100% arsenic activity), the black line represents a fully colorized solution (0% arsenic-binding activity). (B) In blue is presented the fully colorized As-$_m$CAS solution (150 µL methanol + 150 µL of As-$_m$CAS) and in yellow is presented the fully-decolorized solution (150 µL EDTA 83.3 mM + 150 µL of As-$_m$CAS).

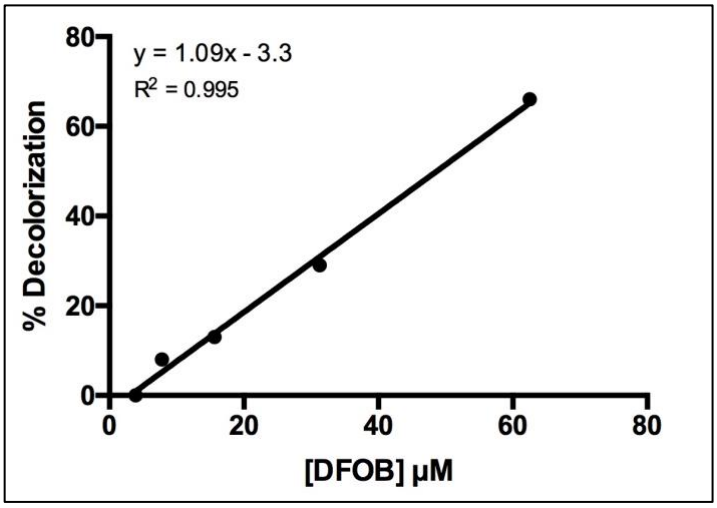

Figure S4.- Desferroxamine B (DFOB) Calibration curve for Fe-CAS assay. Decolorization percentage values were interpolated in the linear regression equation. Measurements with values above linear regression were diluted until they could be interpolated.

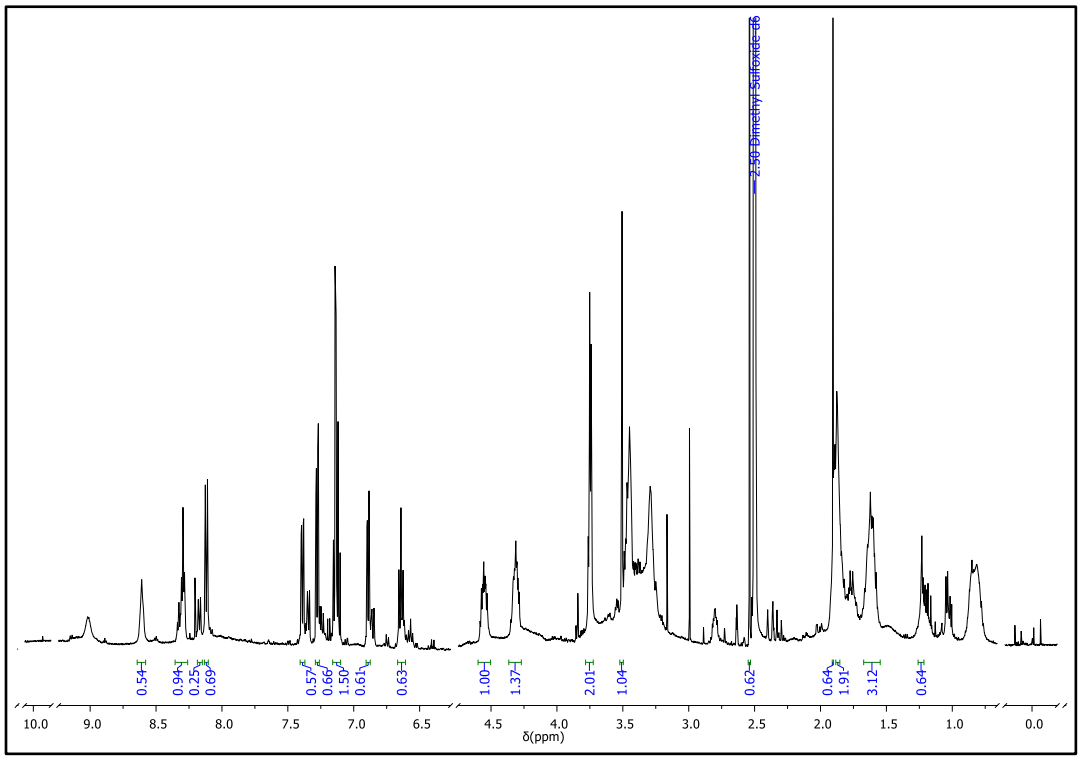

Figure S5.- ^{1}H-NMR spectrum in d6-DMSO of the absorbance peak at retention time 11.8 min with CAS / As-$_{m}$CAS activity. The spectrum obtained from the 80% methanol fraction of *R. erythropolis* S 43 cultured in Fe-free M9 medium (without arsenic addition).

LSI A-domain function predictor (Baranasic et al. 2014)

Rhodococcus erythropolis S43

Adenylation Domain	Substrate Prediction	LSI Score	HMMER E-value	Bit Score
htbE	2,3 dihydroxibenzoic acid	0.795	1.1E-27	83.0 +/- 0.0
htbG A1	Glutamate	0.666	1.3E-28	86.0 +/- 0.1
htbG A2	Glycine	0.724	2.4E-36	111.0 +/- 0.2
htbG A3	Ornithine	0.821	4.8E-35	106.8 +/- 0.0

Rhodococcus erythropolis PR4

Adenylation Domain	Substrate Prediction	LSI Score	HMMER E-value	Bit Score
htbE	2,3 dihydroxibenzoic acid	0.795	1.1E-27	83.0 +/- 0.0
htbG A1	Glutamate	0.666	1.3E-28	96.0 +/- 0.1
htbG A2	Glycine	0.724	2.4E-36	111.7 +/- 0.1
htbG A3	Ornithine	0.821	4.8E-35	106.4 +/- 0.0

NRPSsp (Prieto, 2016)

Rhodococcus erythropolis S43

Adenylation Domain	Substrate Prediction	Score (HMMER bit-score)	Prediction-conditioned fallout
htbE	2,3 dihydroxibenzoic acid	914	0.0037
htbG A1	Ornithine	330	0.14
htbG A2	Glycine	495	0.13
htbG A3	Ornithine	499	0.13

Rhodococcus erythropolis PR4

Adenylation Domain	Substrate Prediction	Score (HMMER bit-score)	Prediction-conditioned fallout
htbE	2,3 dihydroxibenzoic acid	916	0.0041
htbG A1	Ornithine	329	0.13
htbG A2	Glycine	485	0.13
htbG A3	Ornithine	480	0.13

Figure S6.- Substrate prediction for Adenylation-domains of NRPS for heterobactin production in *R. erythropolis* S43 and *R. erythropolis* PR4. LSI A-domain function predictor and NRPSsp bioinformatic platforms were used to predict the substrate specificity of each adenylation site in the amino acid strands of the genes *htbE* and *htbG* of the strains S43 and PR4. All scores show high specificity for each of the substrates present in the figure.

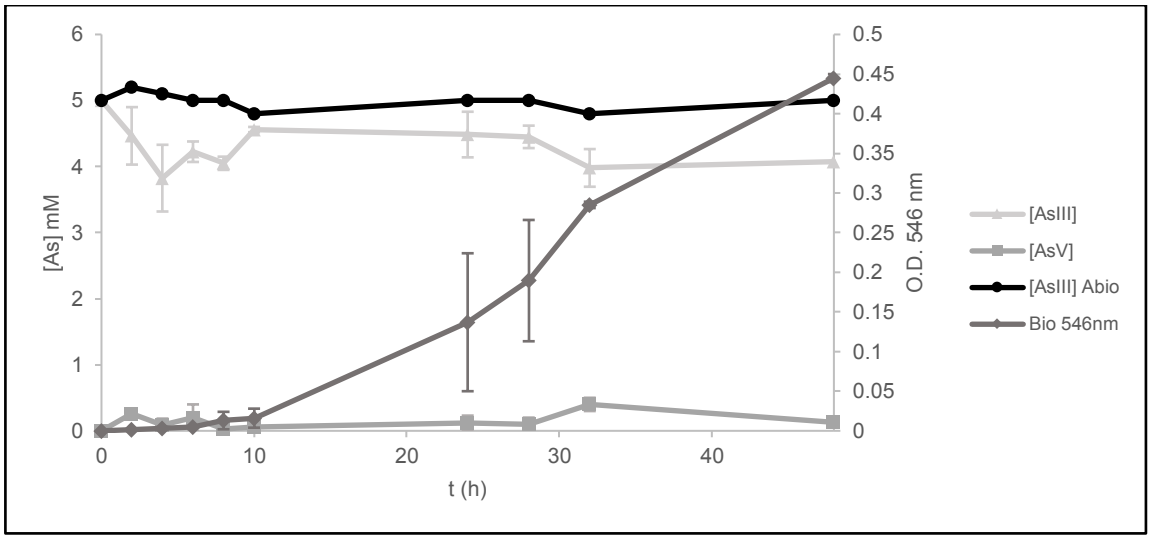

Figure S7.- Growth curve of *R. erythropolis* S43, with monitoring of arsenite oxidation. Graph shows the growth curve of *R. erythropolis* S43 in M1 medium (Sultana et al. 2012) with addition of As(III) as $NaAsO_2$ 5mM. Gray triangles represent As(III) (mM) concentration, grey squares represent As(V) (mM) concentration, black circles represent As(III) (mM) concentration in an abiotic control, grey diamonds represent bacterial growth, measured by turbidity at 546 nm. Measurements of As(III) and As(V) concentration were performed by ICP-MS in the Institue of Biosciences of the University of Freiberg (TUBAF) by MgSc. Fabian Giebner. Graphed data represent the average and standard deviation of three independent measurements.

PUBLICATIONS AND PARTICIPATIONS

Publications

Retamal-Morales, G., Mehnert, M., Schwabe, R., Tischler, D., Schlömann, M., Levicán, G. (2017). Genomic characterization of the arsenic-tolerant actinobacterium, *Rhodococcus erythropolis* S43. *Solid State Phenomena,* **262:** 660-663.

Mehnert, M., **Retamal-Morales, G**., Schwabe, R., Vater, S., Heine, T., Schlömann, M., Levicán, G., Tischler, D. (2017). Revisiting the chrome azurol S assay for various metal ions. *Solid State Phenomena,* **262:** 509-512.

Retamal-Morales, G., Mehnert, M., Schwabe, R., Tischler, D., Zapata, C., Chávez, R., Schlömann, M., Levicán, G. (2018). Detection of arsenic-binding siderophores in arsenic-tolerating Actinobacteria by a modified CAS assay. *Ecotoxicology and Environmental Safe*ty, **157:** 176-181.

Retamal-Morales, G., Heine, T., Tischler, J., Erler, B., Gröning, J., Kaschabek, S., Schlömann, M., Levicán, G., Tischler, D. (2018). Draft genome sequence of *Rhodococcus erythropolis* B7g, a biosurfactant producing actinobacterium. *Journal of Biotechnology,* **280**: 38–41.

Chilean Conferences

2018. Heterobactin-like arsenic-binding siderophores produced by the arsenic tolerant actinobacterium *R. erythropolis* S43. **Retamal-Morales Gerardo**, Schwabe Ringo, Mehnert Marika, Tischler Dirk, Schlömann Michael, Levicán Gloria. XXIV Congreso Latinoamericano de Microbiología , ALAM 2018. November 13th –17th, Santiago, Chile.

2017. Caracterización de Genes de Tolerancia a Arsénico de la Actinobacteria *Rhodococcus erythropolis* S43. **Retamal-Morales Gerardo**, Mehnert Marika, Schwabe Ringo, Tischler Dirk, Schlömann Michael, Levicán Gloria. XXXIX Congreso de Sociedad de Microbiología Chilena, SOMICH. La Serena, Chile.

2016. Arsenic-binding siderophores from arsenic-tolerant environmental bacteria. **Retamal Gerardo**, Mehnert Marika, Schwabe Ringo, Schlömann Michael, Tischler Dirk, Claudia Zapata, Levicán Gloria. XXXVIII Congreso de Sociedad de Microbiología Chilena, SOMICH. Valdivia, Chile.

2014. Analysis in silico of a complete draft genome of *Rhodococcus erythropolis* S43, isolated of a highly contaminated with arsenic soil. **Retamal Gerardo**, Rivera Javier, Valdés Natalia, Levicán Gloria.
XXXVI Congreso de Sociedad de Microbiología Chilena, SOMICH. La Serena, Chile.

International Conferences

2018. Producción y Caracterización de Heterobactina B de *Rhodococcus erythropolis* S43, un sideróforo quelante de arsénico. **Retamal-Morales Gerardo**, Schwabe Ringo, Mehnert Marika, Tischler Dirk, Schlömann Michael, Levicán Gloria. Jornada de Jóvenes Investigadores, Universidad de Cuyo, Mendoza, Argentina.

2018. Arsenic-binding heterobactin produced by the tolerant actinobacterium *R. erythropolis* S43. **Retamal-Morales Gerardo**, Schwabe Ringo, Mehnert Marika, Tischler Dirk, Schlömann Michael, Levicán Gloria.
European Geosciences Union, EGU 2018, April 8th, Vienna, Austria.

2017. El problema del Arsénico, inspiración alemana para un problema en Chile.
Retamal-Morales Gerardo. Simposio de Desarrollo Sustentable, Red INVECA, November 16th, Cologne, Germany.

2017. Genomic characterization of the arsenic-tolerant actinobacterium, *Rhodococcus erythropolis* S43.
Retamal-Morales Gerardo, Mehnert Marika, Schwabe Ringo, Tischler Dirk, Schlömann Michael, Levicán Gloria. IBS, Dechema, September 24th Freiberg, Germany.

2016. Metal (and metalloide) binding of different metallophores from bacteria and fungi.
Marika Mehnert, **Gerardo Retamal**, Thomas Heine, Ringo Schwabe, Michael Schömann, Gloria Levicán J., Dirk Tischler. AMERICAN SOCIETY FOR MICROBIOLOGY 2016, June 20th. Boston, USA.:

2016. Arsenic-binding siderophores from arsenic-tolerant Actinobacteria.
Retamal Gerardo, Mehnert Marika, Schwabe Ringo, Schlömann Michael, Tischler Dirk, Claudia Zapata, Levicán Gloria. BIOHYDROMET 2016, June 20th-22th. Falmouth, Cornwall, UK.

2016. Metallophores selectively bind metals. Dirk Tischler, Marika Mehnert, Sabine Vater, Vivian Schulz, **Gerardo Retamal M.,** Ringo Schwabe, Thomas Heine (2016). UFZ Energy Days 2016, Leipzig, Germany.

Internships Abroad

July 2017 – December 2017. Institute of Biociences, TU Bergakademie Freiberg, Germany.

October 2015 – January 2016. Institute of Biociences, TU Bergakademie Freiberg, Germany.

Funding

This project was funded by Conicyt Scholarship for PhD Students from the government of Chile, Fondecyt Project (117099) of Prof. Dr. Gloria Levicán, University of Santiago Scholarship for internships abroad, GraFA-DAAD funding for international students (TU Freiberg) and *Baksolex* Junior Research group of Prof. Dr. Dirk Tischler.